



Editor-in-Chief

Dr. Jose Navarro Pedreño

University Miguel Hernández of Elche, Spain

Associate Editor

Prof. Kaiyong Wang

Chinese Academy of Sciences, China

Editorial Board Members

Peace Nwaerema, Nigeria

Fengtao Guo, China

Aleksandar Djordje Valjarević, Serbia Han Yue, China

Han Yue, China

Sanwei He, China

Christos Kastrisios, United Fei Li, China

Adeline NGIE, South Africa

Arumugam Jothibasu, India

Zhixiang Fang, China

Ljubica Ivanović Bibić, Serbia

Rubén Camilo Lois-González, Spain

Jesús López-Rodríguez, Spain

Keith Hollinshead, United Kingdom

Rudi Hartmann, United States

Mirko Andreja Borisov, Serbia

Ali Hosseini, Iran

Kaiyong Wang, China

Virginia Alarcón Martínez, Spain

Krystle Ontong, South Africa

Jesús M. González-Pérez, Spain

Pedro Robledo Ardila, Spain

Guobiao LI, China

Federico R. León, Peru

Eva Savina Malinverni, Italy

Alexander Standish, United Kingdom

Samson Olaitan Olanrewaju, Nigeria

Kabi Prasad Pokhrel, Nepal

Zhibao Wang, China

María José Piñeira Mantiñan, Spain

Levent Yilmaz, Turkey

Kecun Zhang,China

Cheikh Faye, Senegal

Damian Kasza, Poland

Thomas Marambanyika, Zimbabwe

Chiara Certomà, Italy

Christopher Robin Bryant, Canada

Naeema Mohamed, United Arab Emirates

Nwabueze Ikenna Igu, Nigeria

Muhammad Asif, Pakistan

Novin Özdəmir Turkov

Nevin Özdemir, Turkey

Marwan Ghaleb Ghanem, Palestinian

Liqiang Zhang, China

Bodo Tombari, Nigeria

Kaveh Ostad-Ali-Askari, Iran

Lingyue LI, China

John P. Tiefenbacher, United States

Mehmet Cetin, Turkey

Arnold Tulokhonov, Russian

Somaye Vaissi, Iran

Najat Qader Omar, IRAQ

Binod Dawadi, Nepal

Keshav Raj Dhakal, Nepal

Julius Oluranti Owoeye, Nigeria

Yuan Dong, China

Carlos Teixeira, Canada

James Kurt Lein, Greece

Angel Paniagua Mazorra, Spain

Ola Johansson, United States

Zhihong Chen, United States

John Manyimadin Kusimi, Ghana

Safieh Javadinejad Javadinejad, UK

Susan Ihuoma Ajiere, Nigeria

Zhiguo Yao,China

Shengpei Dai, China

Xiaoli Ren, China

Journal of Geographical Research

Editor-in-Chief

Dr. Jose Navarro Pedreño





Volume 5 | Issue 2 | April 2022 | Page 1-81

Journal of Geographical Research

Contents

Articles

- 1 An Automated Process of Creating 3D City Model for Monitoring Urban Infrastructures
 - Mirko Borisov Vladimir Radulović Zoran Ilić Vladimir M. Petrović Nenad Rakićević
- 11 Sixteenth-Century Bulge on the Coast of Chile
 - A. Terry Bahill
- Assessment of Urban Morphology through Local Climate Zone Classification and Detection of the Changing Building States of Siliguri Municipal Corporation and Its Surrounding Area, West Bengal Ivana Hoque Sushma Rohatgi
- 44 Assessment of Stakeholders' Perceptions of Landuse/Landcover Change Drivers in Abuja, Nigeria
 Sani Abubakar Mashi Amina Ibrahim Inkani Safirat Sani Hassana Shuaibu
- 52 A Hybrid Geostatistical Method for Estimating Citywide Traffic Volumes A Case Study of Edmonton, Canada

Mingjian Wu Tae J. Kwon Karim El-Basyouny

Open Space Implications in Urban Development: Reflections in Recent Urban Planning Practices in Nepal

Krishna Prasad Timalsina Bhim Prasad Subedi

Retraction Notice

51 RETRACTED: Innovative Practices for the Promotion of Local/Indigenous Knowledge for Disaster Risk Reduction Management in Sudur Paschim Province, Nepal

Kabi Prasad Pokhrel Shambhu Prasad Khatiwada Narayan Prasad Paudyal Keshav Raj Dhakal Chhabi Lal Chidi Narayan Prasad Timilsena Dhana Krishna Mahat



Journal of Geographical Research

https://ojs.bilpublishing.com/index.php/jgr

ARTICLE

An Automated Process of Creating 3D City Model for Monitoring Urban Infrastructures

Mirko Borisov^{1*} Vladimir Radulović¹ Zoran Ilić² Vladimir M. Petrović³ Nenad Rakićević⁴

- 1. Faculty of Technical Sciences, University of Novi Sad, Trg Dositeja Obradovića 6, 21000 Novi Sad, Serbia
- 2. Academy of Technical and Educational Vocational Studies, Aleksandra Medvedeva 20, 18000 Niš, Serbia
- 3. Department for Ecology and Technoeconomics, University of Belgrade, Institute of Chemistry, Technology and Metallurgy, Njegoševa 12, 11000 Belgrade, Serbia
- 4. Republic Geodetic Authority, Nikodija Stojanovića 2, 18400 Prokuplje, Serbia

ARTICLE INFO

Article history

Received: 12 November 2021 Revised: 06 February 2022 Accepted: 11 February 2022 Published Online: 22 February 2022

Keywords:
3D city model
Infrastructure

Automated processing

Point cloud Model builder

ABSTRACT

This paper describes the process of designing models and tools for an automated way of creating 3D city model based on a raw point cloud. Also, making and forming 3D models of buildings. Models and tools for creating tools made in the model builder application within the ArcGIS Pro software. An unclassified point cloud obtained by the LiDAR system was used for the model input data. The point cloud, collected by the airborne laser scanning system (ALS), is classified into several classes: ground, high and low noise, and buildings. Based on the created DEMs, points classified as buildings and formed prints of buildings, realistic 3D city models were created. Created 3D models of cities can be used as a basis for monitoring the infrastructure of settlements and other analyzes that are important for further development and architecture of cities.

1. Introduction

The need for visualization of populated places, and especially the objects in them, has been present since ancient times. There are various forms of visualization of objects and buildings, starting from two-dimensional (2D), three-dimensional (3D), all the way to multidimensional

visualization. At the same time, three-dimensional visualization has become indispensable in spatial planning and city management. The need for the third dimension and spatial analysis arises especially as a result of the construction of large buildings and complexes. Also, there is the idea of smart cities that relate to the modern and

Mirko Borisov,

Faculty of Technical Sciences, University of Novi Sad, Trg Dositeja Obradovića 6, 21000 Novi Sad, Serbia;

Email: mborisov@uns.ac.rs; mirkoborisov@gmail.com

DOI: https://doi.org/10.30564/jgr.v5i2.4093

Copyright © 2022 by the author(s). Published by Bilingual Publishing Co. This is an open access article under the Creative Commons Attribution-NonCommercial 4.0 International (CC BY-NC 4.0) License. (https://creativecommons.org/licenses/by-nc/4.0/).

^{*}Corresponding Author:

urban future, and as such require a third dimension ^[1,2]. In addition, many settlements and cities contain a large number of buildings of different classes, different models and structures, and are most often divided according to the degree of detail of the display of the building-level of detail (LoD) ^[3-5]. Object models are created on the basis of data obtained from various sources (photogrammetry, LiDAR imaging, remote sensing, etc.).

Due to the increasingly frequent requirements for credibility and timeliness in the display of 3D cities and buildings, there is a need for mass and fast data collection. At the same time, the manual data processing procedure is in principle time consuming and it is impossible to repeat procedures with the same results, primarily due to subjectivity in the work. Automated procedures enable a larger amount of data that needs to be processed in the shortest possible time and credibly. Also, the fields of application of 3D models of cities are quite different, such as planning and construction of infrastructure facilities, environmental monitoring (air pollution, noise propagation), observation of roads and green areas, solving emergencies ^[6].

Recently, space data can be obtained by active and passive sensors in the form of point clouds (LiDAR recording). Point cloud data represent a specific surface geometry using an object-independent distribution of points with uniform quality. However, this form of representation is not suitable for many applications. Some more sophisticated tasks require generalization and simplification of data models. The process of generating 3D models of buildings and structures are just such a case.

The ideas and approaches taken to aid the problem of geometry construction have two strands: the creation of imagined geometry for virtual worlds and the reconstruction of geometry as it exists in the real world from measured data. Both commercial and academic spheres of research have investigated the automated reconstruction of geometry from point clouds [7-12].

New approaches to boundary detection employ different properties of the data. Some authors make use of LiDAR data to automatically extract the boundary of water bodies [13]. They present two algorithms for boundary detection. For the first, the centroid of the region of interest is computed and an imaginary line is generated between the centroid and the farthest point. Then, more imaginary lines are generated between the centroid and each point in the region of interest. The angle between the main line and each generated line is computed to create a range between 0° and 360°, then for each degree the furthest point from the centroid is assigned as a boundary point. The second algorithm converts the cloud data into

an image format. The resulting image is transformed into a binary representation and after that the pixels between the white and black colors are assigned as the object boundary ^[13]. The collected data are further processed to obtain fully developed photorealistic virtual 3D city models. The goal of this research is to develop a virtual 3D city model based on airborne LiDAR surveying and to analyze its applicability to Smart Cities applications ^[14]. They identify each roof patch from the LiDAR dataset firstly and secondly an improved Canny detector is used to extract the initial edges from the imagery data. Finally, the boundary is computed by fusing the roof patches with the initial boundary segmented from the images ^[15].

Automatic object modelling from point cloud data spans across a wide variety of domains. Multiple attempts use different segmentation methods with varying results. It seems that the more promising methods employ a combination of segmentation methods and semantic information, with a boundary extraction component. The boundary extraction component may be used to aid in segmentation of objects with the characteristic shape where segmentation methods based on local descriptors may exceed object boundary resulting in improper segmentation [6,9,16,17].

3D models of cities are especially interesting. There are various terms used for 3D city models, some of which are: "Cybertown", "Cybercity", "Virtual City", or "Digital City" [18]. The first 3D city models began to be applied at the end of the last century, accompanied by great difficulties, primarily due to the lack of appropriate application tools as well as standards that prevented the wider use of such models. The City Geography Markup Language Open Geospatial Consortium (CityGML OGC) standard is the first standard in the field and describes five LoDs for structuring the geometric and semantic characteristics of 3D data, however these LoDs have been shown to be ambiguous and limited (Figure 1) [19].



Figure 1. The five LoDs of the OGC CityGML [19]

In the past, virtual city models were most often used for visualization or simple graphical search of urban areas. Today, however, virtual 3D city models provide important information for various aspects of urban area management. Their application becomes extremely important during the construction, use and management of urban infrastructure [18]. The amount of detail that is captured in a 3D model, both in terms of geometry and

attributes, is collectively referred to as the LoD. In fact, the LoD concept is important in all steps of a typical 'life cycle' of a 3D city model, even prior to any acquisition has taken place. When creating 3D models of cities, LoD determines the data collection technologies that should be used, because different models are the result of different data collection approaches. For example, LoD defines the minimum point cloud density when using aerial laser scanning technology. When collecting data, LoD serves as the main guide on how detailed the data should be collected [19].

2. Methodology and Technology of the Study

2.1 Case Study Area

Tuborg Havn or Port of Tuborg is a marina and surrounding mixed-use neighbourhood in the Hellerup District of Copenhagen, Denmark. Located on a peninsula on the north side of Svanemølle Bay, just north of the border to Copenhagen Municipality, it is the result of a redevelopment of the former industrial site of Tuborg Breweries which ceased operations in 1996. The marina is operated by the Royal Danish Yacht Club which also has its club house at the site (Figure 2). Other local landmarks include the Experimentarium science centre, the Waterfront shopping centre and the Saxo Bank headquarters [20].



Figure 2. Tuborg Havn area [20]

2.2 Experimental Program

The experimental design was performed in the ArcGISPro software. It supports data visualization, advanced analysis, and authoritative data maintenance in 2D, 3D, and 4D. Also, it supports data sharing across a suite of ArcGIS products such as ArcGIS Online and ArcGIS Enterprise, and enables users to work across the ArcGIS system through Web GIS [21]. It is used to perform raster analysis and work with large sets of LiDAR

data in 3D ^[22]. In ArcGIS Pro, a body of related work-consisting of maps, scenes, layouts, data, tables, tools, and connections to other resources-is typically organized in a project. A project has its own geodatabase and its own toolbox ^[22].

Model builder is an application within ArcGIS Pro that is used to create, edit and manage models. Models are workflows that combine a number of geoprocessing tools, using the output of one tool as input to another tool. The model usually consists of at least three elements:

- input data (blue circles);
- geoprocessing tools (yellow squares);
- output data (green circles).

Model builder can also be considered a visual programming language for building workflows ^[23]. Instead of running each tool one at a time, a created model takes the input data, transforms it with a series of tools, and then creates the output data. The tools needed to form a model can be added in two ways. The first is by searching in the Add Tools To Model window and adding tools by double-clicking on the model. Another way is to simply drag the geoprocessing tool into the model from the Geoprocessing window or the Catalog window ^[24,25].

There is a possibility that several different users use the created model for the same purpose. Therefore, the input data and the output data have completely different names. Instead of static inputs and outputs, they need to be set dynamically as parameters. When input or output data are set as parameters, users can enter their data and set their output paths or storage locations ^[26].

3. Processing of Data

The created model for performing the task of work can be divided into two parts that are interconnected (Figure 3). The main result of the first part of the model is a digital elevation model (DEM). Within the second part of the model, the classification of point clouds were performed with the aim of obtaining the points of the roofs of buildings and the necessary data processing was performed. The final results of the second part of the model are 3D models of objects and 2D polygons in .shp format with information on the maximum and minimum height of 3D models of objects.

The tools used in the model are described below, starting with the first part of the model. Although the model is universal, for a concrete example, a point cloud related to the settlement of Tuborg Havn in Copenhagen, Denmark was used as input data (Figure 4). All data used comes from the Danish government website [27,28] and is also available through the website [29].

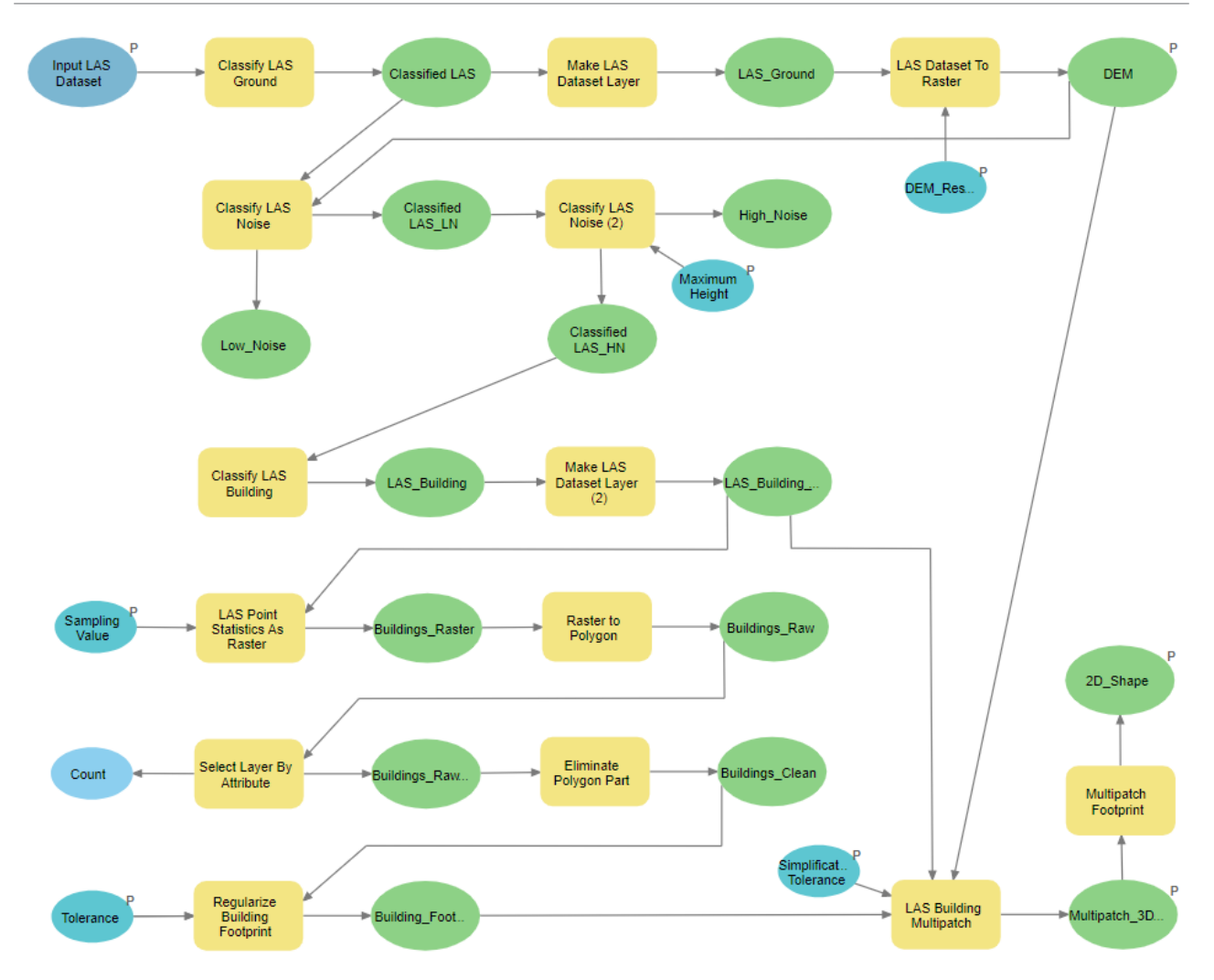


Figure 3. Appearance of the created model



Figure 4. Orthophoto of area of interest (Tuborg Havn)

The point cloud data were split into two files, so it was necessary to merge them into a single file. The two LAS point clouds come from a project managed by the Danish government and resulting in lidar coverage for the entire country. The merging of these two files was done by creating a new LAS dataset. The created LAS dataset called Tuborg_Havn.lasd, which represents the input data is shown in Figure 5.

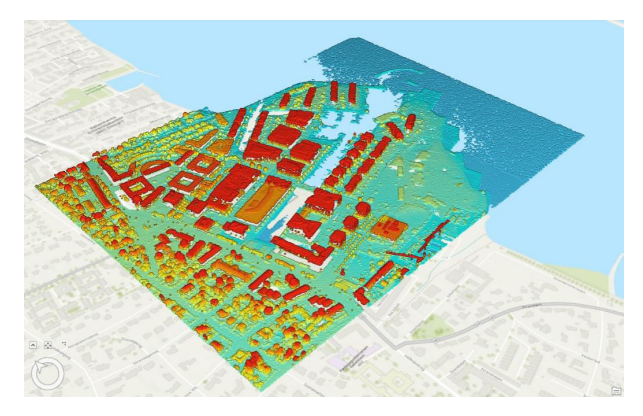


Figure 5. View the created LAS dataset

Prior to the model creation process, a new Toolbox was created in the Catalog called Building_Extraction. tbx. Within the toolbox, a model with the same name Building_Extraction was created. The tools used in the first part of the model are: Classify LAS Ground, Make LAS Dataset Layer, LAS Dataset To Raster, Classify LAS noise (Figure 6).

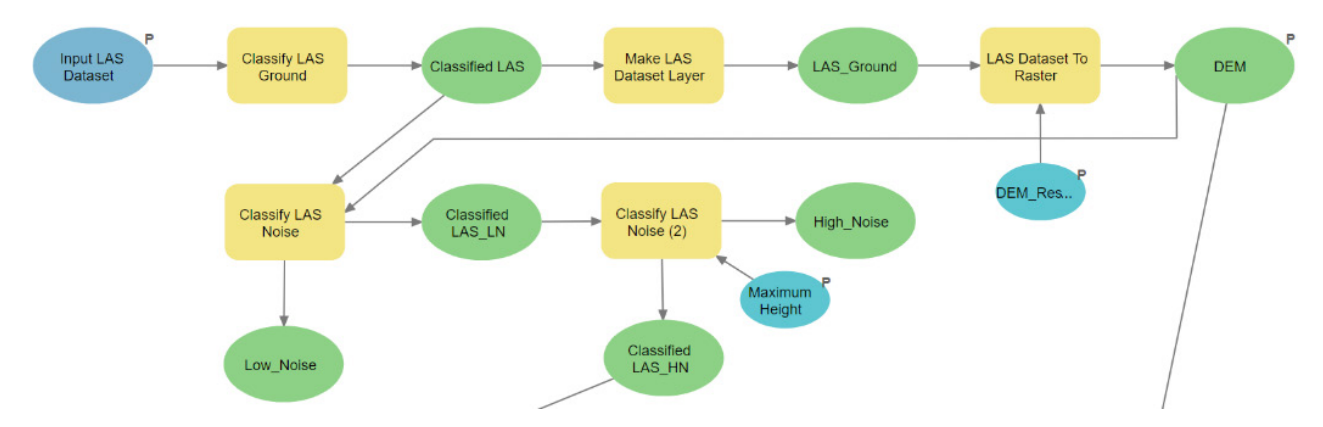


Figure 6. Presentation of the first part of the model

The Classify LAS Ground tool was used at the beginning of the model. The result of the tool is a modified point cloud Classified LAS to which the classification code 2 - Ground has been added (Figure 7).



Figure 7. Classification code 2 – Ground

After the ground classification was performed, the Make LAS Dataset Layer tool was used. The output layer LAS_Ground represents the layer to which the filter for classification code 2 - Ground was applied. After filtering the point clouds and creating a layer that represents the ground, the DEM was created using the LAS Dataset To Raster tool. The created DEM is displayed in Figure 8.

After determining the ground points, the next step is to identify the noise among the remaining unclassified points. Noise points correspond to points that are too high or low and are probably the result of random errors in lidar data. The Classify LAS noise tool was used for noise determination purposes. The LAS tool classifies points with atypical spatial characteristics as noise. The tool was used twice. The first time for low noises (Low Noise), and the second time for high noises (High Noise).

After the classification of noises, in the second part of the model, the classification of buildings, i.e. points that define roofs, was performed and additional data processing was performed to obtain the final result in a vector format containing 3D models of buildings. The tools used within the second part of the model are: Classify LAS Building, Make LAS Dataset Layer, LAS Point Statistics As Raster, Raster to Polygon, Select Layer By Attribute, Eliminate Polygon Parts, Regularize Building Footprint, LAS Building Multipatch, Multipatch Footprint. Figure 9 shows the appearance of the second part of the model.

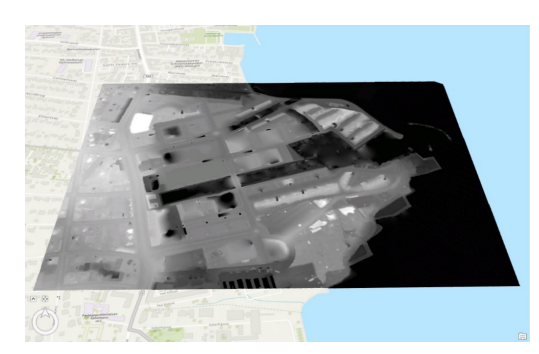


Figure 8. Created DEM resolution 0.5 m

In the second part of the model, the Classify LAS Building tool was used. The tool is used to classify building rooftops and sides in LAS data. The Classify LAS Building tool uses a combination of methods to identify the building points. The ground points must be separated out before running the tool. Among the unassigned points, the tool identifies solid surfaces where there was only one return per laser pulse. In contrast, an area with trees may have several returns per laser pulse because the light reaches and reflects from several levels in the foliage or even the ground. The Minimum Rooftop Height and Minimum Area parameters are also important to make sure that a surface that is too low or too small in the area is not mistakenly classified as a building. The Aggressive method was chosen for the Classification Method. Within this method, points corresponding to the characteristics of a flat roof with a relatively high tolerance to protrusion were discovered. The points identified as buildings are placed in classification code 6 - Buildings (Figure 10).

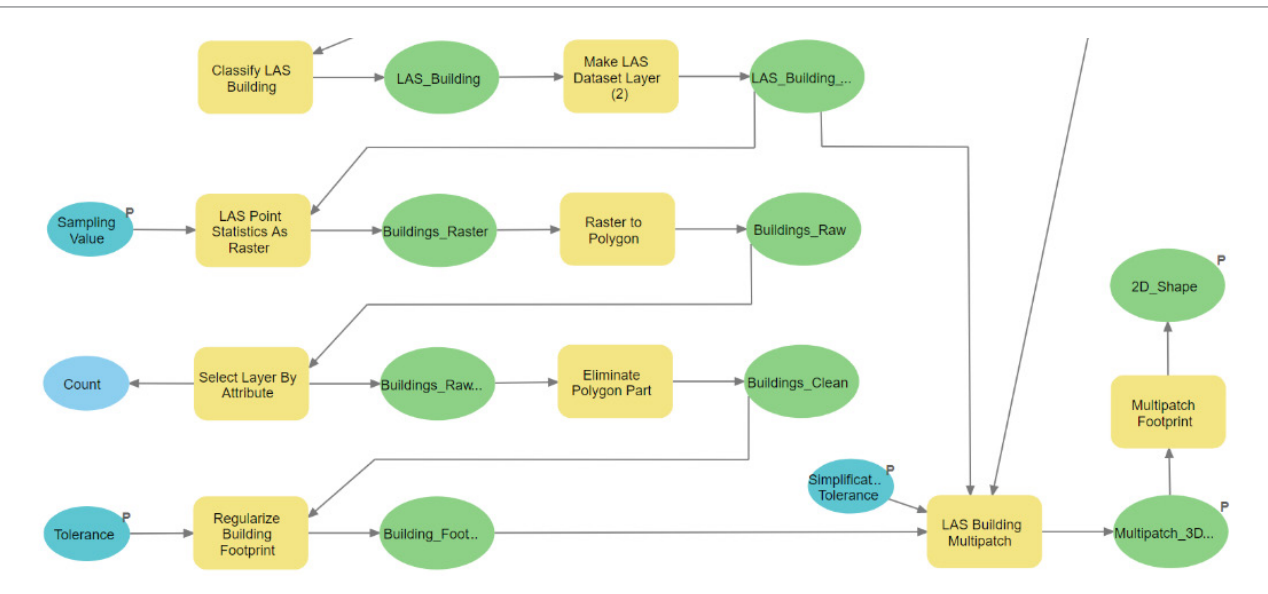


Figure 9. View second part of the model



Figure 10. Classification code 6 – Buildings

After classifying the points of the roofs of the buildings, it was necessary to separate the 2D contours of the buildings. Figure 11 shows the points identified as buildings.



Figure 11. Classification code 6 - Buildings i orthophoto (2D)

Orthophoto provides insight into what real buildings look like. However, the perspective in a photograph can make it difficult to achieve a complete visual match between the contour of the building (or the LAS points of the building) and the building below it. In the continuation, a raster was formed that corresponds to the location of the LAS points of the building. Before forming the raster, the Make LAS Dataset Layer tool was used again to create the layer LAS Building Layer. The LAS Point Statistics As Raster tool was used to form the raster Buildings Raster. The next step was to convert Buildings Raster to a polygon layer. The Raster to Polygon tool was used for this process. A polygon named Buildings Raw has been created that contains defects. The first step in eliminating the defects was to eliminate the smallest polygons based on the value of the Shape Area attribute. Based on the analysis of all facilities, 70 m² was selected for the limit value. Then, polygons larger than that value selected and the others were eliminated. The polygon selection procedure was performed using the Select Layer By Attribute tool. The next step was to remove the cavities within the polygon using the Eliminate Polygon Part tool. In this case, cavities with an area of 50 m² or less were eliminated. The next tool used is the Regularize Buildings Footprint tool. This tool is used to correct the stepped edges of polygons, i.e. to eliminate errors in their geometry. The Right Angles method was chosen for the method, which focuses on buildings with clean right angles. The result of the tool was a feature class called Buildings Footprints (Figure 12).



Figure 12. Buildings_Footprints

The LAS Building Multipatch tool was used to create realistic 3D models of objects. The tool is used to create models of buildings derived from roof points recorded in lidar data. The building model is generated by constructing a triangulated irregular network (TIN) from selected LAS points located within the building contour. The contour is embedded in this TIN as a truncated polygon whose height is defined by the lowest point of the LAS within its range. The ground height is the foundation of the building and can be reported either from the field in the attribute polygon attribute table or from the elevation surface (DEM). The created data were used for input data: DEM, LAS dataset points classified as buildings (LAS Building Layer) and building contours (Buildings Footprints). The result is a multipatch layer, a format that can store complex 3D vector characteristics.

At the end of the model, the Multipatch Footprint tool was used. The tool is used to create 2D polygon object contours in .shp format, created within a multipatch variable. The attributes Z_min and Z_max are added to the existing attributes based on the height of the created object models. The layout of the created polygons is the same as Buildings_Footprints, but with added attributes. The name of the output .shp file is user-defined. Figure 13 shows a pop-up window with information showing the attributes that have been added

For the created model to be universal and to be able be used with different input data, certain input and output data are set as parameters. When input and output data are set as parameters, users can enter their data and set their output paths or storage locations. After saving the model with parameters, the model can be launched by double-clicking within the Toolbox in which it is located, as well as other tools (Figure 14).

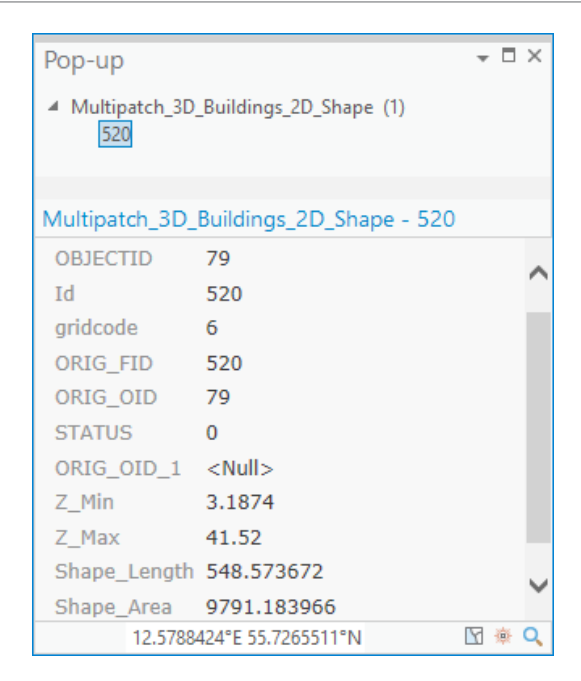


Figure 13. Pop-up window with object information (2D Shape)

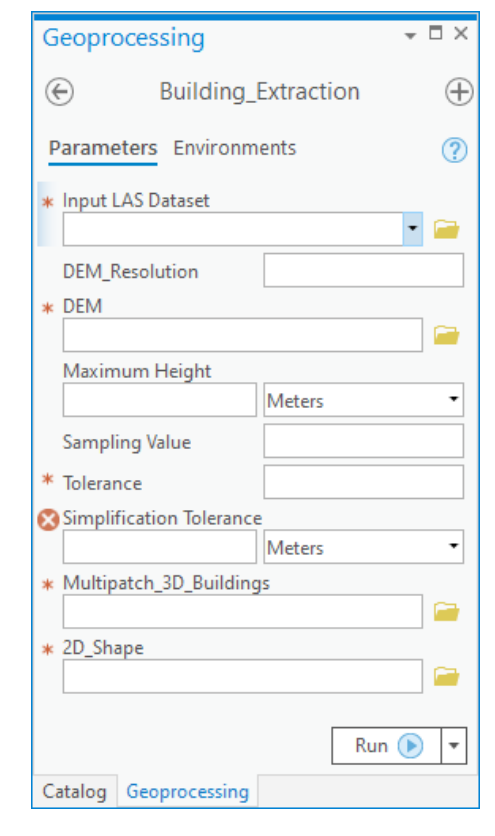


Figure 14. Appearance of the running model window

4. Results and Discussion

The point cloud, obtained by laser scanning, is classified into several classes: ground, high and low

noise and buildings. As stated in the paper, after the classification of ground points, a DEM was created, which was further used in the tools in which it was needed. Primarily in the classification of low noise based on the soil surface. After the calcification of noise inside the cloud of points, the classification of roofs of buildings was performed, i.e. facilities. Then, a raster was created from those points, and after that a polygon to which certain tools were applied in order to obtain the most realistic contours of the objects. The last step was to create realistic 3D models of objects, as well as 2D polygons obtained from point clouds. To create the final result, the previously obtained results in the model were used, and they are: DEM, points classified as buildings and contours of buildings, i.e. facilities.

The results of the work are models or tools for the automated process of creating 3D models of objects based on the raw point cloud. Within the tool, the classification of point clouds was performed, a DEM was created, and after that, the geometry of the objects was extracted. The last step was to create 3D objects. The final results represent a set of 3D objects, i.e. buildings in vector format, as well as 2D polygons of created 3D objects. The created multipatch layer with realistic 3D models of objects and with the created DEM set as a reference of the ground surface is shown in Figure 15.



Figure 15. Multipatch_3D_Buildings

Some of the buildings are located just above ground level. This is because they are generated using the created DEM as a reference for the ground level. Because the DEM is created from very precise lidar data, it represents a slightly different and more detailed terrain than the default WorldElevation3D / Terrain3D layer used within the display scene to model the ground in 3D. For a more accurate view of the terrain within the Contents window, below Elevation Surfaces, the created DEM has been added for Ground using the Add Elevation Source option and selected as a ground surface reference. A

zoomed view of the created 3D object models is shown in Figure 16.



Figure 16. Multipatch_3D_Buildings, close-up

Within the tools in the model, the values obtained by the analysis of the localities for which the data were collected were used. Although the model is universal, one should still take into account the locality and characteristics of the objects within it. The main advantage of the created tool is the possibility of automatic data processing, based on the parameters defined by the user.

5. Conclusions

In this paper, a model was formed, and later a tool for creating an automated procedure for creating a 3D city model based on a raw point cloud. The main intention was to create a tool that is universal for designing. In this way, the tool can be used by all users who need it. Also, there is a possibility for free choice of input and output parameters, and most importantly the input LAS dataset, i.e. point clouds.

The entire process is fully automated. The main disadvantage of the tool is the need for very high quality input data. The processing of different data sets showed that in order to achieve high-quality object models, it is necessary to use a very dense point cloud as an input. The application of a sparse point cloud results in the creation of lower quality object models. As stated in the paper, the obtained 3D models can be used for various purposes such as flood simulation, noise estimation, solar energy estimation, visibility analysis, spatial planning and many others. Advances in data collection methods and technologies for the automatic realization of 3D models are evolving very rapidly, which will make it easier to describe spatial data and their photorealism in the future [16,30]

A procedure was created to perform the task, which was later converted into a tool within the Model Builder application, in the ArcGIS Pro software environment. The input data are an unclassified point cloud obtained by the LiDAR system, which is subsequently structured through the application. Based on the classified point cloud, a DEM was created, object geometry was extracted, and realistic 3D object models were formed in the form of a multipatch layer, a format that can store complex 3D vector features.

References

- [1] Ostrowski, W., Pilarska, M., Charyton, J., Bakuła, K., 2018. Analysis of 3D Building Models Accuracy Based on The Airborne Laser Scanning Point Clouds. The International Archives of the Photogrammetry, Remote Sensing and Spatial Information Sciences, Volume XLII-2.
 - DOI: https://doi.org/10.5194/isprs-archives-XLII-2-797-2018
- [2] Billen, R., Cutting-Decelle, A.F., Marina, O., de Almeida, J.P., Caglioni, M., Falquet, G., Leduc, T., Métral, C., Moreau, G., Perret, J., et al., 2014. 3D City Models and Urban Information: Current Issues and Perspectives. European COST Action TU0801, EDP Sciences.
 - DOI: https://doi.org/10.1051/TU0801/201400001
- [3] Gröger, G., Plümer, L., 2012. CityGML-Interoperable semantic 3D city models. ISPRS Journal of Photogrammetry and Remote Sensing. 71.
 - DOI: https://doi.org/10.1016/j.isprsjprs.2012.04.004
- [4] Wang, R., Peethambaran, J., Chen, D., 2018. LiDAR Point Clouds to 3D Urban Models: A Review. IEEE Journal of Selected Topics in Applied Earth Observations and Remote Sensing. 99.
 - DOI: https://doi.org/10.1109/JSTARS.2017.2781132
- [5] Biljecki, F., Ledoux, H., Stoter, J., 2016. An improved LOD specification for 3D building models. Computers Environment and Urban Systems. 59. DOI: https://doi.org/10.1016/j.compenvurbsys.2016. 04.005
- [6] Hron, V., Halounová, L., 2014. Automatic Generation of 3D Building Models from Point Clouds. Conference: Symposium GIS Ostrava 2014 - Geoinformatics for Intelligent TransportationAt: Ostrava, Czech Republic.
- [7] Thomson, C., 2016. From Point Cloud to Building Information Model: Capturing and Processing Survey Data Towards Automation for High Quality 3D Models to Aid a BIM Process. PhD Thesis. DOI: https://doi.org/10.13140/RG.2.2.19058.71366/1
- [8] Andriasyan, M., Moyano, J., Nieto, J.E., Antón, D., 2020. From Point Cloud Data to Building Information Modelling: An Automatic Parametric Workflow

- for Heritage. Remote Sensing. 12(7). DOI: https://doi.org/10.3390/rs12071094
- [9] Căluşer, A., Cristian, G., 2018. Semiautomatic Building Information Modelling from point clouds, Master's Thesis, Department of Development and Planning, Aalborg University, Denmark.
- [10] Rusu, R.B., Blodow, N., Marton, Z.C., Dolha, M., Beetz, M., 2007. Towards 3D Point Cloud Based Object Maps for Household Environments, Robotics and Autonomous Systems. Volume 56. DOI: https://doi.org/10.1016/j.robot.2008.08.005
- [11] Awrangjeb, M., 2016. Using point cloud data to identify, trace, and regularize the outlines of buildings. International Journal of Remote Sensing. 37(3). DOI: https://doi.org/10.1080/01431161.2015.1131868
- [12] Zahn, C.T., 1996. A formal description for two-dimensional patterns, Stanford Linear Accelerator Center Stanford University, Stanford, California. pp. 621-628.
- [13] Canaz, S., Karsli, F., Guneroglu, A., Dihkan, M., 2015. Automatic boundary extraction of inland water bodies using LiDAR data, Ocean & Coastal Management, Volume 118, Part B. pp. 158-166. DOI: https://doi.org/10.1016/j.ocecoaman.2015.07. 024
- [14] Jovanović, D., Milovanov, S., Ruskovski, I., Govedarica, M., Sladić, D., Radulović, A., Pajić, V., 2020. Building Virtual 3D City Model for Smart Cities Applications: A Case Study on Campus Area of the University of Novi Sad. ISPRS International Journal of Geo-Information. 9 (476).
 DOI: https://doi.org/10.3390/ijgi9080476
- [15] Li, Y., Wub, H., Ana, R., Xua, H., Hea, Q., Xua, J., 2013. An improved building boundary extraction algorithm based on fusion of optical imagery and LIDAR data. Optik - International Journal for Light and Electron Optics. 124(22). DOI: https://doi.org/10.1016/j.ijleo.2013.03.045
- [16] Bellakaout, A., Cherkaoui, M., Ettarid, M., Touzani, A., 2016. Automatic 3D Extraction of Buildings, Vegetation and Roads from LIDAR Data. Remote Sensing Spatial Inf. Sci., XLI-B3. DOI: https://doi.org/10.5194/isprs-archives-XLI-B3-173-2016
- [17] Nys, G.A., Poux, F., Billen, R., 2020. CityJSON Building Generation from Airborne LiDAR 3D Point Clouds. ISPRS International Journal of Geo-Information. 9(9).
 - DOI: https://doi.org/10.3390/ijgi9090521
- [18] Biljecki, F., Stoter, J., Ledoux, H., Zlatanova, S., Çöltekin, A., 2015. Applications of 3D City Models:

- State of the Art Review. ISPRS International Journal of Geo-Information. 4(4).
- DOI: https://doi.org/10.3390/ijgi4042842
- [19] Biljecki, F., 2017. Level of detail in 3D city models, PhD thesis, TU Delf. pp. 353.DOI: https://doi.org/10.4233/uuid:f12931b7-5113-47ef-bfd4-688aae3be248
- [20] C.F. Møller Architects. https://www.cfmoller.com/p/tuborg-nord-general-og-bebyggelsesplan-i215.html. (Accessed 06 October 2021).
- [21] ESRI, ArcGIS Pro. https://www.esri.com/en-us/arcgis/products/arcgis-pro/overview. (Accessed 06 October 2021).
- [22] ESRI, ArcGIS Blog, Available online: https://www.esri.com/arcgis-blog/products/3d-gis/3d-gis/arcgis-pro-reinventing-desktop-gis/. (Accessed 06 October 2021).
- [23] ESRI, ArcGIS Pro, What is ModelBuilder? https://pro.arcgis.com/en/pro-app/latest/help/analysis/geo-processing/modelbuilder/what-is-modelbuilder-.htm. (Accessed 07 October 2021).
- [24] ESRI, ArcGIS Pro, Use ModelBuilder. https://pro.arcgis.com/en/pro-app/latest/help/analysis/geopro-

- cessing/modelbuilder/modelbuilder-quick-tour.htm. (Accessed 07 October 2021).
- [25] ESRI, ArcGIS Pro, Add and connect data and tools and modify elements. https://pro.arcgis.com/en/proapp/latest/help/analysis/geoprocessing/model-builder/add-connect-and-modify-data-and-tools-in-a-model.htm. (Accessed 07 October 2021).
- [26] ESRI, ArcGIS Pro, Model parameters. https://pro.arcgis.com/en/pro-app/latest/help/analysis/geoprocessing/modelbuilder/model-parameters.htm. (Accessed 07 October 2021).
- [27] Styrelsen for Dataforsyning og Effektivisering. https://kortforsyningen.dk/. (Accessed 07 October 2021).
- [28] Styrelsen for Dataforsyning og Effektivisering, Danmarks højdemodel Punktsky. https://dataforsyningen.dk/data/3931. (Accessed 07 October 2021).
- [29] ArcGIS, Building_Extraction. https://www.arcgis.com/home/item.html?id=d0966e35258847e1903e3d4525786b40. (Accessed 07 October 2021).
- [30] Learn ArcGIS, Extract 3D buildings from lidar data. https://learn.arcgis.com/en/projects/extract-3d-buildings-from-lidar-data/ (Accessed 05 February 2022).



Journal of Geographical Research

https://ojs.bilpublishing.com/index.php/jgr

ARTICLE Sixteenth-Century Bulge on the Coast of Chile

A. Terry Bahill*

Systems and Industrial Engineering, University of Arizona, Tucson AZ 85704, USA

ARTICLE INFO

Article history

Received: 17 January 2022 Revised: 21 February 2022 Accepted: 28 February 2022 Published Online: 25 March 2022

Keywords:
Coast of Chile
Evolution of maps
Traceability
Sixteenth-century world maps
Nautical charts
Systems engineering

1. Introduction

In the mid-sixteenth century, printed world maps began showing the west coasts of the South and North American continents. Most maps were similar: each subsequent map maker just added details. Examining Sebastian Cabot's 1544 map (Figure 1) shows an incipient bulge on the southern coast of Chile. This bulge might have grown into the bulge of Girolamo Ruscelli and subsequently into the bulges of Abraham Ortelius and Gerard Mercator 1569-70 (Figure 2). In the next thirty years, dozens of

ABSTRACT

This paper traces the sixteenth-century addition and removal on maps of a bulge on the southern coast of Chile. Abraham Ortelius was primarily responsible for these changes and many cartographers followed his lead. Then, Ortelius rotated the coastline of Chile from northwest to north. Later, he dropped the latitude of the islands of San Pablo and Isla de los Tiburones down six degrees. He named the Amazon River "Río de las amazons." Finally, he removed the cities with fake Native-American-sounding names along the Pacific coast of North America. The research underlying this paper examined over seven-hundred sixteenth-century maps made by sixdozen cartographers. This paper cites five-dozen maps by four-dozen cartographers. In the traceability section of this paper, this information was condensed into a traceability diagram, which shows the chronological flow of information among a score of cartographers. Using this information, this paper traced the influence of one cartographer on another: it showed who influenced whom. It showed the spread of knowledge. Ortelius was at the center of most of this knowledge explosion.

cartographers followed their lead.

The next world-shaking change occurred in 1588 when Ortelius *removed* the bulge on the southern coast of Chile: again almost everyone followed suit. In 1587 Ortelius rotated the coastline of Chile from northwest to north: other cartographers followed. Once again, Ortelius seems to have been the leader in removing the westward lean of the Chilean coast. Later in 1589, he dropped the latitude of the islands of San Pablo and Isla de los Tiburones down six degrees. For example, on his maps, he moved San Pablo from 15° S latitude to 21° S latitude. Again a whole

A. Terry Bahill,

Systems and Industrial Engineering, University of Arizona, Tucson AZ 85704, USA;

Email: terry@sie.arizona.edu

DOI: https://doi.org/10.30564/jgr.v5i2.4357

Copyright © 2022 by the author(s). Published by Bilingual Publishing Co. This is an open access article under the Creative Commons Attribution-NonCommercial 4.0 International (CC BY-NC 4.0) License. (https://creativecommons.org/licenses/by-nc/4.0/).

^{*}Corresponding Author:

group of cartographers followed him. In 1570 he invented the name "Río de las amazons" (River of the Amazons) and dozens of cartographers did likewise. Finally, in 1589, he removed the cities with fake Native-American-sounding names along the Pacific coast of North America: others eventually followed him.

These actions (adding ^① and removing the bulge on the southern coast of Chile, rotating the coast of Chile, 'moving' San Pablo and Isla de los Tiburones, naming the Amazon River, and removing the cities with Native-American sounding names) indicate that Ortelius was the leader and a dozen or more cartographers followed his lead.

Aim: The aim of this paper is to show the sixteenthcentury evolution of the bulge on maps of the southern coast of Chile.

Scope: The scope of this paper is printed sixteenth-century nautical world maps.

The Literature Review for this paper consists of listing the cartographer, the name of the map being cited, and its year of publication. This literature review is in the appendix. These 65 maps listed in the appendix are then linked to their URLs with http://sysengr.engr.arizona.edu/URLsForSixteenthCenturyMaps.xlsx.

2. Materials and Methods

This paper traces changes from cartographer to the cartographer. Our most successful technique for exploring the traceability of sixteenth-century nautical maps was analyzing visually distinct features on these maps. For example, we investigated the bulge on the southern coast of Chile. Features like that are the focus of this paper. This is not a traditional history paper as is common in the field of geographic exploration and discovery. It does not present the religious, familial, or national relationships of the cartographers. Rather it introduces systems engineering tools into nautical cartography. In this study, these tools are traceability and tradeoff studies. We did not make a statement about a map and then reference an earlier paper that made a similar statement. Rather we made a statement and then pointed to a feature on a map that supported the statement. Furthermore, the "literature review" section of this paper is given in the appendix as a list of maps that have relevant information. Using these maps, this paper traces particular geographical features and suggests who instigated the changes.

Fourteenth- and fifteenth-century Portolan charts ²⁰ and sixteenth-century world maps had features, and toponyms that came and went. These features and toponyms were moved geographically and their shapes were changed. They were continually added but seldom removed. Changes were rarely explained. An exception that proves this rule is the Francesco Beccario ^[1] (Franciscus Becharius) Portolan chart of 1403. On this chart, he wrote to his readers that he had moved Sardinia and changed the distance scale of the Atlantic with respect to the Mediterranean. This type of explanation was very unusual in Portolan charts.

In contrast, starting with Ortelius in 1570, atlases had much more off-the-map text than they had maps. For example, Ortelius's 1571 atlas *Theatrum Orbis Terrarum* comprises 200 pages of which only 95 are maps. This present paper investigates prominent features like the bulge on the southern coast of Chile precursors of which might have shown up in 1544 and the bulge itself faded away starting in 1587. We suggest that Girolamo Ruscelli was the cause of its appearance and Abraham Ortelius was the cause of its disappearance.

The research underlying this paper examined over seven-hundred sixteenth-century maps made by six-dozen cartographers. This paper cites five-dozen maps by four-dozen cartographers. In the traceability section of this paper, this information was condensed into a traceability diagram. This diagram shows the chronological flow of information among a score of cartographers. Using this information, this paper traced the influence of one cartographer on another: it showed who influenced whom.

3. Results

3.1 Magellan's Voyage, AD 1519 to 1522

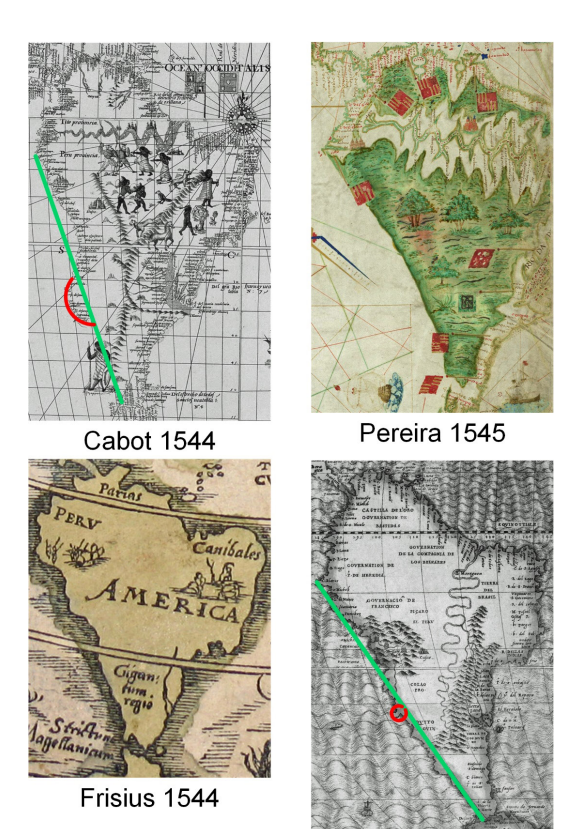
Ferdinand Magellan did not leave a map of his circumnavigation of the world in 1519-22 [3]. However, we do have the logbook of his pilot Francisco Albo [4]. It records that on 2 December 1520, they were off the coast of Chile at 47° S latitude. From there they sailed up the coastline for fourteen days with an average azimuth of 20°, NNE. On 16 December at 36° S, they changed course to go northwest, out into the Pacific Ocean. This means that for two weeks they followed the Chilean coast, and

① We are not saying that Ortelius invented the bulge on the coast of Chile. He did not: Ruscelli did. We are merely saying that many cartographers followed Ortelius. We will discuss this later.

② Portolan charts are mostly fourteenth and fifteenth-century nautical charts of the Mediterranean and Black Seas. Their coastlines are crowded with names of cities, towns, ports, harbors, rivers, points, capes, etc. They are detailed and accurate. They were built on a framework of interconnected rhumb lines emanating from maybe eight or sixteen compass roses encircling the canter of the map. They were the first large-area maps since the lost maps of Ptolemy of the second century AD.

covered 740 miles (we use statute miles in this paper) with an average speed of 50 miles per day (which is reasonable for ships of the day in that region) and an average azimuth of NNE. {In Albo's notation the 16 quarter winds were named using the symbol ¼, for example, "N ¼ NE." This would be an azimuth of 11.25°. The modern notation would call this North by East or NbE.} The point is that Magellan sailed *easterly* up the coast of Chile, not westwardly. [®]

3.2 Add South America to World Maps, AD 1540s



Gastaldi 1546

Figure 1. Sections of contemporary sixteenth-century maps of South America. Land to the west of our green line is defined as the bulge. For most maps in this paper, the meridians of longitude and the parallels of latitude are ten degrees apart. However, on Cabot's map, they are only five degrees apart. All of the maps in this paper are over 400 years old: hence they are not subject to copyright restrictions. Modifications to the original figures belong to the author.

The illustrations in Figure 1 come from these maps.

- Sebastian Cabot, 1544, World Map of A. D. 1544
- Gemma Frisius, 1544, La Cosmographie de Peter Apian ...
- Antonio Pereira, 1545, Early representation of Newfoundland, Lower California, the Amazon, and the Ladrones
 - · Giacomo Gastaldi, 1546, Universalet

We have a database that lists and gives URLs for all maps mentioned in this paper. It is at this location http://sysengr.engr.arizona.edu/URLsForSixteenthCenturyMaps.xlsx.

In Figure 1, Cabot and Antonio Pereira have drawn the Amazon River as a giant snake, as was common between 1544 and 1600. However, Gemma Frisius does not have an Amazon River and Giacomo Gastaldi has his Amazon River running from south to north! Cabot and Gastaldi have a suggestion of a bulge on the coast of Chile, indicated with red arcs.

In 1541-1542, a Spanish conquistador and explorer, Francisco de Orellana, and his crew sailed the length of the Amazon River from west to east. (4) They were the first Europeans to explore this river [5]. The next year, in Portugal, they plausibly shared their travel logs with the Portuguese Captain Antonio Pereira. Then he or some unknown Portuguese cartographer created a world map containing South America. On it, the Amazon River is shaped like a giant snake with its tail in the Andes Mountains and its head on the coast of the Atlantic Ocean (Figures 1 and 2) [6]. At about the same time that Orellana was sailing down the Amazon River, Sebastian Cabot explored the Americas for Spain. From his first-hand knowledge and knowledge from other cartographers. he created his map of the world. ^⑤ A third cartographer, Gemma Frisius, created a globe in 1536 (with the assistance of his graduate student Gerard Mercator) and a world map in 1544. It also had South America. A fourth

③ We assume that Albo's azimuth measurements were made with a magnetic compass. According to https://maps.ngdc.noaa.gov/viewers/historical_declination/ in 1590 the magnetic declination along the coast of Chile between 47° S latitude and 36° S latitude was between +4° and +6° east of north. This means that when Albo thought they were heading 11° east of north, they were actually heading 16° east of true north. This is even farther eastward than we had expected.

④ Orellana and his crew had no intention of sailing to the Atlantic ocean, when they started their trip on the Pacific coast. They merely intended to climb the Andes. But when they found themselves at the bottom on the east side, they decided it would be easier to sail down the Amazon River rather than climb back up the Andes. They had brought nails with them, so they chopped down trees and made boats. Then they sailed east to the Atlantic Ocean. In this paper, we tried to base our judgments strictly on what was on the maps. But in this case, we must comment that this trip was so harrowing, the sailors probably exaggerated all details.

⁽⁵⁾ The year 1544 is widely accepted as the date this map was created/published. However, no copies of the original map exist. The copy in the Boston Public Library contains a date of 1544, which was probably added in 1897: https://collections.leventhalmap.org/search/commonwealth:7h149v62n. There are several older copies in the BnF: Bibliothèque nationale de France, https://data.bnf.fr/12574640/sebastien_cabot/ and https://gallica.bnf.fr/ark:/12148/btv1b55011003p/f1.item_This is the only map attributed to Sebastian Cabot.

cartographer, Giacomo Gastaldi, created his map in 1546. The shape of South America is similar on all four of these world maps in Figure 1. Note that the west coast of Chile slopes at about a 20° angle, NNW, in these maps. This is contrary to the direction given in Albo's log of Magellan's voyage, which was NbE, and contrary to its actual azimuth. Figure 6 shows that from 45 °S latitude up to the Tropic of Capricorn the actual coast slopes 8° eastward. Even so, for the next four decades, the maps of the South America held this incorrect NNW slope, see for example Guillaume Le Testu 1556, Diogo Homen 1558, Paolo Forlani 1560, Bartolomeu Velho 1561, Diego Gutiérrez & Hieronymus Cock 1562, Ortelius 1564, Donato Bertolli 1568, Domingos Teixeira 1573, Giovanni Massa 1580, and Bartolomeu Lasso 1586.

In the Atlantic Ocean, at the Equator, near the mouth of the Amazon River, the maps of Ortelius (and many subsequent maps) have labeled it Rio de las Amazons. Some of the details in this paper, like this label, might be too small to see on the published figures. Therefore, we have provided a list of Internet sources for the maps mentioned here. This list/database is located at http://sysengr.engr.arizona.edu/URLsForSixteenthCenturyMaps. xlsx. This list contains URLs for high-resolution original maps that are mostly in the public domain: that is, they are free of known restrictions under copyright law. Just click on a URL in this file and you will be connected to an original map.

The earliest maps we have found containing the whole continent of South America are those made by Pereira 1545, Frisius 1544, Cabot 1544, and Gastaldi 1546 shown in Figure 1. We do not assert a chronological order amongst these four maps because the dates are only estimates and the cartographers would have been working on these maps concurrently for a long time.

3.3 Add a Bulge to the Coast of Chile, AD 1561-70

Pereira and Frisius have no hint of a bulge on the southern coast of Chile. However, the maps of Cabot and Gastaldi have a suggestion of an incipient bulge on the coast. Two decades later, prominent bulges appeared on maps.

We have a database that lists and gives URLs for all maps mentioned in this paper. It is at this location http://sysengr.engr.arizona.edu/URLsForSixteenthCenturyMaps.xlsx.

Table 1 lists a few cartographers/maps produced between 1544 and 1587 that might have a bulge on the southern coast of Chile. To categorize these maps we used the coordinates of two distinct geographical points: the Pacific Ocean exit from Straits of Magellan, which

has coordinates (52.6° S, 74.7° W), and the westernmost point in South America, the Punta Pariñas, which has coordinates of (4.7° S, 81.3° W). We drew a line between these two points. Everything to the west of this line is called the bulge. We measured the east-west distance between the center of the protrusion and this line and called it the Protrusion Distance.

The 1544 Cabot map shows a small bulge on the southern coast of Chile. Afterward, Gastaldi 1546 and 1548, Tramezzino 1554, and Forlani 1560 followed with small bulges of their own. However, if you were not looking for a bulge on these maps, then you probably would not see one. They are small.

Then, Ruscelli 1561, *Orbis Descriptio*, Forlani 1562, *La.Descrittione. di. Tutto.ll. Peru.* and *Gastaldi and Some Others 1562-65* produced big bulges on their coasts of Chile. These bulges instigated the bulges of the next two decades that are shaded with red in Table 1.

In 1561 Girolamo Ruscelli in his *Orbis Descriptio* map in his *La Geografia di Claidio Tolomeo Alessandrino* ... atlas (which was just one more translation of Ptolemy's *Geographia*) put a bulge on the southern coast of Chile, below the Tropic of Capricorn as shown in Figure 3. Except for this bulge, this map looks like a copy of Gastaldi's 1546 map *Universale*. In seventeen years the bulge was the only addition.

The next maps with prominent bulges are the Forlani 1562 and the Gastaldi and Some Others 1562-65 maps. The text at the bottom of the *Cosmographia Universalis et Exactissima* ... the map indicates the creators as "... Gastaldio Nounullisque Aliis ...," which translates as "Gastaldi and Some Others ..." Therefore we will refer to this map as Gastaldi and Some Others 1562-1565.



Figure 3. Ruscelli's 1561 Orbis Descripto map, contained in his atlas Geography by Claudio Tolomeo Alessandrino, translated from Greek into the Italian vernacular by Girolamo Ruscelli. Land to the west of our green line and below the Tropic of Capricorn is defined as the bulge on the southern coast of Chile. (Only the western hemisphere of his map is shown here.)

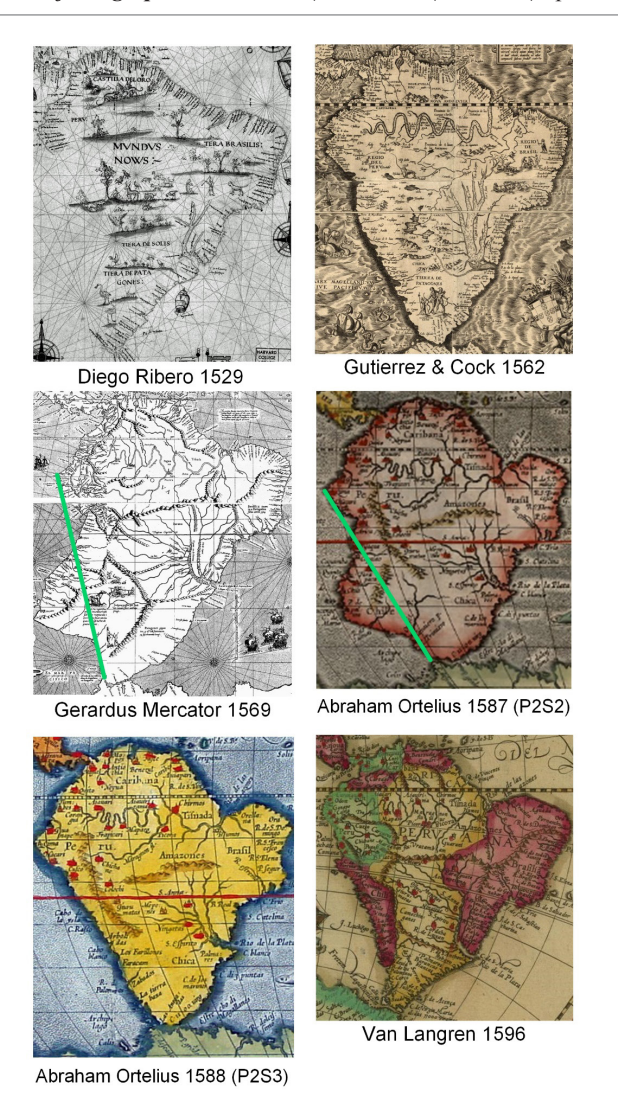


Figure 2. South American sections of sixteenth-century maps. [®] Land to the west of our green line is defined as the bulge. This bulge appears on the southern coast of Chile just below the Tropic of Capricorn on the maps of Mercator 1569 and Ortelius 1587. It is not on the maps by Gutiérrez & Cock 1562 ^[7], Ortelius 1588, or Van Langren 1596. The abbreviations P2S2 and P2S3 will be explained later in section 3.4. Unless noted otherwise, parallels of latitude and meridians of longitude are spaced ten degrees apart on maps in this paper.

The illustrations in Figure 2 come from these maps.

- Ribero 1529, Carta universal en que se contiene todo lo que del mundo se ha ...,
- Gutiérrez & Cock 1562, Americae Sive Quartae Orbis Partis Nova ...,
- Mercator 1569, Nova et Aucta Orbis Terrae descriptio ...,
- Ortelius 1587 (P2S2), Typus Orbis Terrarum,
- Ortelius 1588 (P2S3), Typus Orbis Terrarum, and
- Van Langren 1596, Orbis terrae compendiosa descriptio ...

Port; Puerto, P., Pt.

Cape; cabo, c.

River: rio, R.,

Saint; santo, S., san.,

⁽⁶⁾ Here are some words commonly used on charts and maps of this era followed by some abbreviations: Island; Ilsa, Isla, Iland, Islet, Iles, Isole, ysola, Eylant, I., Y.

In alphabets of this era, the 's' was often elongated (e.g. i | land) making it the tallest letter. This was a characteristic of the Italic type face designed by Ludovico Arrighi 1527. The 'i' is the vowel form of 'i' and the 'j' is the consonant form of 'i'. The 'u' is the vowel form of 'u' and the 'v' is the consonant form of 'u'. The word *diver* means various.

Cartographer	Year	Latitude of the bulge, °S	For the point of the bulge, Degrees west of the Straits of Magellan exit	For the point of the bulge, Degrees east of Punta Pariñas	Protrusion Distance, degrees of longitude	Shape of the bulge	Estimated Area of the bulge in degrees of longitude squared
Actual coast	2021	48 to 50	1	5.6	1	Flat	
Cabot	1544	34	13	5	5	Dome	
Gastaldi	1546	32	8	9	5	Skin tag	
Gastaldi	1548	31	3	1	3	Dome	
Tramezzino	1554	30	8	-2	2	Cone	
Forlani	1560	32	6	10	4	Skin tag	
Ruscelli	1561	22 to 49	30	4	13	Dome	157
Forlani	1562	5 to 41	28	-5	19	Cone	310
Gastaldi and Some Others +	1562-65	5 to 41	28	-5.1	19	Cone	420
D. Homen	1565	24 to 43	33	1	20	Dome	50
Mercator	1569	27 to 47	16	-6	13	Cone	130
Ortelius	1570	34 to 43	20	-6	18	Dome	265
Francois de Belleforest	1575	34 to 43	20	-6	18	Dome	88
Ortelius	1587 P2S2	34 to 43	20	-6	18	Dome	225
+The lines of latitude and longitude are 15 degrees apart on this map by Gastaldi and Some Others							

Table 1. Progression of the size and location of the bulge on the southern coast of Chile

This bulge is centered, on average, at 35° S latitude in Table 1, except for Forlani 1562 and the Gastaldi and Some Others 1562-1565. It was often shaped as in Figure 3. We are still developing a quantitative characterization of the shapes of these bulges.

Ruscelli put this bulge on his *Orbis Descripto* map in all versions of his atlas *La Geografia di Claudio Tolomeo* ... 1561, 1562, 1564, 1574, 1598 and 1599. (He did not put the bulge on his 1562 *Terra Nova* or his 1561 Carta Marina Nuova Tavola.)

The following cartographers/maps of this era do not have this bulge: Frisius 1544, Pereira 1545, Pierre Descelier 1550, Lopo Homen 1554, Velho 1561, Gutiérrez & Cock 1562, and Ortelius 1564. The next cartographers who included this bulge on the southern coast of Chile were Gerard Mercator and Abraham Ortelius in 1569-70.

In 1570, Ortelius published the first modern atlas, *Theatrum Orbis Terrarum*. Then he updated and reissued it just about every year. The *Typus Orbis Terrarum* (TOT) maps in his atlases from 1570 to 1587 had the bulge on the coast of Chile ^[8]. Mercator and Ortelius were early adopters of this big bulge in 1569-70. Others followed suit in adding a bulge to the southern coast of Chile, for example, André Thevet 1575, Nicola Van Sype 1581, Joan Martines 1587, Rumold Mercator 1587, Urbano Monte 1587, Sebastian Munster 1588, Cornelius De Jode 1589 (published in 1593), and Michael Mercator 1595. Some cartographers didn't get the word and continued to publish maps without the bulge after 1569-1570, for example, D. Teixeira 1573, Massa 1580, and Lasso 1586.

3.4 Remove the Bulge from the Coast of Chile, AD 1587-88

In 1587-1588, Ortelius made a dramatic change: he *removed* the bulge on the southern coast of Chile. To be precise, he removed the bulge on the 2nd plate in the 3rd state (P2S3) of the *Typus Orbis Terrarum* (TOT) map printed in 1588 (Figures 2 and 4). He did the same on his *TOT* 1587 P3S1 (published in 1592), his *Americae sive novi orbis nova descripito* ... 1587, and his *Maris Pacifici* 1589. In contrast, the Mercator family kept putting this bulge on their maps into the seventeenth century. These maps by Ortelius do not have the bulge on the coast of Chile: *Typus Orbis Terrarum* 1588 and on, *Americae sive* ... 1587 and on, and all *Maris Pacifici*. These maps were all contained in his atlases: they were not published individually. So these dates have more credibility.

In Figure 4, the only differences between the two maps are to the left of the green line. The bulge is the pink region to the left of the green line. A misalignment of the text can be seen in the bottom part of this figure, to the right of the Straights of Magellan. Otherwise, all of the letters are superimposed.

In Figure 2, the abbreviations P2S2 and P2S3 on the

The year given for each map is only an approximation. I usually list the 1588 P2S3 *Typis Orbis Terrarum* before the 1587 *American Sive ...*, because that is the way they are usually listed in historical documents. There is no absolute of how to list maps chronologically. Should we use the date the map was conceived? When it was finished? When it was published? When the atlas containing it was published? etc. I usually used the year given by the map owner. So take all dates with a grain of salt

Ortelius 1587 and 1588 maps stand for plate-2 state-2 and plate-2 state-3, respectively ^[9]. Most maps of this era were engraved on copper plates and printed from these plates. The printers would print a batch of maps and then set the plates aside. When they needed more maps, they would retrieve the plates and print some more. When the plates wore out, they would engrave a new set of plates. Maps printed with this second set of plates are called plate-2 by modern historians ^[9]. Each set of plates would have occasional changes. Maps printed with these changed plates are called state-1, state-2, state-3, etc.



Figure 4. Superimposing Ortelius's *Typus Orbis Terrarum* (TOT) 1588 P2S3 map of Figure 2 onto his 1587 P2S2 map of Figure 2 shows the size and shape of this bulge on the southern coast of Chile. The bulge comprises almost one million square miles, which is four times the size of Spain.

For the Ortelius *Typus Orbis Terrarum* (TOT) map the first set of copper plates lasted through 16 printings from 1570 to 1575. In 1575 the lower-left corner cracked and was repaired ^[9]. Maps printed with this cracked set of plates are called TOT plate-1 state-2 (P1S2). Ortelius made minor alterations to his plates and in 1579 published his atlas containing TOT plate-1 state-3 (P1S3). In 1584 he published TOT plate-1 state-4 (P1S4) and in 1585 he published TOT plate-1 state-5 (P1S5).

Then, after printing hundreds of maps, the first set of plates wore out. So Ortelius and his engraver Franciscus Hogenberg engraved a new set of plates in 1586. They are called TOT plate-2 state-1, or in our shorthand P2S1.

They erased the date from the plates in 1587 and printed the maps now called TOT plate-2 state-2 (P2S2) as in Figure 2. In 1588 they removed the bulge on the southern coast of Chile and printed TOT plate-2 state-3 (P2S3) also shown in Figure 2 [9]. In 1587 they engraved their third set of plates for TOT. They engraved the date 1587 on them. (Evidentially they did not use these plates for five years.) These plates were used from 1592 to 1612. They are called TOT plate-3 state-1 (P3S1). Finally, plate-3 state-2 (P3S2) maps began to be printed in 1628.

The following maps do not have the bulge on the southern coast of Chile: Ortelius TOT 1588, etc., *American Sive ... 1587*, etc., and *Maris Pacifici* 1589,

After 1588 some cartographers continued to publish maps with the bulge on the southern coast of Chile, for example, Munster 1588, C. De Jode 1589 (first published in 1593), Theodor de Bry 1592, M. Mercator 1595 and into the seventeenth century, and Ruscelli 1599 (this is a different map, but it still has a bulge). Others either followed Ortelius' lead and removed the bulge on the southern coast of Chile, or they had never put it there in the first place, for example, Jodocus Hondius 1595 and 1597, Richard Hakluyt 1589, Emery Molyneux 1592 [10]. Petrus Plancius 1594, Jan Baptists Vrient 1596, João Lavanha & Luis Teixeira 1597, Edward Wright & Emery Molyneux 1598, and Matteo Ricci 1602.

We have found no explanation for *why* Ortelius removed the bulge on the coast of Chile. However, this mistake in the maps seems to have vexed Sir Francis Drake, who wrote [11],

"... we continued our course, *Nouember* 1, [1578] still North-west, as wee had formerly done, but in going on we soone espied, that we miglit easily haue beene deceiued; and therefore casting about and steering vpon another point, wee found, that the generall mappes did erre from the truth in setting downe the coast of *Peru*, [Drake refers to the whole coast as Peru, not differentiating between Chile and Peru. Drake continues describing the section of the coast between 52° S and 40° S latitude.] ... perceiuing hereby that no man had euer by trauell discouered any part of these 12. deg., and therefore the setters forth of such descriptions are not to be trusted, much less honored, in their false and fraudulent coniectures which they vse, not in this alone, but in diuers other points of no small importance."

At the end of his circumnavigation of the world, Drake returned to England in 1580. Molyneux was a crewman on Drake's circumnavigation. We conjecture that they expressed Drake's displeasure to some cartographers because most cartographers later changed their maps. This conjecture is supported by Drake's written words

above, and the *Silver Map* of ca. 1588-89. These maps were stamped onto silver disks about 68 mm in diameter. A photograph of the western hemisphere of one of these is shown in Figure 5. Notice that the bulge on the coast of Chile has been removed. This map also shows Drake's route of circumnavigation with dotted lines.



Figure 5. The *Silver Map*, probably created in 1588-89. Only the western hemisphere is shown here.

The British Museum's two copies of the *Silver Map* are silver medals 68 mm in diameter (2.7 inches, about the size of a baseball) stamped with a map of the world showing Drake's route of circumnavigation with dotted lines. They were probably manufactured in 1588-89 [12]. Neither of these medals has a bulge on the southern coast of Chile. The face of one of them is shown in Figure 5. The Library of Congress also has two medals and lists the locations of all nine existing medals. [®] One of their medals has a cartouche in the ocean near Africa. This cartouche states that the medal's creator was Michael Mercator in 1589. The 1581 map by Van Sype was most likely published before these silver medals because, although it has the same route as Drake's circumnavigation, it still has the bulge on the coast of Chile. [®]

We suggest that Ortelius used information provided by Drake and/or Molyneux when he removed the bulge from the coast of Chile. Other people followed his lead.

3.5 Rotate the Azimuth of the Chilean Coast, AD 1587

We now have another problem to solve. Even if the bulge is gone, the coast of Chile is still wrong because on these maps the coast slopes northwest (Figure 4), instead of northeast (Figure 6).



Figure 6. Present-day South America in a Mercator map projection. The spacing between parallels and meridians is 15 degrees.

One of the cartouches on the Wright & Molyneux 1598 map states [13], "By the discoverie of Sir Francis Drake made in the yeare 1577 ... the southern coast of [South] America called Chili was found, not to trend to the northwestwards as it hath beene described but to the eastwards of the north ..."

The following maps do not have the bulge on the southern coast of Chile; however, they still have an average azimuth for the Chilean coast that is incorrectly west of north: Velho 1561, Gutiérrez & Cock 1562, Forlani 1565, Bertolli 1568, D. Teixeira 1573, Massa 1580, Lasso 1586, Plancius 1594, Vrient 1596, Lavanha & Teixeira 1597, and Hondius 1597.

At the same time that Ortelius removed the bulge from the coast of Chile, he also rotated the azimuth of his coastline between 52° S and 40° S latitude. He did this on his *American Sive* 1587 map by removing a section of Chile making the coast slope north or even northeast.

[®] Library of Congress, The Kraus Collection of Sir Francis Drake, http://hdl.loc.gov/loc.rbc/rbdk.d058a. the Silver Map traces to the Whitehall map, which disappeared in the seventeenth century. The Whitehall map, in turn, traces to Drake's journal that he gave to Queen Elizabeth upon his return. She promptly disappeared it.

⁽⁹⁾ The 1587 map in Hakluyt's publication of Petrus Martyr does not have the bulge on the coast of Chile. The libraries at Brown and Stanford Universities agree with the date on the map of 1587, which matches information on the map, such as the Amazon River being shaped like a giant snake. However, they then state that the creator of the original map was Peter Martyr who died in 1526, which was well before the existence of the bulge on the coast of Chile. This cartographer was clearly from a different era. For example, he did not have the islands of San Pablo, Isla de los Tiburones, S. Felix and S. Nabor, and his zero-longitude meridian was 20 degrees off from everyone else.

The resulting coastline has an average azimuth that is north or even *east* of north: Ortelius *American Sive* 1587, etc., Hondius 1595 and 1597, Wright & Molyneux 1598, and Ricci 1602. We were careful when calculating the azimuth of the coastline of Chile. We used the meridians of longitude because different map projections can be misleading.

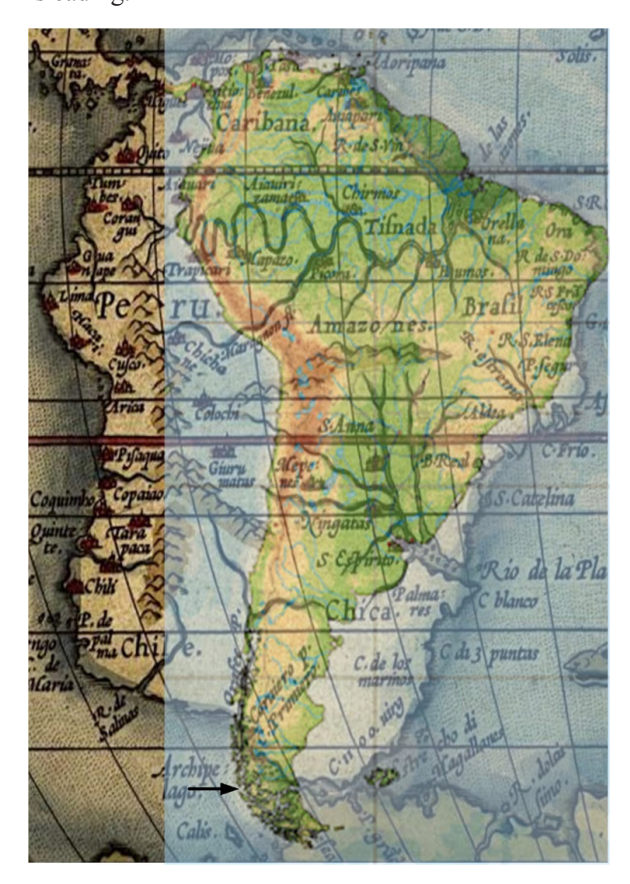


Figure 7. A present-day map of South America overlaid on the Ortelius 1570 *Typus Orbis Terrarum*. These maps were aligned using the north and northeast coasts of South America, the Equator, the Tropic of Capricorn, and the Straits of Magellan. The Pacific side exit for the Straits of Magellan is marked with a black arrow. These maps show that when Drake exited the Straits of Magellan, his maps told him to go Northwest and then West by North, however, he should have gone North and then North by East.

Maps began to show the modern shape of South America at the beginning of the seventeenth century. The southern coast of present-day Chile has an azimuth of 8° eastward from 45 °S latitude up to the Tropic of Capricorn. We now note that the southeast coast of Argentina and Brazil has an azimuth of 37° eastward from 45 °S latitude up to the Tropic of Capricorn. This then defines the shape of southern South America.

Our model for the shape of the southern part of South

America is that of a trapezoid as shown in Figure 8. The Pacific side has an azimuth of 8° and the Atlantic side has an azimuth of 37°. The northern side of this trapezoid is along the Tropic of Capricorn and is 50° of longitude wide (3173 miles). The southern side of this trapezoid is along the forty-fifth parallel and is 17° of longitude wide (1079 miles). Throughout the seventeenth century, most maps used this shape for South America.

The Wright & Molyneux 1598 map shown in the background of Figure 8 is close to our model with azimuths of 7° eastward and 42° eastward respectively. So its shape is good but it's South America is too wide.

The purpose of creating such a model is to allow quick easy comparison of a large number of charts. Just put the trapezoid on top of the map and you can quickly see how accurate the map is.



Figure 8. A portion of the Wright & Molyneux 1598 map *By the discouerie of Sr Francis Drake made in the yeare 1577* is in the background. Our model for South America is the red trapezoid.

3.6 Drop the Latitude of San Pablo and Isla de los Tiburones, AD 1589

Now we have another complication to resolve. Removing the bulge from the coast of Chile in 1587-1588 and redirecting the Azimuth of the coastline northward might have caused Ortelius to reconsider the route of Magellan in 1519-1522 and consequently the locations

of San Pablo and Isla de los Tiburónes. Their locations are important because no one had ever visited these uninhabited islands except for Magellan and his crew. And we do not know where these islands were. Therefore, information about their locations had to come from word of mouth, letters, texts, atlases, charts, and other maps, not from first-hand observations, measurements, or calculations. Ortelius dropped the latitude of these islands on his Maris Pacifici 1589 map (Figure 9) and his Typus Orbis Terrarum 1587 P3S1 (published 1592). Maps published before 1589 (for example Agnese 1541, Gastaldi 1546 and 1565, Forlani 1560 and 1565, Bertelli 1568, G. Mercator 1569, Ortelius TOT 1570 to 1587, R. Mercator 1587, Hondius 1589, and C. De Jode 1593) have San Pablo island at, on average, 15° S latitude and Tiburones at 9° S. Whereas maps published after 1589 (for example Ortelius 1589 Maris Pacifici, Plancius 1594, Hondius 1597 and Wright & Molyneux 1598) have San Pablo island at, on average, 21° S and Tiburones at 15° S. Ortelius instigated this shift but we do not know why he did it. Perhaps he did it because removing the bulge altered his concept of Magellan's route.

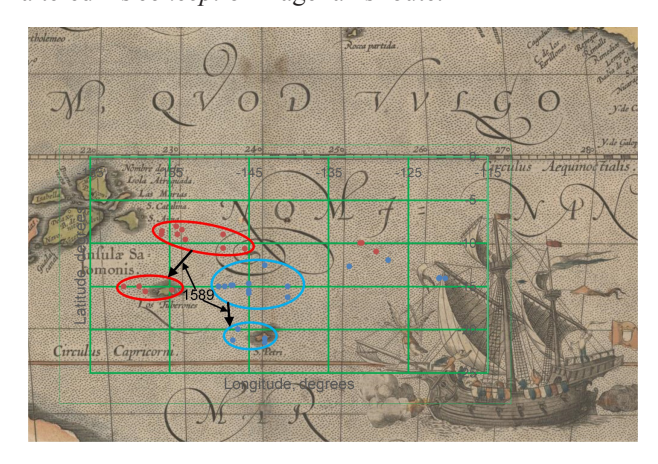


Figure 9. In this *Maris Pacifici* 1589 map, Ortelius lowered San Pablo island and Isle de la Tiburones by about six degrees in latitude. Others followed his lead as shown by the arrows between the ellipses. The numbers inside the green box in the Ariel font are present-day latitudes and longitudes. Magellan's ship the Victoria is being guided by the angel above its prow https://jcb.lunaimaging.com/luna/servlet/s/35yp7r

3.7 Traceability Analysis

Traceability is an important part of the Discovering System Requirements activity of the System Design process [14]. It has been used for decades in the field of system design and systems engineering. As far as we can tell, it has not been used in the field of geographic exploration and discovery. We have used processes from

this activity to trace the ancestry of sixteenth-century cartographers/maps. This section traces cartographers/maps based on toponyms (names of cities, rivers, bays, capes, mountains, etc.) and the visual appearance of objects on ancient maps.

In this section, we review previous material and organize it into the traceability diagram of Figure 10. The dates are not strictly chronological, because in the sixteenth-century information did not travel at the speed of the Internet.

At the start of our traceability analysis of sixteenth-century cartographers/maps, we refer to four maps that were made around 1544-1546 by Pereira, Cabot, Frisius, and Gastaldi (Figure 1). There is one prominent visual difference between them. The Pereira and Cabot maps have the Amazon River represented as a giant snake with its tail in the Andes Mountains and its head on the coast of the Atlantic Ocean ^[6] as shown in Figure 1. The Frisius map does not have this representation. For this and many other reasons, the Frisius map is not included in our traceability chart in Figure 10. The *Carta universal en que se* ... by Diego Ribero 1529 (Figure 2) also lacks the Amazon River, however, it has many other features such as a label for the Straits of Magellan that inclined us to include it in Figure 10. ⁽¹⁾

The ghost information flow path from the Pereira and Cabot box, which is the *Padrón Real* inside the *Casa de Contratación* in Spain, to Gastaldi's workshop in Genoa Italy is light gray. It would have been implemented with stolen documents.

We did not include all sixteenth-century cartographers in our traceability diagram. For example, cartographers in the Dieppe school in France made a series of world maps in the 1540s, 1550s, and 1560s, but they were not included in Figure 10. They had some similarities to these maps/cartographers, but no evidence of information flow.

We also omitted the Venetian cartographers Forlani, and Bertolli. They had similarities to these maps/cartographers, but not enough to include them in Figure 9. They formed an isolated branch. We have not proven a link between Forlani and Ortelius.

The same with Ruscelli. He was isolated in Venice. We cannot prove that Ortelius got his idea for the bulge on the southern coast of Chile from Ruscelli. We know

⁽¹⁾ The history books state that Cabot never explored the Amazon River, so Cabot probably got his information from Pereira and his cartographers and possibly from Diego Ribero's 1529 *Map of America*. Therefore, Ribero is included in our traceability chart of Figure 10. His map may be the first to label the Straights of Magellan. Ribero worked on the *Patron Real* (1508-1606) at the Casa de la Contratacion in Seville as did Pereira, Cabot, Diego Gutiérrez (father), Diego Gutiérrez (oldest son) and Sancho Gutiérrez (middle son).

that Ruscelli published his map about nine years before Ortelius. But we cannot prove causality. Also, we cannot prove that there were a group of cartographers who copied from Ruscelli. Whereas we have made a case that many cartographers copied from Ortelius.

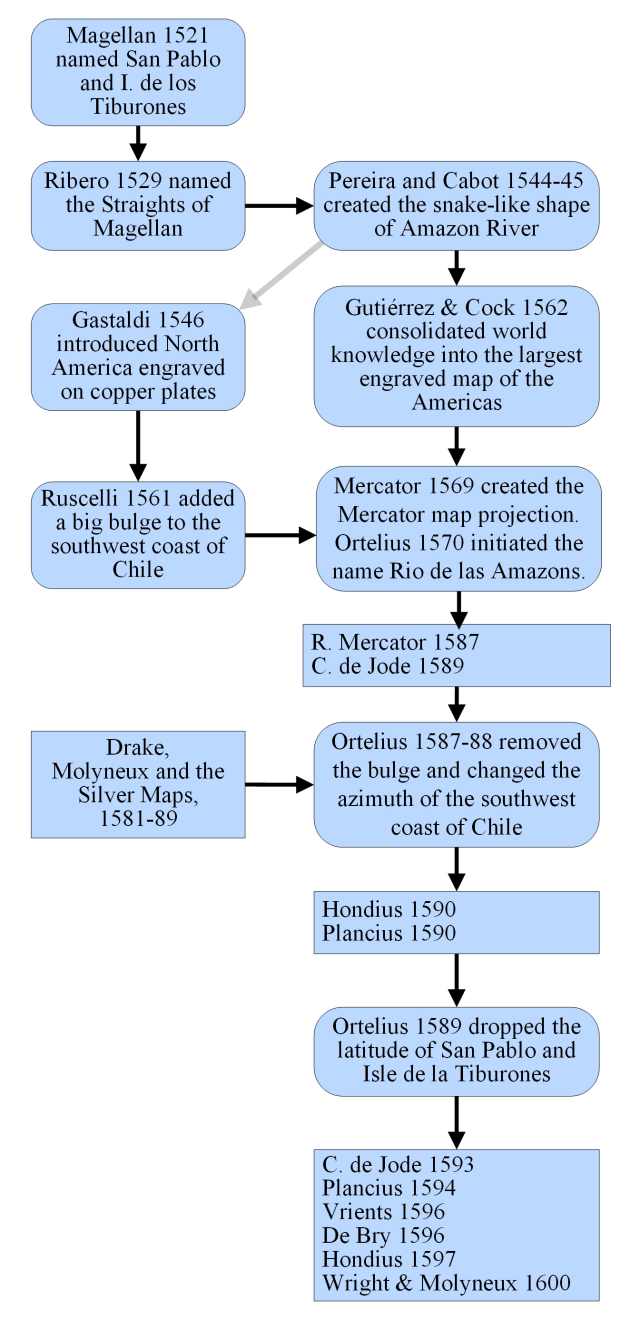


Figure 10. Traceability diagram for sixteenth-century cartographers/maps that contain South America. This diagram was derived from information on the maps themselves. Therefore, the dates are only approximations. Actions (verbs) are in boxes with rounded corners and objects (nouns) are in rectangles.

The following maps have visual appearances that are similar to each other but dissimilar to all other maps: R.

Mercator 1587, Plancius 1590 and 1594, Hondius 1592, M. Mercator 1595, De Bry 1596, and Vrients 1596. Some have a bulge on the coast of Chile and some don't. They have a distinct appearance because they used the Mercator bi-hemispheric stereographic projection function introduced by R. Mercator in 1587. It uses curved parallels of latitude. We considered map projection functions but did not use them elsewhere in this paper.

3.8 Synopsis

The following page or so summarizes sections 3.3 to 3.7 of this paper. In the early sixteenth century, world maps began to present the Pacific Ocean coasts of South and North America. Most subsequent maps were similar: they just added details. We found no lead-cartographer or school of cartographers that initiated these changes.

Then in 1561, Ruscelli made a dramatic addition. He added a big bulge on the southern coast of Chile. In the next four decades, dozens of other cartographers produced maps with similar erroneous bulges on the coast of Chile.

At the end of his circumnavigation of the world in 1580, Sir Frances Drake most certainly pointed out the error of the bulge on the southern coast of Chile.

The next important change in maps occurred in 1588 when Ortelius removed the bulge on the southern coast of Chile (*Typus Orbis Terrarum* P2S3). He also made this change on his 1587 *Americae sive* map. Again everyone followed suit. After 1587-1588 some cartographers continued to publish maps with the bulge, for example, M. Mercator 1595. Others followed Ortelius' lead and removed the bulge on the southern coast of Chile, including the *Silver Maps* of 1588-1589.

At the same time, Ortelius realigned his coastline of Chile to make it north rather than northwest. The other cartographers followed. Ortelius modified his coastline so that from 52° S latitude to 40° S it had an azimuth of due north or perhaps slightly northeast. Once again Ortelius seems to have been the leader in taking out the westward lean of the Chilean coast.

On his *Maris Pacifici* 1589 map and his *Typus Orbis Terrarum* 1587 P3S1 (published in 1592) Ortelius dropped the latitude of San Pablo and Isla de los Tiburones about six degrees each: again the whole group of cartographers followed him. Maps published before 1589 have San Pablo island at, on average, 15° S latitude and Isla de los Tiburones at 9° S. Whereas maps published after 1589 have San Pablo island at, on average, 21° S and Isla de los Tiburones at 15° S (Figure 9).

The first cartographer to name the Amazon River was Cabot 1544, who wrote: "Río de las amazona descubrio Francisco de orillana" (River of the amazon discovered



Figure 11. Rumold Mercator 1587 Orbis Terrae Compendiosa Descriptio

by Francisco de Orellana) [15]. The *river* is not named on the Pereira 1545 and L. Homen 1554 maps: instead, the province is named [15]. Cabot was followed by Sancho Gutiérrez 1551 who wrote "El Río ... amazonae," Velho 1561 who labeled it "Río de sa iohan de las amazonas" (River of Saint John of the Amazons) and Gutiérrez & Cock 1562 who labeled it "El grand rio de las amasons" (The grand river of the Amazons). Ortelius 1564 labeled it "Río de las Amasona sive Oregliana." Later, Ortelius 1570 shortened this to "Río de las amazons" (River of the Amazons). Some of these are shown in Figure 2.⁽¹⁾ On this map, in the ocean next to the mouth of the river, the equator cuts between the words "Rio" and "de las" and between "Am" and "azones." This name and partitioning were then used on maps by R. Mercator 1587, Hondius 1590, Plancius 1590 and 1594, DeBry 1592 and 1596, and Vrients 1596. This same name with a different partitioning was used by C. de Jode 1589, Hondius 1597, and Wright & Molyneux 1598.

In 1540-1542 Francisco Vázquez de Coronado et al. journeyed through what is now New Mexico. They encountered many Native-American cities and villages, such as Tuchana, Quivira, Cicuic, and Tiguex. These names were probably attempts by Coronado to write in Spanish Native-American names that were only *spoken*

by Native Americans. Later, the cartographers Ortelius 1564, Gastaldi 1565, Forlani 1565, and Bertelli 1568 spread these cities across the American west on their maps. In 1569-1570, Mercator and Ortelius moved these cities to the Pacific coast of North America. Dozens of cartographers followed their lead.

In 1589 Ortelius made a major change that was not immediately followed by other cartographers. Ortelius removed the cities with Native-American-sounding names: Tuchana, Quivira, Cicuic, and Tiguex from his *Maris Pacifici* 1589 map. He left Quivira as a region, however. Other cartographers did not follow his lead right away. A possible reason may be that he did not remove these cities from his *Typus Orbis Terrarum* maps. Tuchana, Cicuic, and Tiguex lasted on other maps into the second decade of the seventeenth century before disappearing.

In his Americae sive 1587 map, Ortelius added the islands of S. Felix and S. Nabor. Of course, each successive edition of this atlas also had this same map. Subsequently, C. de Jode 1593 *Brasilia et Peruvia* and Mercator & Hondius 1608 *Americae Descrip* also had these islands. Much later Claes Janszoon Visscher's 1650, map had them labeled S. Felix and S. Ambrosio. So, adding these islands did not immediately develop a lot of followers.

Ortelius developed the concept of an atlas. This is our eighth unique action by Ortelius. Before Ortelius, maps were designed, made, sold, and used separately. But in 1570, Ortelius published the first modern atlas of maps.

① If the letters are too small in this journal paper then see http://sysengr.engr.arizona.edu/URLsForSixteenthCenturyMaps.xlsx. This list contains URLs for high-resolution original maps that are mostly in the public domain: that is, they are free of known restrictions under copyright law.

It was a collection of uniform map sheets and supporting text bound together to form a book. Copper plates were specifically engraved for the maps. This book was 37.5 by 50.5 cm (14.5 by 19.6 inches). It contained 70 maps on 53 sheets. It went through over twenty editions in four languages. It was followed by atlases by Gerard de Jode in 1578 and M. Mercator in 1595.

These eight actions (adding and removing the bulge on the southern coast of Chile, rotating the coast of Chile, 'moving' San Pablo and Isla de los Tiburones, naming the Rio de las Amazons, removing the cities with Native-American sounding names, adding the islands of S. Felix and S. Nabor, and creating an atlas) indicate that Ortelius was the leader and a dozen or more cartographers followed his lead.

This information is summarized in the traceability diagram of Figure 10 and Table 2. To be included in this diagram the specified map must have had most of the eight actions listed above. The blue shaded cells in Table 2 show abrupt changes in features. Time runs roughly from left to right.

4. Discussion

In keeping with our policy of using only information contained in the maps themselves, we now speculate that the cartographers Ortelius, G. Mercator, R. Mercator, M. Mercator, C. de Jode, Plancius, Hondius, De Bry, Vrients, and Molyneux formed a clique and shared common knowledge that was not necessarily in their published atlases or maps mentioned in this paper. We formulated this concept of a clique based on the maps. We did not rely on (1) historical texts, (2) sixteenth-century family, friendship and religious relationships, language, geographical location, or professional feuds, or (3) present-day human biases, speculation, and mistranslations.

In breaking with our policy of using only information contained in the maps themselves, we can observe that we have no maps with a bulge on the coast of Chile that was created by Spanish cartographers. This was unexpected because the Spanish were the only ones sailing the Pacific Ocean in the sixteenth century: it was a 'Spanish lake.' This could have been caused by the requirement that all Spanish maps are reconciled with the *Patron Real* (the master map) at the *Casa de la Contratacion* in Seville. This may have helped them avoid the mistake of the bulge on the coast of Chile. (I do not classify Martinis 1582 as Spanish.)

4.1 A Fly in the Ointment

Our results have shown that Ruscelli was the originator of the big bulge on the southern coast of Chile. His 1561 *Orbis Descripto* map (Figure 3) was the first map to show

de Jode 1593, Brasilia et Peruvia C. de Jode, 1589, Totis Orbis Terrae Ortelius, 1589, Maris Pacifici 1599 Ortelius, 1588, TOT P2S3 Ortelius 1587, Amer sive Ortelius, 1570 *TOT M. Mercator, 1595 G. Mercator, 1569 R. Mercator, 1587 Wright & Molyneux, Plancius, 1594 Hondius, 1590 Hondius, 1597 Vrients, 1596 DeBry, 1596 Plancius, Ortelius' Actions $\sqrt{}$ Include the bulge on the coast of Chile Remove the bulge on the coast of Chile Rotate the coast of Chile northeast $\sqrt{}$ $\sqrt{}$ No No No No No No $\sqrt{}$ $\sqrt{}$ Draw San Pablo at 15° S and Tiburones $\sqrt{}$ V at 9° S Drop the latitude of San Pablo to 21° S $\sqrt{}$ $\sqrt{}$ $\sqrt{}$ $\sqrt{}$ $\sqrt{}$ and Tiburones to 15° S Represent the Amazon River as a giant $\sqrt{}$ $\sqrt{}$ No No snake Use the name Rio de las Amazons $\sqrt{}$ $\sqrt{}$ $\sqrt{}$ No $\sqrt{}$ $\sqrt{}$ $\sqrt{}$ $\sqrt{}$ No $\sqrt{}$ $\sqrt{}$ $\sqrt{}$ $\sqrt{}$ Contain cities with Native-American- $\sqrt{}$ $\sqrt{}$ No sounding names Include the islands S. Felix and S. Nabor No No No $\sqrt{}$ No No No No *TOT stands for Typus Orbis Terrarum. Checkmarks ($\sqrt{}$) mean yes, No means No, and blanks mean no data is available or the cell is not applicable

Table 2. Major changes in the evolution of sixteenth-century world maps

this bulge. The date is verified because this map was published in his atlas of 1561.

However, there is a slight problem here because the Forlani 1562 *La Descrittione* (Figure 12) and the Gastaldi and Some Others 1562-65 maps also have big bulges on their southern coasts of Chile. Furthermore, these maps were probably created at about the same time.

The Forlani map is straightforward and is shown in Figure 12. However, the Gastaldi and Some Others 1562-65 *Cosmographia Universalis et Exactissima* map would not reproduce well in a journal. So it requires some explanation.

The text at the bottom of the *Cosmographia Universalis* et *Exactissima* ... map indicates its creators as "... Gastaldio Nounullisque Aliis ...," which translates as "Gastaldi and Some Others ..." Therefore we will refer to this map as Gastaldi and Some Others 1562-65. We do not know which sections of this map were created by which authors. So its authorship is fuzzy.



Figure 12. Forlani 1562, *La.Descrittione. di. Tutto.ll. Peru.*

The bulge on the Forlani 1562 map is identical to that on the Gastaldi and Some Others 1562-1565 map. Also, both maps have the same inconsistent shadows on the cartouches. So Forlani was probably responsible for the portion of the Gastaldi and Some Others 1562-1565 map

that included South America. However, Forlani did not engrave this bulge on any of his other maps, e.g. Forlani 1560, 1562b, 1565, 1568, or 1570.

Looking further at the Gastaldi and Some Others 1562-1565 map we see about twenty animals spread across a large Antarctic continent. Some are real, like the wolf, elephant, lion, grasshopper, and armadillo, and some are mythical like the unicorn and the griffin. These animals are similar to the twenty on the map of Forlani 1565 (Figure 13) in looks and placement. The obvious conclusion, therefore, is that Frolani was responsible for the animals in Antarctica and the bulge on the coast of Chile on the Gastaldi and Some Others 1562-1565 map. Both of these maps have about a dozen ships and a dozen sea monsters. However, the ships and sea monsters are different on the two maps.

There is also some fuzziness here about the date of the Gastaldi and Some Others 1562-65 map because the map has little documentation. The Bibliothèque nationale de France (BnF) dates it from 1539 to 1565. Shirley ^[9] dates it as 1561 conjectured on a rare booklet published sometime around 1562.

So the authorship and date of this map are fuzzy. However, it still seems that this map was created after Ruscelli's.

The bulges on the coast of Chile on the Forlani 1562 La Descrittion and Gastaldi and Some Others 1562-65 maps are huge. They make South America diamond-shaped (Figure 12). See also Tommaso Porcacchi 1572, Discorso Intorno alla Carta da Navigare. These bulges extend from the Straights of Magellan all the way up to the Equator. Their sizes average 365 degrees squared. In contrast, the other big bulges listed in Table 1 are completely below the Tropic of Capricorn and have an average area of only 150 degrees squared ($\sigma = 80$). Therefore, the big bulge of Forlani does not seem to have been copied by later cartographers. He did not even include it in his own subsequent maps.

In summary, the Ruscelli 1561 *Orbis Descripto* map not only preceded the Forlani 1562 *La Descrittione* and the Gastaldi and Some Others 1562-65 maps but it was also the map followed by other cartographers for the next 27 years with regard to the bulge on the coast of Chile.

4.2 Area for Future Research

We were not successful in determining why the bulge was added to and removed from the southern coast of Chile. We searched the English language translation of Ortelius' *Theatrum Orbis Terrarum* looking for an explanation for the appearance and removal of the bulge but found none: perhaps the 1588 Latin version has an

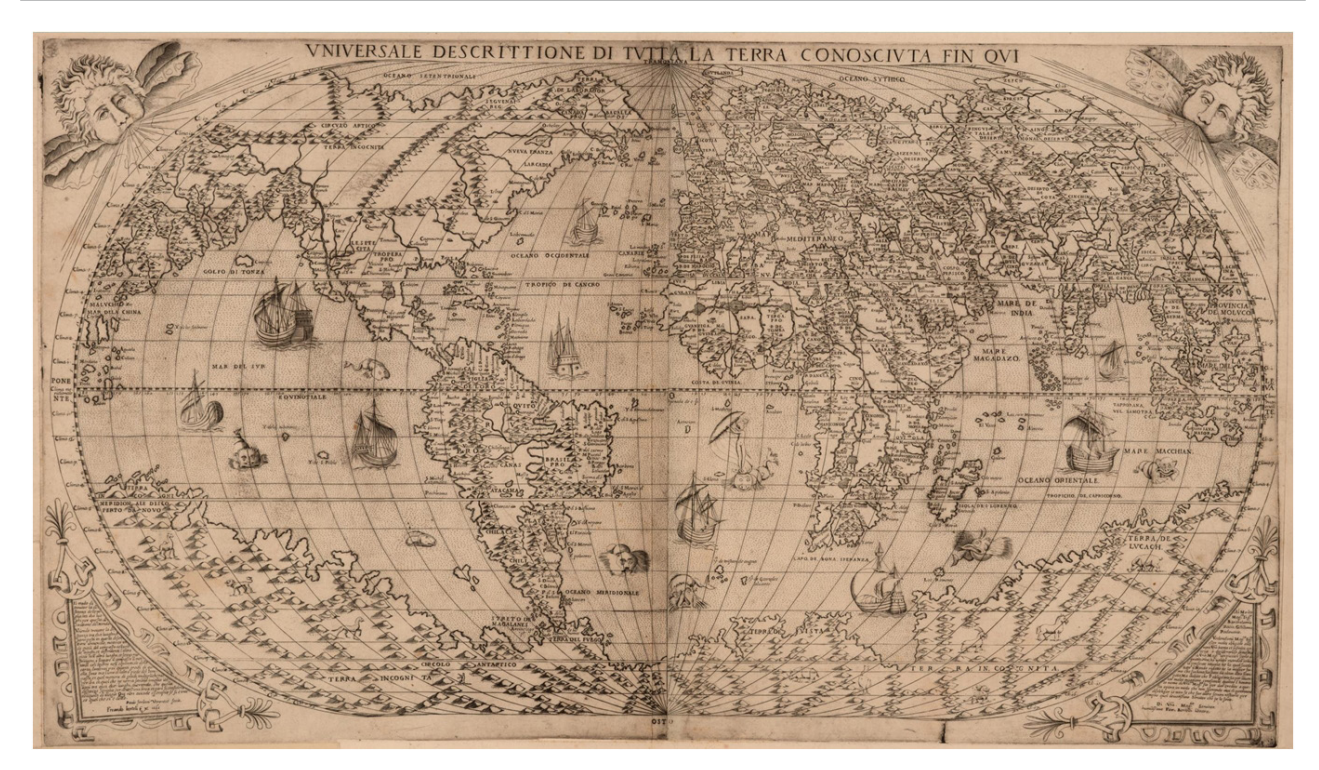


Figure 13. Paolo Forlani 1565 P3S2 *Universale Descrittione Di Tutta la Terra Conosciuta Fin Oui*. Note that (1) Antartica is very large, (2) there are 20 animals in Antartica and (3) there is no bulge on the coast of Chile.

explanation. Likewise, there could be an explanation for the addition of the bulge in Ruscelli's Italian language atlas of 1599, Geografia di Claudio Tolomeo Alessandrino, tradotta di greco nell'idioma volgare italiano da Girolamo Ruscelli.

5. Conclusions

In the first half of the sixteenth century, world maps began to appear that contained the Pacific Ocean coasts of South and North America. Most subsequent maps were similar. The cartographers just added details over the years. Then in 1561, Ruscelli made a unique addition. He added a big bulge on the southern coast of Chile. In 1569-70 Mercator and Ortelius added bulges on *their* southern coasts of Chile. Dozens of cartographers followed their lead and produced maps with a bulge on the southern coast of Chile.

Using the information given to him after Drake circumnavigated the world, Ortelius removed the bulge from his *Typus Orbis Terrarum* 1588 and realigned the coast of Chile on his *Americae sive* 1587 and his *Maris Pacifici* 1589 maps. Again most cartographers followed suit

At about this same time Ortelius also dropped the latitude of San Pablo and Isla de los Tiburones about six degrees: a whole group of cartographers followed him.

The first cartographer to name the Amazon River

was Cabot 1544, named it the "River of the Amazon discovered by Francisco de Orellana." Ortelius 1570 shortened this to "River of the Amazons." Dozens of cartographers followed suit.

These eight actions (adding and removing the bulge on the southern coast of Chile, rotating the coast of Chile, 'moving' San Pablo and Isla de los Tiburones, naming the Amazon River, removing the cities with Native-American sounding names, adding the islands of S. Felix and S. Nabor, and creating an atlas) indicate that Ortelius was the leader and dozens of cartographers followed his lead.

In the sixteenth century, on printed world maps containing South America, a bulge four times the size of Spain appeared on the southern coast of Chile. Ruscelli first created this bulge. No one knows why, and no one back then questioned it. But dozens of cartographers followed his lead. Then 27 years later, without explanation, Ortelius removed the bulge from the coast of Chile. All cartographers followed his lead and soon the phantom bulge was gone forever.

Conflict of Interest

The author has no conflicts of interest.

Funding

This research received no external funding.

Ethical Approval

No ethical approval was necessary.

References

- [1] Becharius, F., 1403. Francischus becharius cuius lanue [con]posuit, Genoa, Yale University, Beinecke Library. This is a Portolan chart.
- [2] Valjarević, A., 2020. The Size of the Ecumene of the Mediterranean in Ancient Times. Journal of Geographical Research. 3(4), 1-7. DOI: https://doi.org/10.30564/jgr.v3i4.2030.
- [3] Nunn, G.E., 1934. Magellan's route in the pacific. Geographical Review. 24(4), 615-633.DOI: https://doi.org/10.2307/208851.
- [4] Albo, F., 1874. Logbook of Francisco Albo, in Antonio Pigafetta, The First Voyage Round the World, translated by Lord Stanley of Alderley, London, https://en.wikisource.org/wiki/The_First_Voyage_Round_the_World/Logbook_of_Francisco_Alvo_or_Alvaro
- [5] Cortesao, A., 1939. António Pereira and His Map of Circa 1545: An Unknown Portuguese Cartographer and the Early Representation of Newfoundland, Lower California, the Amazon, and the Ladrones. Geographical Review. 29(2), 205-225.
- [6] Bahill, A.T., Gitzen, G.D., 2021. The Amazon River Modeled as a Giant Snake, KN - Journal of Cartography and Geographic Information. 71(3), 173-194. DOI: https://doi.org/10.1007/s42489-021-00082-3.
- [7] Hébert, J.R., 2021. The 1562 Map of America by Diego Gutiérrez, Library of Congress, https://www.loc.

- gov/rr/hispanic/frontiers/gutierrz.html
- [8] Van den Broecke, M., Van den Broecke-Günzburger, D., 2021. Cartographica Neerlandica. http://www. orteliusmaps.com/index.html This is presumably the biggest collection of Ortelius maps.
- [9] Shirley, R.W., 1983. The Mapping of the World: early printed world maps 1472-1700, London, Holland Press. This is the 'bible' of sixteenth and seventeenth-century nautical world maps. pp. 145.
- [10] Wallis, H.M., 1951. The first English globe: A recent discovery, The Geographical Journal. South America is two pages after page 282. Stable URL: https:// www.jstor.org/stable/1791852. 117, 275-290. DOI: https://doi.org/10.2307/1791852.
- [11] Drake, F., 1628. *The* World Encompassed by Sir Francis Drake. https://archive.org/details/worldencompassed16drak/page/n14. pp. 46.
- [12] Christy, M., 1900. The silver map of the world a contemporary medallion commemorative of Drake's great voyage (1577-80) a geographical essay... H. Stevens, son, & Stiles in London.
- [13] Gitzen, G.D., 2014. Edward Wright's World Chart of 1599, *Terrae Incognitae*; The Journal of the Society for the History of Discoveries. 46(1), 3-15.
- [14] Bahill, A.T., Madni, A.M., 2017. Discovering Systems Requirements, Chapter 4 in Tradeoff Decisions in System Design, Switzerland, Springer International Publishing.
- [15] Bahill, A.T., 2021. The Second Engraver of the Library of Congress Mystery Map, International Journal of Cartography.
 - DOI: https://doi.org/10.1080/23729333.2021.1988042

Appendix

Literature Review

Table 3. Maps that are mentioned in this paper. They are listed in alphabetical order by the last name of the cartographer. URLs for these maps can be found at http://sysengr.engr.arizona.edu/URLsForSixteenthCenturyMaps.xlsx.

Cartographer	First Year Published	Title of Map		
Agnese, Battista	1541	Nautical Atlas of Battista Agnese		
Anonymous	1588-89	Silver Map		
Becharius, Franciscus	1403	Francischus becharius cuius lanue [con]posuit		
Bertelli, Donato	1568	Universale Descrittione Di Tutta la Terra Conosciuta Fin Qui.		
Belleforest, François de	1575	Typus Orbis Terrarum		
Cabot, Sebastian	1544	World Map of A. D. 1544 (The Sebastian Cabot Map)		
De Bry, Theodor	1592	Americae Pars Magis Cognita		
De Bry, Theodor	1596	America Sive Novus Orbis Respectu Europaeorum Inferior Globi Terrestris		
De Bry, Theodol		Pars		
De Jode, Cornelius	1589	Brasilia et Peruvia		
De Jode, Cornelius	Dated 1589, published	Totius Orbis Cogniti Universalis Descriptio		
De Jode, Comenus	1593			
De Jode, Gerard	1578	Americae Peruvi aque ita ut post		

Descelier, Pierre	1550	Chart of the Atlantic and Indian Oceans
Forlani, Paolo	1560	Paulus de furlanis Veronensis opus hoc exmi Cosmographi
Forlani, Paolo	1562	La.Descrittione. di. Tutto.ll. Peru
Forlani, Paolo	1565	Universale Descrittione Di Tutta la Terra Conosciuta Fin Oui,
Frisius, Gemma	1544	La Cosmographie de Peter Apian
Gastaldi, Giacomo	1546	Universalet
Gastaldi, Giacomo	1548	Universale Novo
Gastaldi, Giacomo, and Some Others	1562-65	Cosmographia Universalis et Exactissima
Gastaldi, Giacomo	1565	Universale della parte
Gutiérrez, Diego & Cock, Hieronymus	1562	Americae Sive Quartae Orbis Partis Nova et Exactissima Descriptio
Gutiérrez, Sancho	1551	Esta Gerale en plano hizo Sancho Gutierrez Cosmographo
Hakluyt, Richard	1589	Typus Orbis Terrarum
Homen, Diogo	1558	A América meridional
Homen, Diogo	1565	Coastline of South America
Homen, Lopo	1554	Nautical mappamundi in four sections
Hondius, Jodocus	1589	America Novissima Descripto
Hondius, Jodocus	1590	Nova Universi Orbis Descripto
Hondius, Jodocus	1595	Vera totius expeditionis nauticæ: descriptio D. Franc. Draci.
, in the second		Typus Totius orbis Terrarum in Quo
Hondius, Jodocus	1597	(The Christian Knight map)
Janszoon, Claes	1650	None
Le Testu, Guillaume	1556	Cosmographie Universe
Van Langren, Arnold	1596	Orbis terrae compendiosa descriptio
Lasso, Bartolomeu	1586	Portugaliae Monumenta Cartographica
Lavanha, João & Teixeira, Luís	1597	Atlas-cosmografia
Martines, Joan	1587	Portolan chart of South America
Martyr, Petrus	1587	Novus Orbis (Map of the New World)
Massa, Giovanni	1580	America et Proximar Regionumorae Descriptio
Mercator, Gerard	1569	Nova et Aucta Orbis Terrae descriptio,
Mercator, Michael	1595	America sive India Nova
Mercator, Rumold	1587	
Mercator, Gerard & Hondius, Jodocus	1608	Orbis Terrae Compendiosa Descriptio
		Americae Descrip
Monte, Urbano	1587	Planisphere of 1587
Molyneux, Emery	1592	The Petworth Globe
Munster, Sebastian	1588	Die erst GeneralTafel die Beschreibung Nova Totius Terrarum Orbis iuxta
Ortelius, Abraham	1564	Typus Orbis Terrarum Typus Orbis Terrarum
Ortelius, Abraham	1570	71
Ortelius, Abraham	1587	Americae sive novi orbis nova descriptio
Ortelius, Abraham	1587 P2S2	Typus Orbis Terrarum
Ortelius, Abraham	1588 P2S3	Typus Orbis Terrarum
Ortelius, Abraham	1589	Maris Pacifici
Pereira, Antonio	1545	Early representation of Newfoundland, Lower California, the Amazon, and to
		Ladrones
Plancius, Petrus	1590	Orbis Terrarum Typus de Integro
Plancius, Petrus	1594	Orbis Terrarum Typus de Integro
Ribero, Diego	1529	Carta universal en que se contiene todo lo que del mundo
Ricci, Matteo	1602	Kun Yu Wan Guo Quan Tu
Ruscelli, Girolamo	1561	Orbis Descriptio
Ruscelli, Girolamo	1562	Tierra Nova
Ruscelli, Girolamo	1599	Orbis Terrae Compenduiso Descriptio
Ruscelli, Girolamo	1599	Geografia di Claudio Tolomeo Alessandrino, tradotta di greco nell'idioma volgare italiano da Girolamo Ruscelli
Van Sype, Nicola	1581	La Herdike Enterprinse Faict Par Le Signeur Draeck D'Avoir Cirquit Toute I Terre
Teixeira, Domingos	1573	World map
Thevet, André	1575	Le Nouveay Monde Descuvert
Tramezzino, Michele	1554	Wereldkaart in twee halfronden
Velho, Bartolomeu	1561	Mapa de Bartolomeu Velho
Vrient, Jan Baptists	1596	Orbis terrae compendiosa descriptio ex peritissimorum
Wright, Edward & Molyneux, Emery	1598	By the discouerie of Sr Francis Drake made in the yeare 1577



Journal of Geographical Research

https://ojs.bilpublishing.com/index.php/jgr

ARTICLE

Assessment of Urban Morphology through Local Climate Zone Classification and Detection of the Changing Building States of Siliguri Municipal Corporation and Its Surrounding Area, West Bengal

Ivana Hoque * Sushma Rohatgi

Department of Geography and Applied Geography, University of North Bengal, West Bengal, India

ARTICLE INFO

Article history

Received: 05 January 2022 Revised: 17 February 2022 Accepted: 25 February 2022 Published Online: 03 March 2022

Keywords:

LCZ classification Urban land cover

SMC

Changing urban building types

ABSTRACT

Progressive population concentration in the urban centres has fuelled urban expansion in both horizontal as well as vertical directions, with consequences in the urban landscape change. This growth resulted in posing many complexities towards sustainable urban development which can be counted by observing the changing proportions of natural landscapes and built up areas. Local climate zones (LCZs), a systematic classification of natural lands and built up lands, are identified in Siliguri Municipal Corporation (SMC) and its surrounding region to explore the spatio temporal complexity of urban growth in recent years. Rapid urbanization and population growth of SMC have led to changes in the building states from low-rise to mid and high-rise which added an important feature to the urban landscape dynamics of the area. The work intends to provide the vision of the spatial urban morphology of the area through the investigation of its changing land use and changing urban built space using the LCZ classification. The study shows that the WUDAPT method can accurately generate LCZs, especially the built type LCZs. The results of the proposed LCZ classification scheme are tested using an error matrix for the years 2001 and 2021 having coefficient values of 0.79 and 0.81 respectively. The study explores the changing pattern of building states of SMC using LCZ products, which is essential for proper urban planning implementations.

1. Introduction

Urban growth incorporates both horizontal and vertical expansion through its complex spatio temporal process. With the physical expansion of built up land internal urban morphology also altered. In the context of rapid urban

growth and limited territories, a new approach is needed for urban space planning through vertical construction [1]. Building distribution patterns, especially the upward growth of buildings can significantly transform urban built up morphology with compact rise, open rise and sparsely built areas [2]. This urges the need to study the

Ivana Hoque,

Department of Geography and Applied Geography, University of North Bengal, West Bengal, India;

Email: ivana01102009@gmail.com

DOI: https://doi.org/10.30564/jgr.v5i2.4329

Copyright © 2022 by the author(s). Published by Bilingual Publishing Co. This is an open access article under the Creative Commons Attribution-NonCommercial 4.0 International (CC BY-NC 4.0) License. (https://creativecommons.org/licenses/by-nc/4.0/).

^{*}Corresponding Author:

complexities of horizontal as well as vertical urban growth of cities in the field of urban analysis. In developing countries' morphological unevenness can be vividly noticed in the town and cities were parts of the city is comprised of concrete and metal structured medium and high-rise buildings, metallic pavements, parking lots and parts of the city are still composed of low-rise buildings constructed of mud, tin and semi concrete materials that are compact or sparsely arranged with open and green space [3]. So it is necessary to quest the differences in the urban landscape at a local scale. A universal scheme of the local climatic zone was suggested by Stewart and Oke to characterise and capture this shot of micro level variations within the entire urban landscape [4].

A number of urban classification schemes such as Urban Terrain Zone (UTZ), Urban Climate Zone (UCZ) have been developed to facilitate knowledge in urban studies [5,6]. The previous classification of Oke on Urban Climatic Zone (UCZ) has been expanded and improved through LCZ scheme to make a standardised classification of the 'urban' and 'rural' (or built and land cover classes) landscapes [4]. Local climate zones are defined by Stewart and Oke as "regions of uniform land cover, surface structure, construction material and human activity that span hundreds of meters to several kilometres on a horizontal scale". It is a more effective classification system to study the spatial characteristics of landscapes on a local scale that fall in the category of 'urban' and 'rural'. LCZ mapping is considered the first step in the development of urban climate maps that contain information on the spatial distribution of land use classes [7]. Large extents of research works have applied the classification scheme for extracting the LCZ classes in their target regions [8-12]. The outcomes from the application of this process can be applied as input data for urban planning purposes. LCZ classification scheme has been applied to many cities of the world to classify urban surface conditions based on remote sensing data and primary observations [13]. A complex urban scenarios can be differentiated through analysis of the dissimilarity of textures of different urban LCZ types using high resolution satellite data set [14]. The findings of the case study of Hong Kong provide an in-depth understanding of different LCZ mapping methods and their advantages and limitations [9]. Zheng et al. examine the spatial sensitivity and spatial characteristics of LCZ classification in Hong Kong and establish the LCZ database [15]. The results of LCZs scheme can be implemented for modelling and mapping of intra urban structures based on various geometric properties [16-18]. The study by Ren et al. examines the relationship between socio economic status and LCZ products of the cities of China, essential for further implementations and urban growth monitoring [19].

Most of the previous studies attempted to explore the transformation of an urban landscape with the rapid transformation of LULC [20-22]. But LULC changes can only provide the horizontal transformation of the landscape. It fails to capture the vertical transformation which is an integral part of urban landscape study and that can be well understood in local climatic zones. The subdivision within the built up land can accurately determine the changes of built up types from sparse lowrise to compact high density high-rise built up land [23]. The LCZ classification scheme can provide distinct and unique partitions of landscapes that cover major urban forms and land cover types. In this context, LCZs provide a great potentiality to explore changing dynamics of the urban landscape in response to changing LULC and the inter categorical transformation of building states. In developing countries, information related to urban morphological characteristics remains scarce where the heterogeneous complex urban surface characteristics needed to be monitored. Various studies successfully incorporated WUDAPT method to derive LCZ maps in the cities having a homogeneous built surface with planned development [24-26]. But there are few studies of LCZ mapping in the cities of developing countries with heterogeneous built form having mixed urban fabric [26,27]. Those countries where land use information is not readily available are needed to generate LCZ classification results to meet the planning requirements of urban areas [9]. LCZ data sets can be developed from generalised knowledge of built forms and land cover types to enhance their usefulness especially in data poor but rapidly changing tropical cities [27]. So geospatial technologies should be adopted by the planners and scientists of those countries to enhance the understanding of urban forms of cities and promote sustainable urban development [28]. Documentation and presentation of proper data to describe the specific local features of urban built form in Indian cities are less in number. Most Indian cities are characterised by heterogeneous types of built form. The complex urban form and data inefficiency of such cities pose difficulties in the identification and classification of LCZ [29]. They have detected the variations in built LCZ classes in Nagpur, India, as a result of the intermi of compact lowrise areas with slums and squatters.

In recent years upward construction has become inevitable with the rapid population increase in the major cities of India to fulfil the growing demand for housing and Siliguri is none the exception. Siliguri Municipal

Corporation (SMC) is undergoing significant demographic growth and economic development hence, experiencing rapid conversion of its land use land cover pattern and built up forms. A number of high-rise multi storied complexes have come up both in SMC and its surrounding areas, as it tries to adjust its population pressure and land scarcity which added a new dimension its built up scenario. Expansion of the city brings changes in the land use and land cover (LULC) pattern, affecting its spatial characteristics. Being a town located near the Himalayan mountain region, high-rise construction was restricted in Siliguri. But after 2011, as high-rise constructions became permissible (The West Bengal Municipal building rules, 2008), the built up scenario of Siliguri has changed rapidly with the increasing number of high-rise buildings. To maximise the development potentials mid-rise and high-rise building development is adopted in SMC urban areas. The areas around the railway station considered the central business district, characterised by high density with mid to high-rise structures, have adversely affected the area under green cover and open spaces (City development plan for Siliguri-2041).

The city requires proper identification of the arrangement of built space associated with urban development for giving a proper direction to the growth and urbanization process. To meet this requirement the study employs the classification scheme of 'Local Climatic Zones' to conduct a spatiotemporal analysis of changing LULC condition and built up types of Siliguri and its surrounding area. No studies have yet been done to analyze the internal urban morphology and building alteration process using the LCZ scheme in SMC. So it is essential to investigate the spatial characteristics of urban land systematically in the context of the urban the predominance of SMC for the future implication of suitable policies in North Bengal.

Hence, the present study aims i) To delineate the local climate zones and identify the built up types and natural land cover types of SMC and its surrounding. ii) To investigate the change and alteration of building states in Siliguri Municipal Corporation through the output of LCZ classification scheme. The study tries to develop a local climate zone classification map using spatial data obtained from Landsat images in remote sensing and GIS environment to analyse urban morphology and establish the association between urban growth and the internal variations of building states within the city. This will ultimately help in understanding the local complexities in growing urban land and meeting the future planning

requirements of the city by balancing the proportion of land use and land cover types.

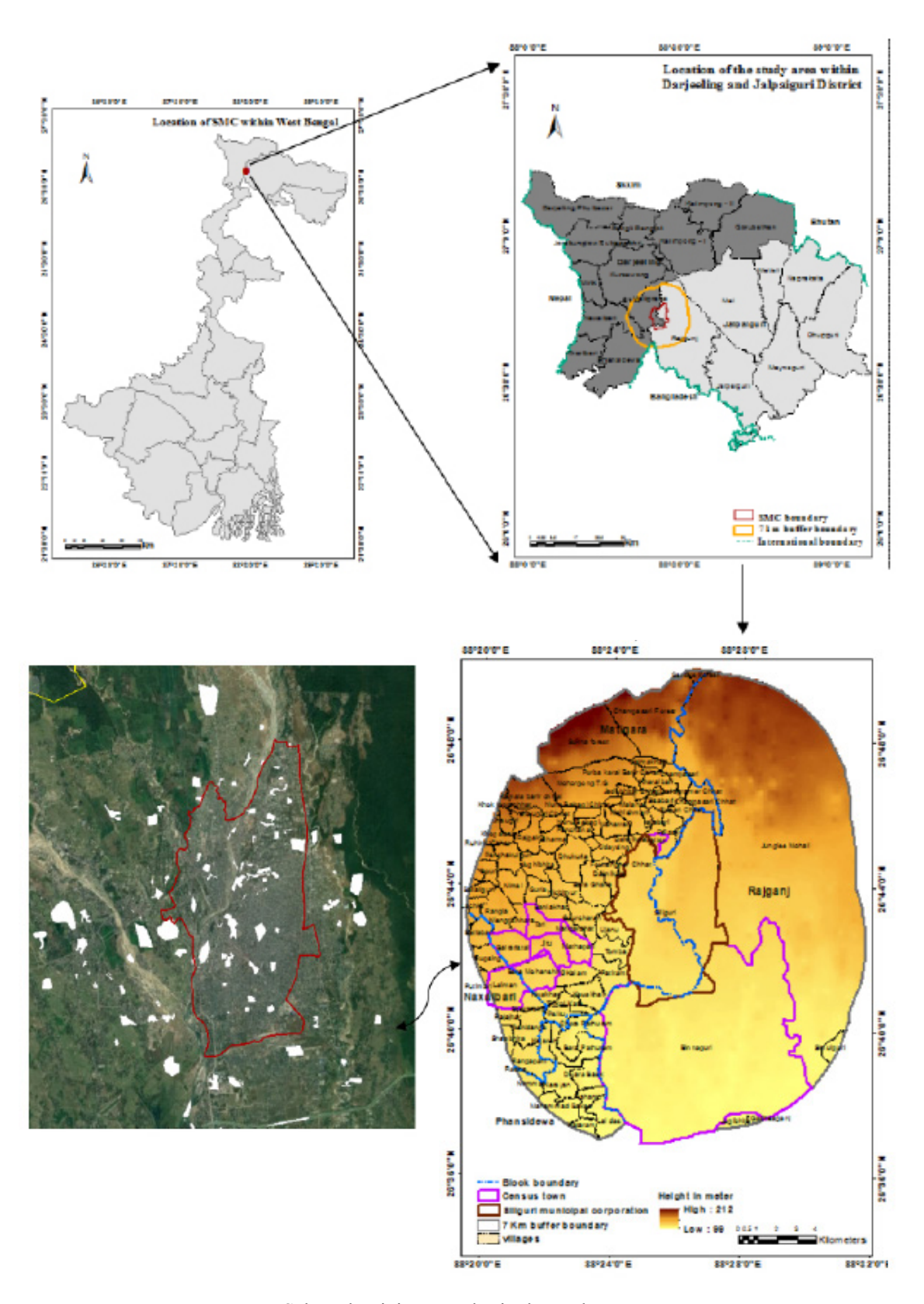
2. Study Area

The study area includes Siliguri Municipal Corporation (SMC) and its buffer of seven kilometres, taken as the area of interest (AoI), comprising both urban main land and suburban areas. SMC is the nodal unit of development of Siliguri Jalpaiguri planning area and has immense importance as a rapidly developing urban area in West Bengal. Siliguri is the gateway of the whole of North East India for its strategic location and is one of the fastest growing urban entities of the state. The town is located at the foot of the southern Himalayas which fall under the Terai physiographic region, connecting north east border states with the rest of India. SMC lies at 26° 41' N to 26° 42' N and 88° 23' E to 88° 28' E coordinates near the Mahananda river at an elevation of 121 meter above sea level with an area of 41.9 sq.km. The upgradation of Siliguri urban area from Municipal town in 1949 to the status of Municipal Corporation in 1994 was an indicator of its rapid pace of urbanization.

The study area comprises Siliguri Municipal Corporation, 9 census towns (namely Kalkut, Lalman, Tari, Bairatistal, Bara mohansing, Jitu, Mathapari, Dabgram and Binnaguri) and 92 villages within the buffer boundary of 7 km, covering total of 384 sq.km of area (Figure 1). Total population of Siliguri town as per the census report of India recorded 216950 in 1991 which has increased to 513,264 in 2011. Although SMC has a population of 513,264, according to the last census report, its urban agglomeration population is 705,579. It registered a population growth rate of 8.65% in the decade 2001-2011. Its population density has increased from 5178 persons per sq.km (in 1991) to 12250 persons per km² in 2011. Over the last 20 years, SMC has experienced rapid changes in terms of population density, land use pattern and building types.

3. Materials and Method

Landsat 8 TM and OLI TRIES images are used for preparing Local Climate Zones (LCZs) maps for the year 2001 and 2021. These input image data contain land use information and urban built up information which can be used by analysing their spectral and spatial information to develop the LCZ map. Details specifications of these Landsat images are shown in Table 1. downloaded from the U.S. Geological Survey website after considering their availability and quality.



Selected training samples in the study area.

Figure 1. Location map of the study area and selected training samples

Source: Google earth image

Table 1. Characteristic of Land sat Satellite Images used in the Study

Satellite	Sensor ID	Year	Acquisition date	Resolution	Path/Row	Projection
LANDSAT 5	TM	2001	2001-01-19	30 m	139/41	UTM-WGS1984
LANDSAT-8	OLI_TIRS	2021	2021-01-11	30 m	139/41	UTM-WGS1984

Source: earth explorer USGS

3.1 Methods for Delimitation of Local Climate Zones (LCZ)

The LCZ classification scheme is applied to Siliguri and its 7 km surrounding area, taken as an area of interest (AOI) following the World Urban Database and Access Portal Tools (WUDAPT) methodology ^[30]. WUDAPT is the remote sensing satellite image based method for LCZ mapping, which is adopted and applied by many researchers in their urban morphological and UHI studies ^[31,32]. WUDAPT gathers information on the form and functional aspects of urban areas that are used worldwide in a consistent manner. Based on the LCZ scheme, WUDAPT classifies natural and urban landscapes into climate relevant surface properties ^[30,33].

Out of 17 LCZ classes (Table 2), as developed by Stewart and Oke, a total of 15 types LCZ i.e. 10 built types and 5 natural surface covers were identified based on the LCZ classification criteria. 15 training samples, selected for each LCZ class, were collected through GPS survey according to the building heights and spacing. The total area of a training site for each LCZ has to range between 1 to 5 sq.km, collected from a place where homogeneous conditions covered at least 1 sq.km area as stipulated by Danylo et al. [26]. The area polygons for creating signature sample files are selected which consist of buildings and theirs close vicinity. After transferring the points on Google earth for extracting sample signatures for each LCZ class, polygons were digitized and saved in Kml format. The training samples selected for the LCZ classification are shown in Figure 1.

Table 2. LCZ classes and respective codes (Stewart and Oke, 2012)

Built types	Land cover types	Variable Land cover properties
LCZ 1- compact high-rise	LCZ A- dense trees	b - bare trees
LCZ 2- compact mid-rise	LCZ B- scattered trees	s - snow cover
LCZ 3- compact low-rise	LCZ C- bush, scrub	d - dry ground
LCZ 4- open high - rise	LCZ D- low plants	w - wet ground
LCZ 5- open mid-rise	LCZ E- bare rock/paved	
LCZ 6- open low-rise	LCZ F- bare soil/sand	
LCZ 7- lightweight low-rise	LCZ G- water	
LCZ 8- large low-rise		
LCZ 9- sparsely built		
LCZ 10- heavy industry		

Pre processed Landsat images, AOI and training samples are imported into the system for Automated Geosci-entific Analyses (SAGA) programme and then LCZ classifications are executed by using random forest classifier algorithm [33,34]. A random forest classifier is a prediction model with high computational accuracy which considers the similarity between training samples and the rest of the AOI to classify the whole input image into different LCZ types [35]. Lastly the final output of SAGA GIS software has been imported into ArcGIS to prepare the thematic map of LCZ. The whole methodological the procedure of LCZ classification using the WADPT method is summarised in Figure 2.

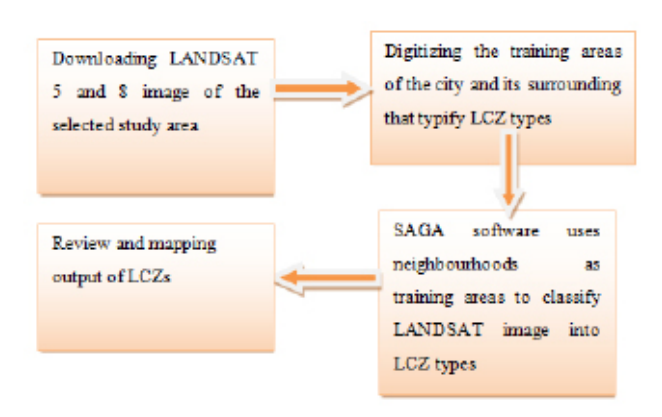


Figure 2. Methodological steps of LCZ classification using WUDAPT method.

3.2 Accuracy Assessment of LCZ Classes

Accuracy assessment was conducted through the confusion matrix to validate the LCZ classification scheme used in the study. Total of 225 reference points, collected randomly from field surveys, were generated on 2021 LCZ classification map for assessing user's accuracy, producer's accuracy, overall accuracy, and Kappa coefficient. In the case of LCZ 2001, the sample sites have been identified from Google earth image of 2001 and field interview of residents living there before 2001 to compare the land use/land cover and building types for validating the LCZ of 2001. Selected points are then superimposed on classified images to compare LCZ types of each point with existing ground truth using Google Earth data. The Kappa

coefficient, one of the most reliable accuracy indicators is computed by the following formula:

$$K = \frac{\sum_{N}^{a} - \sum ef}{1 - \sum ef}$$

Where, a is the sum of diagonal frequency, N is the total number of data in LCZ classes, and ef is the expected frequency. Expected frequency (ef) can be computed using the following formula:

$$ef = \frac{\text{Row total X column total}}{N}$$

3.3 Method for Detecting Conversion of Urban Built Type LCZs

Local climatic classified image pairs of two different time phases (2001 and 2021) are compared using cross-tabulation in order to determine the quantitative aspects of the conversion of buildings. Using the output data sets of LCZ mapping from SAGA GIS, a change matrix is generated from this alteration process over the ArcGIS platform. Quantitative areal data of the conversion of built type LCZ changes are then determined by compiling the amount of high and mid-rise buildings gained from each category of low-rise buildings and natural land use types. It is necessary to investigate such conversion of building states through LCZ classification for urban space planning.

4. Results

4.1 Delimitation of Local Climate Zones

Using the method described above, two LCZ maps of SMC and its surroundings have been prepared for the years 2001 and 2021. Figure 4 shows the spatial pattern of occurrence of individual LCZ class areas where, in 2001, thirteen and 2021, fifteen LCZs are identified. Ten built type LCZ classes were identified according to building height (high-rise, mid-rise and low-rise) and building compactness (compact and sparse). The descriptions of built type LCZs have been given in Figure 3. Classification of land use type LCZs reveals five dominant land cover types of the study area. The result features areal extent of built up LCZs has increased drastically from 2001 (43 sq.km) to 2021 (83.9 sq.km) in the study area with an increasing rate of 2.1 sq.km. per year.

Within this 20 year of interval, some significant reorientation of LCZs is recognized e.g. in the previous phase, there was absolutely no open and compact highrise class but in a late phase it significantly emerged in the north and north western part of the city and its periphery. Most of the pre-existing vacuum open spaces are now replaced with mid and high-rise buildings. Out of the total built up land of the study area, 5.62 sq.km and 18.1 sq.km areas are now covered with high-rise and midrise buildings respectively. Different low-rise built types prevail over 56.05 sq.km area out of 83.94 sq.km of the total built up land. LCZ 3 and LCZ 5 dominate the central parts of the city, LCZ 5 areas prevail with the fragments of LCZ 6, which spread from the external city centre borders up to the edge of the compact urban development, and LCZ 8 and 10 produce projections of significant development into the surrounding areas of SMC. The rapid growth of LCZ 7 and LCZ 8 indicates sprawling of the city. Changing built type and land cover type LCZs and their areal extension has shown details in Table 3. It can be observed that low-rise building categories are sometimes converted to midrise and high-rise buildings. The study has focussed on Siliguri Municipal Corporation to identify the alteration process of building states over the last decades.

4.2 Accuracy Level of LCZs

Four indices, overall accuracy, user's accuracy, producer's accuracy and Kappa coefficient, were applied for validation of the classification scheme. The results of accuracy assessment of LCZ classification shows that for the year 2001, the overall accuracy level is 82.66% and the kappa a coefficient is 0.79 (Table 4) and for the year of LCZ 2021, overall accuracy level is 83.56% and the kappa coefficient is 0.81 (Table 5). So the accuracy results of LCZ model for both the time period suggest validly and encouragement in using the classification scheme in this region. Though in the case of accuracy level variations were found in different LCZs. The highest degree of accuracy was recorded for LCZ 2 (92.86% in 2021) and the lowest degree of accuracy was recorded for LCZ 4 (68.75% in 2021).

4.3 Conversion of Building Types

An investigation is focussed on Siliguri Municipal Corporation to detect intra-zonal variability in built up LCZs. In the context of complex urban morphology and high density area, it is needed to study the morphological alteration of building types over time. The population of Siliguri is growing at a rapid pace which are subjected to the transformation of built up land and natural land cover. Significant alteration of buildings is predominant at the core and immediately surrounding areas of SMC with the expansion of urban land over the two decades.

Built types LCZ	Description	Building stories	By Stewart and Oke	Real photograph
Compact high rise LCZ 1	Dense mix of tall buildings. Few/ no trees. Mostly paved land cover. Concrete, steel, stone Construction materials.	> 9		
Compact mid rise LCZ 2	Dense mix of midrise buildings. Few/ no trees. Mostly paved land cover with stone, brick, tile and concrete construction materials.	3-9		
Compact low rise LCZ 3	Dense mix of low rise buildings. Few/no trees. Mostly paved land cover. Stone, brick, tile and concrete construction materials.	1-3		
Open high rise LCZ 4	Open arrangement of tall buildings. Abundance of pervious land covers having low plants, scattered trees. Concrete, steel, stone and glass construction materials.	>9		
Open mid rise LCZ 5	Open arrangement of mid rise buildings. Abundance of pervious land cover having low plants, scattered trees. Concrete, steel, stone and glass construction materials.	3-9		
Open low rise LCZ 6	Open arrangement of mid rise buildings. Abundance of pervious land cover having low plants, scattered trees. Wood, brick, stone, tile and concrete construction materials.	1-3		
Light weight low rise LCZ 7	Dense mix of one story buildings. Few/no trees. Mostly hard packed land cover. Lightweight construction materials e.g. Wood, thatch, corrugated metal.	1		

Large low rise LCZ 8	Open arrangement of large low rise buildings. Few/no trees. Land cover is mostly paved. Steel, concrete, metal and stone construction materials.	1-3	
Sparsely built LCZ 9	Sparse arrangement of small or medium-sized buildings in natural settings. Abundance of Lowplants, scattered trees.	1-3	
Heavy industry LCZ 10	Low rise and mid rise industrial Structures. Few/no trees. Land cover is mostly paved or hard packed. Metal, steel and concrete construction materials.	1-3	

Figure 3. Description of Local Climate Zones (after Stewart and Oke, 2012) identified in Siliguri Municipal Corporation.

Table 3. Areal extension of the Local Climatic Zones (LCZ) of the study area

	2	001		2021	
Class name	Pixel count	Area in sq. Km	Pixel count	Area in sq. Km	Remark
LCZ 1 - compact high-rise	0	0	1950	1.76	Newly emerged
LCZ 2 - compact mid-rise	2633	2.37	12349	11.11	Increased significantly
LCZ 3 - compact low-rise	1408	1.27	9300	8.37	Increased significantly
LCZ 4 - open high – rise	0	0	4288	3.86	Newly emerged
LCZ 5 - open mid-rise	7982	7.18	7772	6.99	Decreases slightly
LCZ 6 - open low-rise	10841	9.76	6451	5.81	Decreases
LCZ 7 - lightweight low-rise	8596	7.74	22056	19.85	Increased significantly
LCZ 8 - large low-rise	4348	3.91	17527	15.77	Increased significantly
LCZ 9 - sparsely built	11571	10.41	6944	6.25	Decreases
LCZ 10 - heavy industry	337	0.30	4635	4.17	Increased significantly
LCZ A-dense trees	96081	98.47	107491	96.74	Decreases
LCZ B - scattered trees	41997	46.44	44376	39.94	Decrease
LCZ D - low plants	217648	177.88	134229	136.81	Decreases significantly
LCZ F - bare soil/sand	13868	9.48	29912	11.05	Increases
LCZ G - water	9312	8.38	17342	15.61	Increases

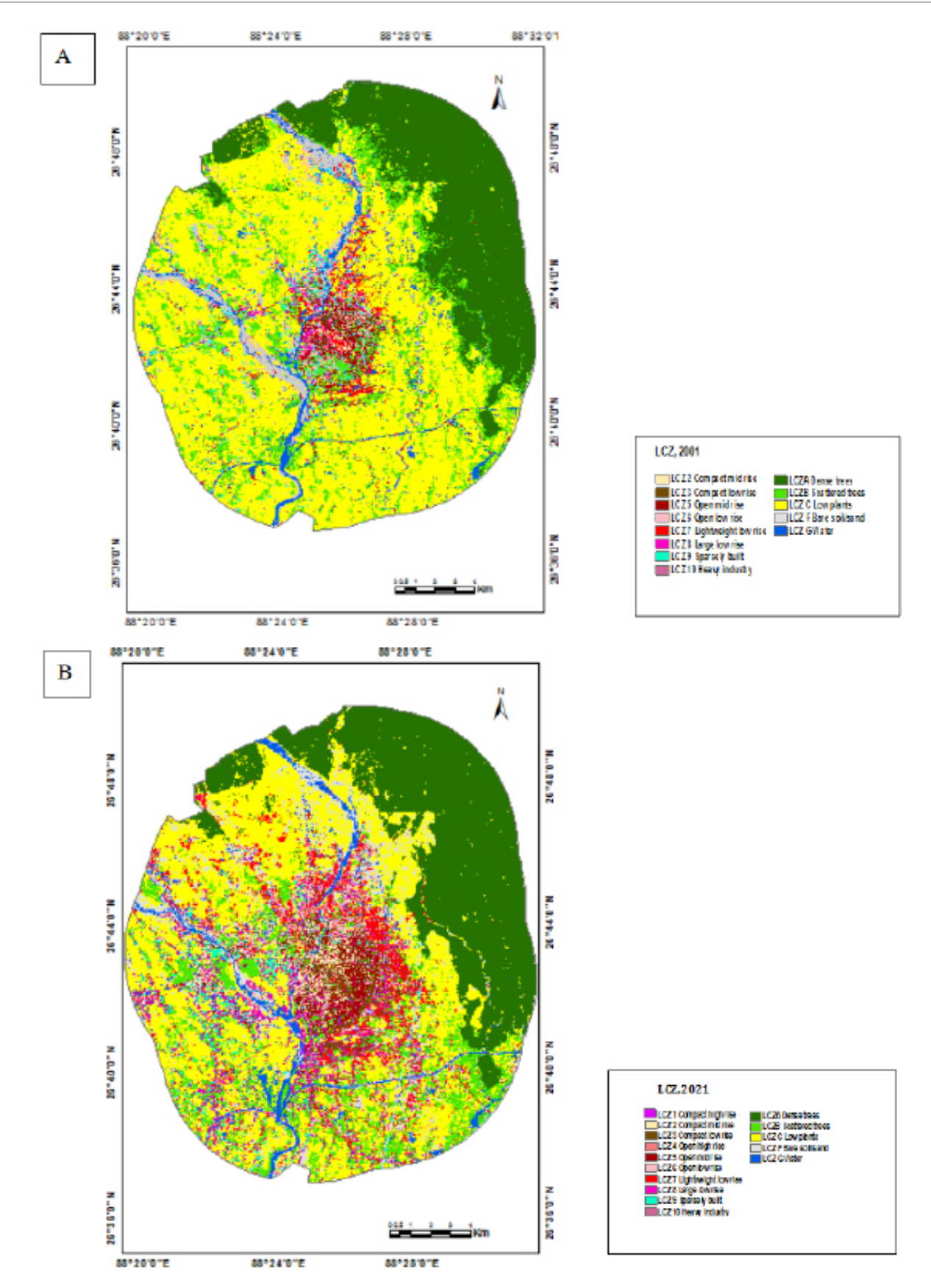


Figure 4. Local Climate Zones map of SMC and its surrounding. (a) 2001 (b) 2021

Table 4. Confusion matrix for classification accuracy assessment of LCZ, 2001.

LCZs	LCZ1 LCZ2		LCZ3	LCZ4 I	LCZ5 I	LCZ6 I	LCZ7	LCZ 8	LCZ 9	LCZ 10	LCZ A	LCZB	LCZD	LCZF	LCZ G	Row total	User accuracy(in %)
LCZ 1	11	0	0	0	0	1	0	1) ()	0 0	1	()	1 1:	5 73.33
LCZ 2	0	14	0	0	0	0	0	0	1)	0 0	0	0) (1.	93.33
LCZ 3	0	0	13	0	1	0	0	0) ()	1 0	0	0) (1.	86.66
LCZ 4	1	0	0	11	0	1	0	0) :		0 0	0	1	1 (1.	73.33
LCZ 5	0	0	0	0	12	0	1	0	1)	0 0	0	0)	1 1	5 80
LCZ 6	0	0	0	0	0	14	0	0) ()	0 1	. 0	0) (1.	93.33
LCZ 7	0	0	0	1	0	0	13	0) ()	0 0	0	1	1 (1	86.66
LCZ 8	0	1	1	0	0	1	0	10) 1		1 (0) (1	5 66.66
LCZ 9	0	0	1	0	0	0	1	0	11	. ()	0 1	1	() (1:	73.33
LCZ 10	0	0	0	1	0	0	0	0	() 13	3	0 0	0	()	1 1	86.66
LCZ A	1	0	1	0	1	0	0	0) () 1	1 0	0	1	1 (1	73.33
LCZB	0	0	0	1	0	0	0	0) ()	0 14	. 0) (1	93.33
LCZD	0	1	0	0	0	0	0	0) 1		0 0	13	0) (1.	86.66
LCZF	0	0	0	0	0	0	1	0) ()	0 0	0	14	1 (1	93.33
LCZ G	1	0	1	0	0	0	0	1) ()	0 0	0	0	1	2 1	5 80
Column total	14	16	17	14	14	17	16	12	13	16	5 1	3 16	15	17	1	5 22	5
Producer accuracy (in%)	78.57	87.5	76.47	78.57	85.71	8235	81.25	83.33	84.62	81.25	84.6	1 87.5	86.66	82.35	8	0	
Over all accuracy (in %)	82.66																
Карра	0.79																

Table 5. Confusion matrix for classification accuracy assessment of LCZ, 2021

																	User accuracy (in
LCZs I	CZ1	LCZ2 LCZ3	1	LCZ 4	LCZ5	LCZ 6	LCZ 7	LCZ 8	LCZ9	LCZ 10	LCZ A	LCZB	LCZD	LCZF	LCZG	Row total	%
LCZ1	12	0	0	1	0	0	0	0	1	0	1	. 0) () (0 () 1:	80
LCZ2	0	13	0	0	0	0	1	0	0	0	0	0)]	. (0 () 1:	86.67
LCZ3	1	0	12	0	0	0	0	1	0	1	0	0) () (0 () 1:	80
LCZ4	0	0	1	11	0	1	0	0	0	1	0	0) () 1	1 () 1:	73.33
LCZ 5	0	0	0	1	13	0	0	1	0	0	0	0) (0 () 1:	86.67
LCZ 6	0	0	0	0	1	12	0	0	0	1	0	1	. () (0 () 1:	5 80
LCZ7	1	0	0	0	0	0	14	0	0	0	0	0) () (0 (1:	93.33
LCZ 8	0	0	0	1	0	0	0	13	1	0	0	0	0) (0 (1:	86.67
LCZ9	0	0	1	0	0	0	1	0	12	0	0	0) 1	. (0 (1:	5 80
LCZ 10	1	0	0	0	0	0	0	0	0	14		0) () (0 (1:	93.33
LCZA	0	0	0	0	1	0	0	1	0	0	12	. 0) () 1	1 () 1:	5 80
LCZB	0	1	0	1	0	0	0	0	0	0	0	13) (0 (1:	86.67
LCZD	0	0	1	0	0	1	0	0	0	1	0	0	12	2 (0 (1:	5 80
LCZF	0	0	0	1	0	0	0	0	0	0	0	0) () 1/	4 (1:	93.33
LCZG	1	0	0	0	1	0	0	1	0	0	1) () (0 11	1 1:	73.33
Column total	16	14	15	16	16	14	16	17	14	18	14	14	14	1 16	5 11	22:	5
Profuser accuracy (in	75	92.86	80	68.75	813	85.71	87.5	76.47	85.71	77.78	85.71	92.9	85.71	87.5	5 100)	
Over all accuracy (in %	83.	56															
Карра	0.81																

Transition matrix based on 'from' and 'to' changes of LCZs between 2001 and 2021 has been produced (Table 7) to assess this trend of changing building states in SMC. Figure 5 shows some LCZ training samples collected in SMC areas, documenting the intra urban alteration of building types from low-rise to high and mid-rise. Table 6 highlights that low-rise zone consisting of open low-

rise, compact low-rise, lightweight low-rise, large low-rise and sparsely built cover, are collectively increased from 17 sq.km to 18.22 sq.km. Open and compact mid-rise building cover area has been increased from 7.58 sq.km to 11.64 sq.km. Out of the total study area of SMC, the newly emerged open and compact high-rise buildings cover an area of 2.04 sq.km. So, the low-rise zone has slightly

increased within two decades but mid and high-rise zones are rapidly increasing and a major portion of these mid and high-rise buildings are made up from conversion of low-rise building types. From a total 13.68 sq.km area of high and mid-rise zone, 10.8 sq.km area which is 78.95%, is built from the alteration of low-rise buildings and natural lands. The transformation of different low-rise buildings to mid and high-rise buildings is shown in detail in Table 7. It is clearly visible from the conversion map (Figure 7) that the process of alteration to high-rise zone is very much active in the northern part and to mid-rise zone is in the south eastern part of SMC. Because of the presence of industries in the southern part and high density in the central part of the city, high-rise buildings (compact high-rise, open highrise) are mostly spread in the northern part of the city. Significant decrease in open low-rise (4.89 sq.km to 3.59 sq.km) and sparse building cover area (3.94 sq.km to 0.94 sq.km) documents the compact growth of the city from dispersed one. Among the built LCZs, LCZ8 were mostly converted to LCZ 1(28.93%), LCZ 7 to LCZ 4 (18.69%), LCZ 9 converted to LCZ5 (70.97%) and LCZ 3 to LCZ 2 (60.39%). Among natural land cover types, LCZ B was mostly converted to compact high-rise (55.82%) and open mid-rise zone (41.22%) whereas low plant cover converted to compact mid-rise (41.18%). This process is continuous at the present and expectedly that in the near future more such urban capes will be turned into mid or high-rise zones.



Figure 5. Examples of building conversion from A) low-rise (2001) to B) high-rise (2021) of same training samples. Captured from Google earth image.

Table 6. Area (sq.km) of each LCZ in SMC

LCZ types	2001	2021
Compact high-rise	-	0.8
Compact mid-rise	1.61	5.26
Compact low-rise	1.15	6.22
Open high-rise	-	1.24
Open mid-rise	5.97	6.38
Open low-rise	4.89	3.59
Light weight low-rise	4.75	4.76
Large low-rise	2.22	2.71
Sparsely built	3.94	0.94
Heavy industry	0.03	0.77
Scattered vegetation	3.52	2.77
Low plant	11.89	2.68
Waste land	0.53	2.22
Water	1.29	1.44

Table 7. Land transition to mid-rise and high-rise LCZ of SMC, from 2001 to 2021

		LCZ types	(area in Sq.	
		2021	km)	
LCZ types	Compact	Open high-	Open mid-	Compact
(2001)	high-rise	rise	rise	mid-rise
Compact low- rise	0.065(8.55)	0.023(3.02)	0.21(27.63)	0.459(60.39)
Open low-rise	0.172(7.68)	0.134(5.54)	1.063(47.46)	0.875(39.06)
Light weight low-rise	0.221(26.31)	0.157(18.69)	0.233(27.73)	0.233(27.73)
Large low-rise	0.379(28.93)	0.086(6.51)	0.385(29.17)	0.466(35.30)
Sparsely built	0.126(10.24)	0.163(13.25)	0.873(70.97)	0.071(5.77)
Low plant	0.282(14.54)	0.426(21.96)	0.432(22.27)	0.799(41.18)
Scattered tree	1.323(55.82)	0.017(7.17)	0.977(41.22)	0.05(2.11)
West land	0.018(14.75)	0.041(33.60)	0.015(12.29)	0.048(39.34)

Computed by the author from image data extraction

Figures in the row cells depict the amount of former land cover contributed to the current land cover shown in columns. Values in parentheses are the corresponding percentage values.

5. Discussion

The study developed the LCZ classification maps, showing the spatial distribution pattern of LCZ classes which are also consistent with the actual land use pattern of Siliguri and its surrounding area. The importance of the LCZ scheme lies in the detailed classification of urban built types and explaining the conversion of built up forms with time. Intra urban landscapes can be analysed through the LCZ classification which demonstrates the outward and also upward growth of the city. Within the study period low, moderate and high state buildings are co-developed with the urban expansion and constitute an an important feature of the urban landscape of the study area.

5.1 LCZ Classification Based on Building Forms

A high concentration of heterogeneous surfaces in

urban areas produces specific built LCZs units that are well differentiated from each other. The LCZ distribution exhibits compact development at the centre (LCZ 2, LCZ 3) and towards its outer boundary there is an increasing area of LCZ 7 and LCZ 9. LCZ 10 and LCZ 7 occur especially in the outer part of the city. Dominant built type LCZs of the study area is LCZ 7 and the natural type is LCZ D. In SMC the most prevalent built type is LCZ 3, compact low-rise and LCZ 5, open mid-rise and dominant land use type is LCZ D. Most parts of Siliguri and its surrounding areas are mainly covered by mid-rise and low-rise building types with emerging growth of highrise sites. High-rise buildings are mainly developed in the ward no. 43, 41, 42 and 46 of SMC and notably developed in the census towns namely Tari, Jitu and Mathapari. A compact high-rise zone is characterised by closely spaced buildings with few or no trees. Open high-rise buildings set in an open arrangement with scattered trees and abundant plant cover. In some circumstances of low-rise classes (LCZ 9 and LCZ 6), the surface was covered by bare soil. Open low-rise and large low-rise classes outside SMC boundary characterised by well vegetation cover and spacious settlements.

Another significant proportion was lightweight lowrise zone (19.85 sq.km) characterised by a dense mix of single storey buildings mostly in the north eastern and south eastern part around SMC and often it merged with compact low-rise class. Rapid decrease in open lowrise area from 9.76 sq.km to 5.81 sq.km and sparsely built cover area from 10.41 sq.km to 6.25 sq.km signifies compact growth of the region.

Siliguri is witnessing immense demographic expansion due to migration from outside areas leading to housing demand that has changed its residential structure with a varied mix of buildings. In the last two decades midrise and high-rise high density dwelling types have significantly developed in the city. Increase of urban population, growth of socioeconomic activities of the a city with its hinterland and limited territory has led to an increase in the number of storeys of buildings.

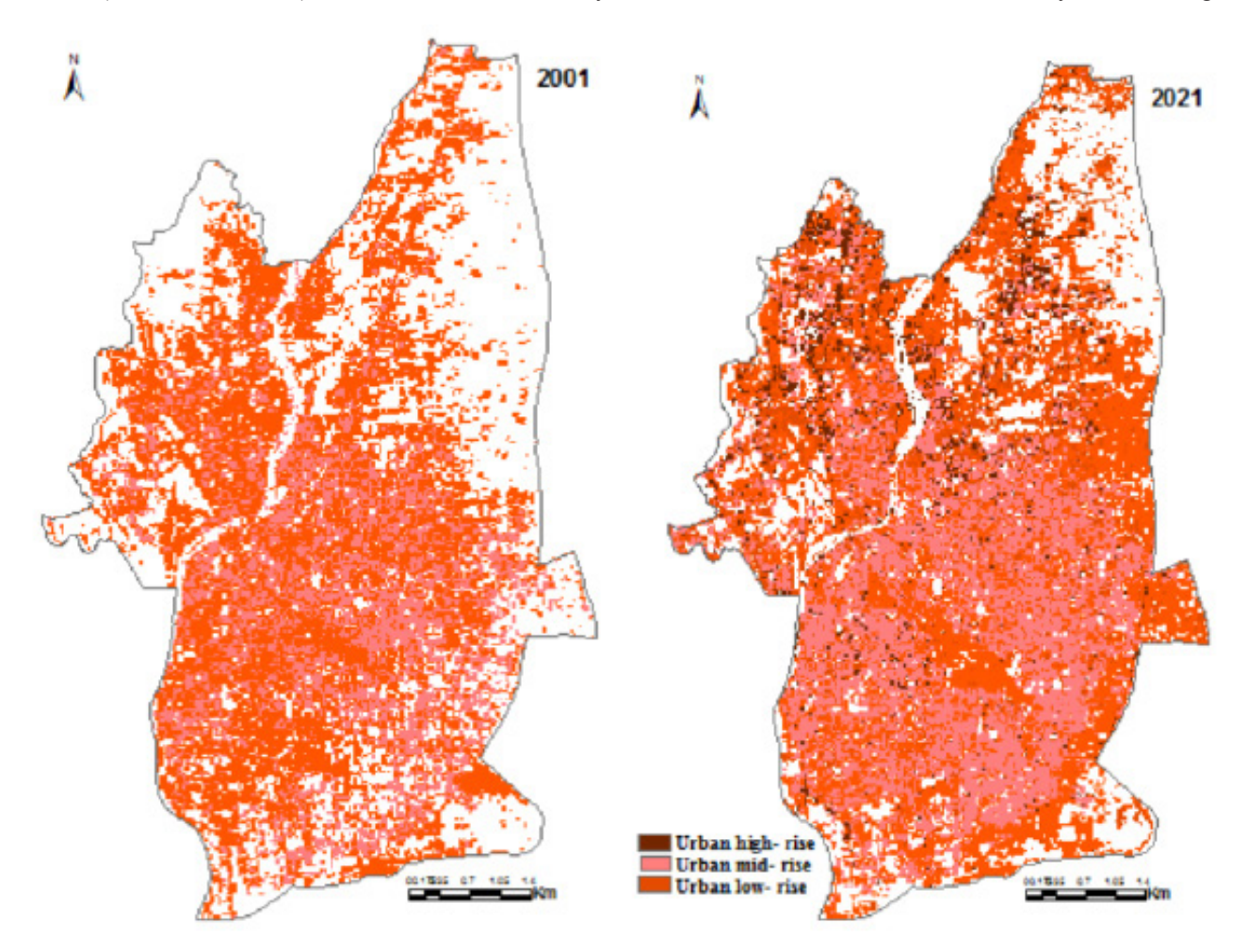


Figure 6. Spatial distribution of building states (low, moderate, high) of SMC in 2001 and 2021.

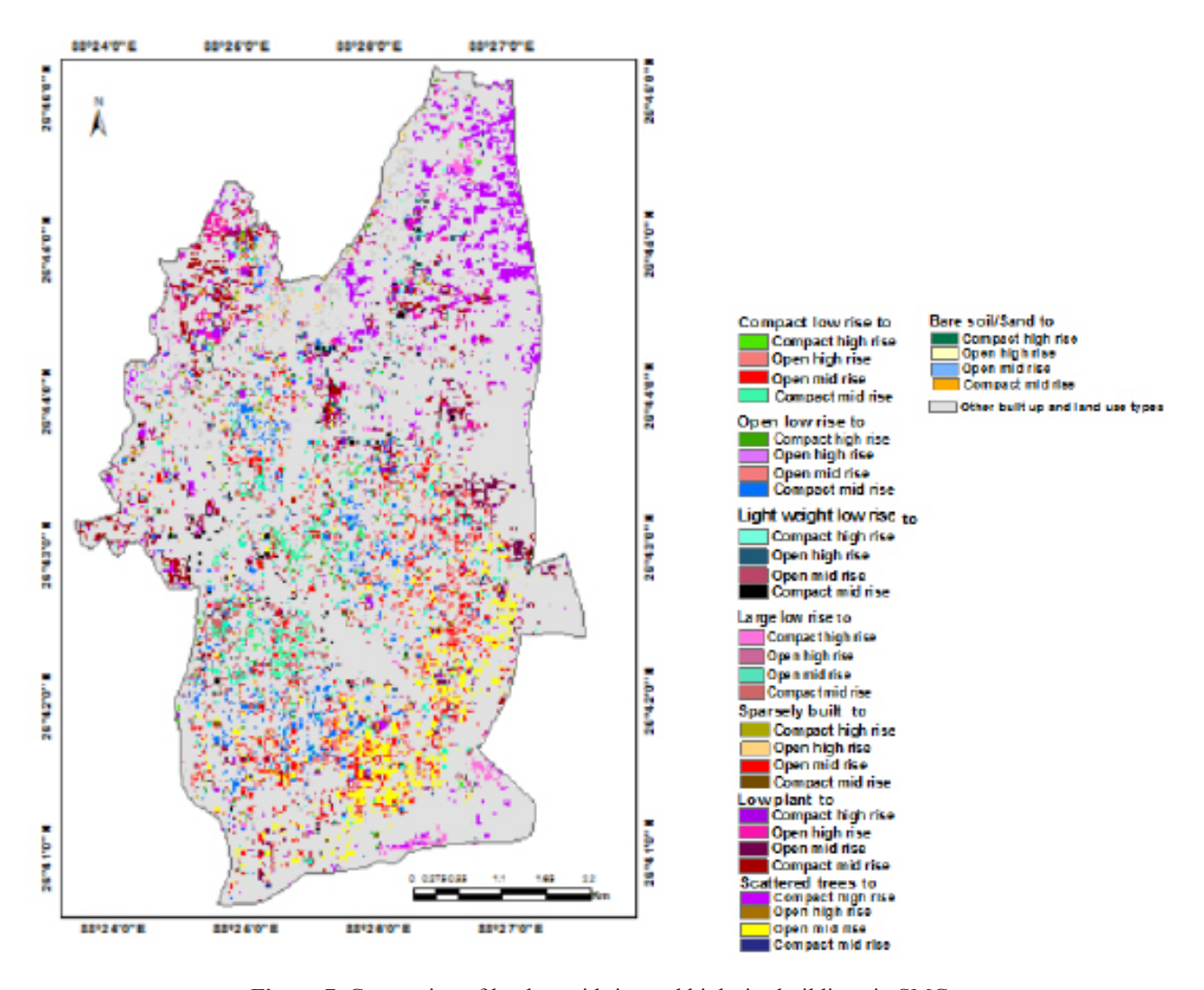


Figure 7. Conversion of land to mid rise and high rise buildings in SMC.

This upward rise of buildings allows being built within a smaller area of land to accommodate its population pressure.

5.2 LCZ Classification Based on Land Covers Forms

The generated LCZ maps assorted 5 natural land cover classes, where dense natural trees categorised as LCZ A, occupied a large portion in the eastern part of this study area. Scattered trees were classified as LCZB, while plantation and agricultural land were classified as low plant cover LCZD. Open space, bare soil and wasteland were categorized as LCZ E. Ponds, reservoirs, streams and nullahs were assigned to LCZ G. Development of compact buildings, sparsely built and lightweight rise has replaced low plant zone and scattered vegetated areas. The low plant zone has decreased significantly from 177.9 sq.km to 136.8 sq.km (Table 3). The compact growth

of the city is pushing vegetated areas, low plant areas outwards the periphery of the city. The other natural LCZ F is composed of bare soil and sand having low spatial coverage.

5.3 Changing LCZs of SMC

The building distribution pattern of SMC reveals that the areas assigned to compact mid-rise zone are characterised with a denses mix of 3 to 9 storied tall buildings and mostly paved spread in and around the core part of the city. Places with a dense mix of 3 storied (or less) buildings, mostly paved with scanty trees constituted the compact low-rise zone at the centre part of the town, covering the both sides of Siliguri station road and Hill cart road and the places around the city. Older core and some other parts of the town were characterised by low-rise buildings, most of them with poor furnishing.

Built type LCZs classes according to building height

(i.e. low-rise, mid-rise or high-rise) have shown in Figure 6 which reflects built up density is high in the middle and southern parts of SMC. As the conversion of built type LCZs is predominant at the core urban area, SMC has taken to visualize this conversion dynamics clearly (Figure 7). Increasing population pressure in SMC gives rise to the formation of the LCZ built type beyond the city borders. High-rise buildings (comprising LCZ 1 and LCZ 4) covers a total 5.62 sq.km of built up area, which was developed more in outskirts areas (3.58 sq.km i.e. 63.7% area) than SMC (2.04 sq.km i.e. 36.29% area). SMC has experienced an increase of compact low-rise and compact mid-rise buildings at a rate of 0.26 and 0.2 sq.km. per year respectively followed by a significant trend of upward building growth. The results obtained from the conversion matrix fortify the process of changing internal urban built forms. Hence from the analysis of 2001 and 2021 LCZ maps it is evident that with the expansion of urban land significant parts of SMC have undergone a transition in status from low-rise to mid and high-rise built zones.

5.4 Implication in Future Urban Planning

In the context of rapid urban development and planning for new town construction there is a need to delineate and update LCZs results to meet new needs that arise with rapid population growth. LCZs classification scheme using WUDAPT methodology provides a comprehensive database for scientific enquiry of the transformation that could be used in urban land use study. Planners should plan and develop new constructions with green space seeking sustainable urban development. LCZs classification ultimately emphasizes the need to classify urban land into specific local area zones to differentiate complex urban LCZ types. The analysis can assist urban planners estimating and better understanding urban morphological characteristics. The investigation and documentation of changing building states can provide very useful input for creating a proper urban built up plan with a rapidly growing population. LCZ classification recognizes 10 built types which are essential to understand the city morphology and controlling the built environment in terms of building height, plot size and spacing. The study highlights the areas of scanty open and green space that need to be preserved. Conversion of LCZ6, LCZ7 and LCZ8 to the development of LCZ1 and LCZ2 should be avoided, especially at the dense core area.

LCZ classification hierarchy provides useful urban information for the regions underwent unplanned urbanization, consisting of more heterogeneous urban forms and land cover types which are very much needed for further research work. The present study implies that

LCZ is an effective method for urban planners to make appropriate decisions on urban land use planning.

6. Conclusions

LCZs classification map and the changing urban morphology with alteration of building states are the core results of the present work. Local Climate Classification has become the most accepted method in urban studies to explain internal urban forms. The study demonstrates that the adopted scheme can appropriately capture urban morphology through the detailed and comprehensive assessment of natural landscapes and building classes. The findings of LCZ mapping, especially the urban built up statistics of LCZ 1 to LCZ 10 have been identified consistent with those documented by Swert and Oke. Investigation of building distribution patterns through built type LCZs demonstrate that peripheral areas of SMC tend to construct high state LCZ zone while the the core urban area witnessed a significant increase in low and mid-rise LCZ zones. SMC witnessed a higher degree of compact building development, especially at the core city area. Beyond SMC active growth of compact high-rise and open high-rise buildings with lightweight low-rise and large low-rise buildings can be noticed. Analysing the alteration of urban built types plays a significant role in understanding the transformation of urban built up forms. Two-way land transition matrix has been produced to detect every possible land conversion from low-rise built types and other land cover classes to high and midrise zone. Significant growth of midrise and high-rise buildings in Siliguri and its surrounding area demonstrate that the city is undergoing a transition from horizontal to vertical one.

Nonetheless the study presents urban built up growth patterns across space and this would help urban planners in determining the appropriate proportion through integrating low, medium and high-rise buildings for promoting or discouraging building development keeping urban environmental sustainability (such as choice in surface material, planting trees). LCZs classification highlights the influence of large mix of buildings with different froms and structures in the urban scenario. The results pertaining to the of urban built up land influences this pattern greatly. Therefore, the study has established that LCZs classification can efficiently capture the urban surface dynamics through correct classification and characterization of existing urban built up zones. Our a novel approach to evaluating urban morphology is also directly relevant to current theoretical developments in both human geography [36-39] and planning theory [40-43], and future work should explore these theoretical linkages more explicitly.

Conflict of Interest

The authors declare no conflict of interest.

References

- [1] Akristiniy, V.A., Boriskina, Y.I., 2018. Vertical cities - the new form of high-rise construction evolution. E3S Web of Conferences 33.
 - DOI: https://doi.org/10.1051/e3sconf/20183301041.
- [2] Lehnert, M., Geletič, J., Husák, J., et al., 2014. Urban field classification by "local climate zones" in a medium-sized Central European city: the case of Olomouc (Czech Republic). Theor Appl Climatol. 122(3-4), 531-541.
 - DOI: https://doi.org/10.1007/s00704-014-1309-6.
- [3] Song, J., Du, S., Feng, X., et al., 2014. The relationships between landscape compositions and land surface temperature: quantifying their resolution sensitivity with spatial regression models. Landscape and Urban Planning. 123, 145-157.
 - DOI: https://doi.org/10.1016/j.landurbplan.2013. 11.014.
- [4] Stewart, I.D., Oke, T.R., 2012. Local climate zones for urban temperature studies. Bulletin of the American Meteorological Society. 93(12), 1879-1900. DOI: https://doi.org/10.1175/BAMS-D-11-00019.1.
- [5] Ellefsen, R., 1991. Mapping and measuring buildings in the canopy boundary layer in ten US cities. Energy and Buildings. 16(3), 1025-1049.
 - DOI: https://doi.org/10.1016/0378-7788(91)90097-m.
- [6] Oke, T.R., 2004. Initial Guidance to Obtain Representative Meteorological Observations at Urban Sites. WMO/TD No. 1250.
- [7] Lelovics, E., Unger, J., Gál, T., et al., 2014. Design of an urban monitoring network based on local climate zone mapping and temperature pattern modelling. Climate Research. 60(1), 51-62. DOI: https://doi.org/10.3354/cr01220.
- [8] Gál, T., Bechtel, B., Unger, J., 2015. Comparison of two different Local Climate Zone mapping methods. Paper presented at the 9th International Conference on Urban Climate, Toulouse, France.
- [9] Wang, R., Ren, C., Xu, Y., et al., 2018. Mapping the Local Climate Zones of urban areas by GIS based and WUDAPT methods: A case study of Hong Kong. Urban climate. 24, 567-576.
 - DOI: https://doi.org/10.1016/j.uclim.2017.10.001.
- [10] Geleti'c, J., Lehnert, M., Dobrovolný, P., 2016. Land Surface Temperature Differences within Local Cli-

- mate Zones, Based on Two Central European Cities. Remote sensing, 8(10), 788.
- DOI: https://doi.org/10.3390/rs8100788.
- [11] Geleti^{*}c, J., Lehnert, M., Savic, S., et al., 2019. Inter-/intra-zonal seasonal variability of the surface urban heat island based on local climate zones in three central European cities. Building and environment. 156, 21-32.
 - DOI: https://doi.org/10.1016/j.buildenv.2019.04.011.
- [12] Fricke, C., Pongracz, R., Gal, T., et al., 2020. Using local climate zones to compare remotely sensed surface temperatures in temperate cities and hot desert cities. Moravian geographical reports. 28(1), 48-60. DOI: https://doi.org/10.2478/mgr-2020-0004.
- [13] Leconte, F., Bouyer, J., Claverie, R., et al., 2015. Using local climate zone scheme for UHI assessment: evaluation of the method using mobile measurements. Build. Environ. 83, 39-49. DOI: https://doi.org/10.1016/j.buildenv.2014.05.005.
- [14] Xu, Y., Ren, C., Cai, M., et al., 2017. Classification of Local Climate Zones Using ASTER and Landsat Data for High-Density Cities. IJSTAEORS. 10(7), 3397-3405.
 - DOI: https://doi.org/10.1109/jstars.2017.2683484.
- [15] Zheng, Y., Ren, C., Yong, X., et al., 2017. GIS-based mapping of Local Climate Zone in the high-density city of Hong Kong. Urban climate. pp.1-30. DOI: http://dx.doi.org/10.1016/j.uclim.2017.05.008.
- [16] Bechtel, B., Daneke, C., 2012. Classification of local climate zones based on multiple earth observation data. IEEE J. Selected Topics Appl. Earth Observat. and Remote Sensing. 5(4), 1191-1202.
 - DOI: https://doi.org/10.1109/jstars.2012.2189873.
- [17] Alexander, P.J., Mills, G., Fealy, R., 2015. Using LCZ data to run an urban energy balance model. Urban Climate. 13, 14-37.
 - DOI: https://doi.org/10.1016/j.uclim.2015.05.001.
- [18] Danylo, O., See, L., Bechtel, B., et al., 2016. Contributing to WUDAPT: a local climate zone classification of two cities in Ukraine. IEEE J. Sel. Topics Appl. Earth Observations Remote Sens. 9(5), 1841-
 - DOI: https://doi.org/10.1109/JSTARS.2016.2539977.
- [19] Ren, C., Cai, M., Li, X., et al., 2019. Assessment of Local Climate Zone Classification Maps of Cities in China and Feasible Refinements. Scientific Reports.
 - DOI: https://doi.org/10.1038/s41598-019-55444-9.
- [20] Lambin, E.F., Turner, B.L., Geist, H.J., et al., 2001. The causes of land-use and land-cover change: moving beyond the myths. Global Environmental

- Change. 11(4), 261-269.
- DOI: https://doi.org/10.1016/s0959-3780(01)00007-3.
- [21] Rindfuss, R.R., Walsh, S.J., Turner, B.L., et al., 2004. Developing a science of land change: challenges and methodological issues. Proceedings of the National Academy of Sciences. 101(39), 13976-13981. DOI: https://doi.org/10.1073/pnas.0401545101.
- [22] Gutman, G., Janetos, A.C., Justice, C.O., et al., 2004. Land change science: Observing, monitoring and understanding trajectories of change on the earth's surface. Dordrecht; New York: Springer.
- [23] Das, M., Das, A., 2019. Estimation of Ecosystem Services (EESs) loss due to transformation of Local Climatic Zones (LCZs) in Sriniketan-Santiniketan Planning Area (SSPA)West Bengal, India. Sustainable cities and society. 47, 1-13.

 DOI: https://doi.org/10.1016/j.scs.2019.101474.
- [24] Brousse, O., Martilli, A., Foley, M., et al., 2016. WUDAPT, an efficient land use producing data tool for mesoscale models? Integration of urban LCZ in WRF over Madrid. Urban Climate. 17, 116-134. DOI: http://dx.doi.org/10.1016/j.uclim.2016.04.001.
- [25] Ng, Y.X., 2015. A study of urban heat island using "Local Climate Zones" the case of Singapore. British Journal of Environment & Climate Change. 5(2), 116-133.

 DOI: https://doi.org/10.9734/BJECC/2015/13051.
- [26] Perera, N.G.R., Emmanueal, R., Mahanama, P.K.S., 2012. 576: mapping "Local Climate Zones" and relative warming effects in Colombo, Sri Lanka. ICUC8-8th International Conference on Urban Climates. Dublin, Ireland.
- [27] Perera, N.G.R, Emmanuel, R., 2016. A "Local Climate Zone" based approach to urban planning in Colombo, Sri Lanka. Urban Climate. 23, 188-203.
 DOI: https://doi.org/10.1016/j.uclim.2016.11.006.
- [28] Mushore, T.D., Dube, T., Manjowe, M., et al., 2019. Remotely sensed retrieval of Local Climate Zones and their linkages to land surface temperature in Harare metropolitan city, Zimbabwe. Urban Climate. 27, 259-271.
 - DOI: https://doi.org/10.1016/j.uclim.2018.12.006.
- [29] Kotharkar, R., Bagade, A., 2018. Local Climate Zone classification for Indian cities: a case study of Nagpur. Urban Climate. 24, 369-392. DOI: https://doi.org/10.1016/j. uclim.2017.03.003.
- [30] Bechtel, B., Alexander, P.J., Böhner, J., et al., 2015. Mapping Local Climate Zones for a Worldwide Da-

- tabase of the Form and Function of Cities. ISPRS Int. J.Geo-Inf. 4(1), 191-219.
- DOI: https://doi.org/10.3390/ijgi4010199.
- [31] Anjos, M., Targino, A.C., Krecl, P., et al., 2020. Analysis of the urban heat island under different synoptic patterns using local climate zones. Building and Environment. pp.185.
- DOI: https://doi.org/10.1016/j.buildenv.2020.107268. [32] Cai, M., Ren, C., Xu, Y., et al., 2018. Investigating the relationship between local climate zone and land
- surface temperature using an improved WUDAPT methodology A case study of Yangtze River Delta, China. Urban climate. 24, 485-502.
 - DOI: http://dx.doi.org/10.1016/j.uclim.2017.05.010.
- [33] Ching, J., Mills, G., Bechtel, B., et al., 2018. World Urban Database and Access Portal Tools (WUDAPT), an urban weather, climate and environmental modeling infrastructure for the Anthropocene. Bulletin of American meteorological society. pp.1-50. DOI: https://doi.org/10.1175/bams-d-16-0236.1.
- [34] Böhner, J., MacCloy, K.R., 2006. SAGA-analysis and modelling applications. Göttingen: Goltze. 115, 1-121.
- [35] Liaw, A., Wiener, M., 2002. Classification and regression by random Forest. R News. 2(3), 18-22.
- [36] Simandan, D., 2011. The wise stance in human geography. Transactions of the Institute of British Geographers. 36(2), 188-192.
- [37] Simandan, D., 2002. On what it takes to be a good geographer. Area. 34(3), 284-293.
- [38] Simandan, D., 2018. Competition, contingency, and destabilization in urban assemblages and actor-networks. Urban Geography. 39(5), 655-666.
- [39] Simandan, D., 2020. Being surprised and surprising ourselves: a geography of personal and social change. Progress in Human Geography. 44(1), 99-118.
- [40] Allmendinger, P., 2017. Planning theory. Macmillan International Higher Education. Economics. 51(5), 569-582.
- [41] Allmendinger, P., 2001. Planning in postmodern times (No. 1). Psychology Press.
- [42] Allmendinger, P., 2002. Towards a post-positivist typology of planning theory. Planning theory. 1(1), 77-99.
- [43] Allmendinger, P., 2006. Zoning by stealth? The diminution of discretionary planning. International Planning Studies. 11(2), 137-143.



Journal of Geographical Research

https://ojs.bilpublishing.com/index.php/jgr

ARTICLE

Assessment of Stakeholders' Perceptions of Landuse/Landcover Change Drivers in Abuja, Nigeria

Sani Abubakar Mashi^{1*} Amina Ibrahim Inkani² Safirat Sani¹ Hassana Shuaibu¹

- 1. Department of Geography & Environmental Management, University of Abuja, PMB 117, Abuja, Nigeria
- 2. Department of Geography, Umaru Musa Yar'dua University, PMB 2128, Katsina, Nigeria

ARTICLE INFO

Article history

Received: 26 December 2021 Revised: 28 February 2022 Accepted: 05 March 2022

Published Online: 15 March 2022

Keywords:

Landuse

Landcover

Change

Drivers

Stakeholders

Rural Urban

ABSTRACT

Landuse/Landcover (LULC) changes are recognised as some of the major causes of environmental problems like land degradation and climate change. To achieve sustainability, we need to properly understand such changes in order to have adequate information that will enable us to design and implement measures to mitigate their negative impacts. Doing this particularly requires a proper understanding of how stakeholders perceive the changes in general and their drivers in particular. Unfortunately, not much is known in many areas about the perspective of landuse stakeholders on drivers of LULC changes. This paper reports the results of a study conducted to examine the perceptions of different landuse stakeholders on drivers of LULC changes in Abuja Federal Capital Territory, Nigeria. A questionnaire survey was utilised, involving 514 households across four settlements, 2 rural (Karshi and Orozo) and 2 urban (Nyanya and Karu) towns in the territory, which were complemented with Focus Group Discussions conducted. The results obtained showed that urban dwellers are largely aware of drivers of changes in socio-economic drivers (physical development on lands, more commercial complex development and more institutional development). Rural dwellers are largely aware of environmental drivers of LULC changes (bush burning, livestock overgrazing, collections of wood and medicinal plants, and agricultural expansion). It was concluded that there is a need to bring about a harmonisation of the perceptions of LULC change drivers by the rural and urban dwellers so as to bring about a common front understanding and response to LULC changes in the study area.

1. Introduction

Landuse and land cover are sometimes used interchangeably but quite refer to different things. Land use involves how the biophysical attributes of the land are

manipulated and the intent underlying such manipulation for which the land is used, whereas land cover implies the biophysical state of the earth's surface and immediate subsurface including biota, soil, topography, surface

Sani Abubakar Mashi,

Department of Geography & Environmental Management, University of Abuja, PMB 117, Abuja, Nigeria;

Email: abubakar.sani@uniabuja.edu.ng

DOI: https://doi.org/10.30564/jgr.v5i2.4273

Copyright © 2022 by the author(s). Published by Bilingual Publishing Co. This is an open access article under the Creative Commons Attribution-NonCommercial 4.0 International (CC BY-NC 4.0) License. (https://creativecommons.org/licenses/by-nc/4.0/).

^{*}Corresponding Author:

and groundwater, human structures etc. ^[1]. Land use change implies the conversion of land use due to human intervention in various purposes such as agriculture, settlement, transportation, etc. ^[2]. While land cover change on the other hand, refers to modification of the existing land cover or complete conversion of a biophysical cover of the land to a new land cover type ^[3].

Human activities (growing food, cutting off trees, building cities, etc.) almost at all times involve the use of land which exerts tremendous effects on land cover (the physical characteristics of the land surface, including grain crops, trees, or concrete). Clearing of new lands, for whatever purpose has long been common in areas with rapidly growing populations [4,5]. It has variously been noted that land resources have been altered by rapid land use and cover changes accelerated by changeable socioeconomic factors including high population growth, rapid urbanization, agricultural intensification and government policies [5]. Human pressure upon land resources and interactions between varying climatic characteristics facilitate changes in land use and cover [6].

Land use and land cover (LULC) change, as one of the main driving forces of global environmental change, is central to the sustainable development debate. Urban growth, particularly the expansion of residential and commercial land to rural areas at the periphery of metropolitan areas, have long been considered a sign of regional economic vitality but a very powerful agent of LULC change. Urban growth is known to exert enormously pressure on LU/LC through processes such as the removal of vegetation cover, replacement of existing vegetation types, reforestation and creation of hardened/ paved/concrete surfaces. Such processes can cause some changes to the LU/LC with consequences to human survival. When towns develop, not only are lands taken for settlement development to accommodate more housing demands of urban dwellers, satellite towns also develop to meet with housing needs of those that serve the towns but are less capable of competing for houses in them. Thus, with the town and satellite down development, massive transformations in LU/LC are introduced which could no doubt have some serious consequences for global environmental change. To continue living in such changes, stakeholders in cities affected by the changes must as of necessity find means of adapting to them.

With advances in techniques for monitoring such changes (especially remote sensing and GIS technologies), a very large amount of research information is now available on nature, extent and consequences of urban development on LU/LC for many areas. A review of this has been presented elsewhere [3]. Most studies focused

mainly on LULC changes, their drivers and their societal and biophysical impacts. To address the likely negative consequences that LULC changes may cause, it is quite appropriate to develop an understanding of how different stakeholders perceive them. Research on LULC change assessment hardly considers the views of stakeholders on especially the drivers of the changes. In most cases where such views were sought, farmers were the main ones consulted as they are typically considered the most notable actors on land and hence can be relied upon in gathering information on stakeholders' perspectives ^[3]. Unfortunately, other stakeholders like non-farm workers, as well as workers in public institutions and the private sector are largely neglected.

In the present study, a contribution is made to this regard by examining the perspectives of some key stakeholders on the drivers of LULC changes in Abuja Municipal Area Council, one of the fastest growing urban and regional areas in the world. The extent of such changes have been well documented elsewhere [3]. The aim of the study therefore is to analyze the perspectives of different landuse stakeholders on the drivers of LULC changes in Abuja Municipal Area Council of Abuja Federal Capital Territory.

2. Study Area

Abuja Federal Capital Territory (FCT) is located between latitudes 8°25"N and 9°25"N and longitudes 6°45"E and 7°45"E, covering a land area of about 8000 square kilometers. It was designated as the capital seat of Nigeria in 1976, with the country's government formally moved there in 1991. The master plan for the territory provides for a 250 km² capital city (FCC) to serve as the seat of the Federal Government of Nigeria, but with several satellite towns to support the teeming population the territory. Abuja FCT is divided into 6 political units, called Area Councils, which include Abaji, Bwari, Gwagwalada, Kwali, Kuje and Municipal Area Councils. The FCC is located within the Municipal Area Council, AMAC and this area council were deliberately chosen to serve as the testing ground for the kind of investigation intended in this study as most of the major public and private establishments in the FCT are located in the AMAC. This has particularly caused massive LULC changes in the area council. The nature of LULC changes that have resulted from these growth processes have been well documented [3] but no research information is available on the perspectives of different stakeholders on the drivers of such changes.

AMAC has a total of twelve wards, namely City Centre, Garki, Gui, Gwagwa, Gwarimpa, Jiwa, Karshi,



Figure 1. Location of Abuja Municipal Area Council (AMAC) in Abuja FCT, Nigeria

Kabusa, Karu, Nyanya, Orozo and Wuse, out of which four (Karshi, Karu, Nyanya and Orozo) which were identified as the most densely populated and the ones in which is the primary occupation of the majority of the dwellers have something to do directly with landuse/land cover were selected for this study.

3. Methodology

Data about the people's perception of the causes of LULC change in the study area were collected through the use of a questionnaire survey involving 514 selected households from the four selected wards, field observations, as well as focus group discussions with people that have been living in the study area for at least the past 30 years from the date of the study (2016). The 514 sample size was calculated from the data on household size of the four wards obtained from the Primary Health Care Department of AMAC. Distribution of the 514 households across the wards is shown in Table 1. The questionnaire utilised was designed to contain both closed and open-ended questions to enable the respondents to have the opportunity of expressing

themselves very well on issues related to drivers of LULC changes. After completing the questionnaire the survey, the contents of the completed questionnaires were coded, summarized and exported into SPSS spreadsheet for statistical analysis to derive mean values and percentages of all the responses received through the questionnaires administered. Four sessions of Focus Group Discussions (FGDs) were held, one per each ward, with selected representatives of the various stakeholders. The motive of the FGDs was to provide a means of cross checking the individual responses received through the questionnaire survey.

Table 1. Distribution of Respondent by ward

Ward	Household Size	Calculated Sample
Karshi	10787	85
Nyanya	11805	117
Karu	28517	249
Orozo	2954	63

4. Results and Discussion

In this study, the causes/drivers of LULC change were identified into two categories as socio-economic or environmental, as this classification has been well discussed in the literature ^[6]. The responses received from the stakeholders on the influence of each of the categories are presented in Tables 2 and 3.

4.1 Socio-Economic Drivers of LULC Change

A close look at Table 2 reveals that there are some levels of variations between the stakeholders in two categories of settlements in the study area on the role of socio-economic drivers in causing LULC change. Demand for higher Income, population pressure increases and need for more housing developments were listed by the

Table 2. Responses Received on Socio-Economic Drivers of LULC Change

No. and % of R	esponses Received	for the V	arious W	ards				
	Ka	ru	Nya	nya	Kai	rshi	Ore)ZO
	No.	%	No.	%	No.	%	No.	%
Demand for higher Income	93	37.4	103	88	63	74.1	53	84.1
Increased access to modern technology	12	4.82	19	16.2	6	7.06	3	4.76
More opportunities for Markets	23	9.24	17	14.5	16	18.8	9	14.3
Increase in access to land	78	31.3	98	86.2	23	27.1	19	30.2
Increase in access to labour	213	85.5	86	73.5	23	27.1	13	20.6
Increase in access to information	15	6.02	12	10.3	16	18.8	5	7.94
Absence of subsidies and credits	8	3.21	15	12.8	5	5.88	3	4.76
Government land policy for more development	206	82.7	95	81.2	32	37.7	21	33.3
Population pressure increase	197	79.1	102	87.2	72	84.7	61	96.8
More housing development	205	82.3	98	83.8	72	84.7	58	92.1
More commercial complex development	194	77.9	101	86.3	6	7.06	3	4.76
More institutional development	186	74.7	89	76.1	39	45.9	26	41.3
Increase in investments	89	35.7	18	29	17	20	24	38.1
Social unrest	8	3.21	15	12.8	5	5.88	3	4.76
Lack of alternative livelihood	21	8.43	46	39.3	68	80	61	96.8
Lack of information on best practices	9	3.61	13	11.1	7	8.24	3	4.76
Shortage of off-farm income-generating activities	11	4.42	27	23.1	75	88.2	58	92.1
Large dependence on natural resources	79	31.7	34	29.1	71	83.5	54	85.7
Lack of land ownership	31	12.5	19	16.2	6	7.06	3	4.76
Beliefs and values leading to more land usage	8	3.21	15	12.8	73	85.9	54	85.7
International trade	1	0.4	0	0	2	2.35	0	0
More Industrialisation	23	9. 24	13	11.1	4	4.71	0	0

Table 3. Responses Received on Environmental Drivers of LULC Change

N	o. and % of Resp	ponses Recei	ived for the	Various Wa	rds			
	Ka	ru	Nya	nya	Kar	shi	Oro)ZO
	No.	%	No.	%	No.	%	No.	%
Reduced rainfall	37	31.6	34	13.7	21	24.7	12	19.1
Increase in heat	14	12.2	19	7.63	6	7.06	3	4.76
Increase in incidence of Soil erosion	23	19.7	17	6.83	16	18.8	9	14.3
Agricultural expansion	43	36.8	21	8.43	65	76.5	52	82.5
Overgrazing	15	12.8	5	2.01	9	10.6	46	73
More Wood collection	45	38.5	64	25.7	69	81.2	57	90.5
More Medicinal plants collection	34	29.1	46	18.5	45	52.9	52	82.5
More Wild foods collection	42	35.9	28	11.2	67	78.8	48	76.2
Reduced river flow	23	19.7	17	6.83	16	18.8	9	14.3
Topographic condition	15	12.8	5	2.01	9	10.6	4	6.35
Pesticide and herbicides use	15	12.8	5	2.01	9	10.6	4	6.35
Bush burning	8	6.84	15	6.02	56	65.9	58	92.1
Livestock grazing	15	12.8	12	4.82	61	71.8	43	68.3
More logging activities	8	6.84	5	2.01	4	4.71	5	7.94
Windstorms	8	6.84	6	2.41	7	8.24	7	11.1
Flooding	23	19.7	19	7.63	6	7.06	3	4.76

majority (more than 80%) of the stakeholders across the four locations as the main drivers of LULC change. Those in urbanised settlements mentioned the government's emphasis in favour of more physical development on lands, more commercial complex development and more institutional development as the major drivers of LULC change. In Ethiopia, Meshesha *et al.* ^[7] have also observed that government's policy of deliberately promoting physical development has contributed largely towards promoting LULC change.

Those in predominantly rural locations indicated beliefs and values of the people leading to more land usage, shortage of off-farm income-generating activities and a lack of alternative livelihood as the major causative drivers of LULC change in the area.

Gbagyi people (one of the major tribes in central Nigeria) is known to hold the belief that ownership of land from where one can gather large quantities of fuelwood will not only increase one's chance of getting rich but will make one absolute control over the spirits that dwell in the forests [8]. With time however, as more lands were taken up for physical development, forest lands are lost leading to a loss of livelihoods. Also taking up of more cultivated lands will imply loss of off-farm livelihood activities especially those related to off-season processing and sale of farm produce. With that, the stakeholders are left with no option but to seek for other alternative livelihood sources which invariably will directly or indirectly lead to more pressure of LULC as the lands are the only option for survival of the rural dwellers. The fact that agriculture and deforestation contribute significantly to LULC change in particular and environmental degradation in general in sub-Saharan Africa has been well documented [9].

During the FGD sessions, it was established that due to loss of livelihoods, many of the rural stakeholders disposed of their lands as survival strategies while those with large holdings from where they used to obtain tree-based wild foods and fodder cleared and prepared them for cultivation, rental by others interested in crop production or sell them to those interested in acquiring lands for physical development.

Enedah *et al.* [10] have shown that though Abuja FCT was created in 1976, it was not until the physical development of both the city of Abuja and its region started in earnest with the provision of the large number of socio-economic infrastructures and developmental institutions through the activities of both the public and private sectors. With this followed a large influx of a large number of Nigerians of diverse ethnic origins into the FCT as employees in the public and private sectors, and as entrepreneurs in the informal sector [8].

As is typical with urbanisation process in sub-Saharan Africa [11,12], the provision of infrastructure in Abuja has been at an unprecedented pace in the country and to date nowhere else in the country has such development been replicated. This created the problem of urban primacy in the country and since the FCT is located at the centre of the country, the problem gave rise to a large influx of Nigerians from all parts of the country leading to massive rise in the human population [3]. To accommodate the ever expanding population, the government has been encouraging massive provision of infrastructure using both public and private funding sources. It is thus not surprising that the stakeholders irrespective of their location almost unanimously identified population pressure increase, demand for more income and housing (which are all products of provision of infrastructure) as among the major drivers of LULC change in the study area. However, as the infrastructure provider has not been evenly provided between rural and urban locations within the territory, it is to be expected that disparity will exist between rural and urban stakeholders in the perception of the extent to which such factors contribute to LULC change. In particular, the stakeholders in the predominantly rural locations comparatively have a lower perception of the role of infrastructure provision in causing LULC change than other stakeholders.

In Nigeria, ownership and use of all lands are defined by Landuse Decree of 1976, which vests power on the Government. Nigerians are only given the right of ownership through the issue of the right of occupancy for a period not exceeding 99 years. Thus, even though allocated lands are not 'permanently' owned by allottees, the fairly lengthy period of occupancy typically given (99 years) more or less make them have a feeling of permanency of ownership. It is sometimes argued that not vesting permanent and complete ownership of lands on the people will discourage them from conserving such lands [13]. In Ethiopia, studies have shown that the possession of all rural and urban lands by the state led to a lack of belongingness to natural resources by the individual farmers, which in turn triggered huge deforestation [14,15]. During discussions with key informants among the stakeholders, it was established that the people generally hold the belief that lands belonging to them whether allocated, purchased or borrowed/rented must be protected for the owner to ensure deriving benefits continuously from them. In sub-Saharan Africa, the fact that rural people' near total dependence on natural resources contribute much to LULC changes have been well recognised [15].

A majority (more than 60%) of the stakeholders across

the four study locations indicated that increased access to modern technology, more opportunities for markets, absence of subsidies and credits, increase in access to information, increase in investments, social unrest, lack of information on best practices, lack of land ownership, International trade and more industrialisation are not major socio-economic causative factors of LULC change in the area. During discussions with the stakeholders, it was however established that the coming of private sector in housing development processes in the study area have brought about a massive transformation of the urban landscape, especially in the two predominantly urbanised settlements of Karu and Nyanya. Also, it was found out that crisis resulting from social unrest in especially central and northeastern parts of the country over the last 5 to 10 years have contributed to a massive influx of people into the FCT. Thus, it was a bit erroneous that the majority of the respondents did not indicate an increase in investment and social unrest as major factors contributing to LULC change in the area.

In general, the stakeholders' perception of a population pressure and lack of alternative livelihoods as among the major socio-economic drivers of LULC change were in line with the findings of studies conducted in different parts of sub-Saharan Africa ^[7,13,16]. As the population grows, competition for available options increases leading to reduced opportunities for livelihood and consequently, alternative livelihoods become scarce. People thus have few options to diversity to other livelihoods options besides the limited ones available (especially exploitation of forest resources and cultivation of crops).

4.2 Environmental Drivers of LULC Change

The main environmental drivers of LULC change on which the perception of the stakeholders was sought are presented in Table 3. It could be seen from the table that majority (over 60%) of the stakeholders in the two predominantly urban settlements did not indicate environmental drivers as the major ones responsible for LULC change in the study area. In the predominantly rural settlements however indicated bush burning, livestock grazing/overgrazing, more wood collection, more medicinal plants collection and agricultural expansion as the major drivers.

Literature on environmental causative factors of LULC change in many areas of the world ^[5,6,14,17-26], has variously described climate change, agricultural expansion, bush burning, collection of timber and non-timber products as the major environmental drivers. It is obvious from the results obtained in this study that it is mainly the stakeholders in rural locations that have some good

level of perception of the role of such environmental factors in causing LULC change perhaps they maintain comparatively stronger interactions with the environment than their urban dwellers' counterparts.

5. Conclusions

The results obtained showed clearly that there are clear differences between rural and urban stakeholders in the perceptions of some of the causes of LULC in the study area. While urban dwellers are largely aware of causes of changes in human aspects (physical development on lands, more commercial complex development and more institutional development) of LULC, and in fact majority (over 60%) of them did not indicate environmental drivers as the major ones responsible for LULC change in the study area. Their rural counterparts on the other hand are largely aware of the causes of changes in the physical aspects (beliefs and values of the people leading to more land usage, shortage of off-farm income-generating activities and lack of alternative livelihood, leading into bush burning, livestock overgrazing, more collections of wood and medicinal plants, and agricultural expansion) of LULC change. For programs aimed at responding effectively to negative effects of LULC change to be designed and implemented in the study area, there is the need to be about effective harmonisation of the level of perceptions and understanding of the change drivers of both the rural and urban dwellers so as to ensure that they develop a common underrating of the problem and how best to tackle it. In this regard, intensive use of environmental education and engagement of stakeholders in policy design and implementation towards responding effectively to LULC changes, are very much needed.

Declaration of Conflict of Interest

The authors declare that they have no individual relationships that could have performed to affected the work reported in this study and have no known conflict of financial interests.

References

- [1] Lambin, E.F., Geist, H., Lepers, E., 2003. Dynamics of land use and cover change in tropical regions. Annual Review of Environment and Resources. 28, 205-241.
- [2] Turner, B.L, Skole, D., Sanderson, S., et al., 1995. Land use and Land-cover Change. Science/Research Planning, IGBP Report No. 35.
- [3] Mashi, S.A., Shuaibu, H.S., 2018. People and sustainable land management: assessment of stakehold-

- ers' knowledge of the nature of landuse/cover change in Abuja, Nigeria. GeoJournal. 83(3), 545-562. DOI: https://doi.org/10.1007/s10708-017-9782-y
- [4] Kates, R.W., Haarmann, V., 1992. Where the poor live: Are the assumptions correct? Environment. 34(4), 4-28.
- [5] Lambin, E., Geist, H., 2007. Causes of land-use and land-cover change. Retrieved from http://www.eo-earth.org/view/article/150964.
- [6] Leemans, R., Lambin, E.F., McCalla, A., et al., 2003. Drivers of change in ecosystems and their services. In Ecosystems and Human Well-Being: A Framework for Assessment, ed. H. Mooney, A. Cropper, W. Reid. Washington, DC: Island Press. ISBN: 1559634030.
- [7] Meshesha, D., Tsunekawa, A., Tsubo, M., 2012a. Continued land degradation: cause-effect in Ethiopia's CRV. Land Degradation Development. 23, 130-143.
- [8] Balogun, O., 2001. Abuja: Geography of its Development. Ibadan, Nigeria, University Press Ltd.
- [9] Angelsen, A., Kaimowitz, D., 2001. Agricultural Technologies and Tropical Deforestation. Wallingford, UK: CABI Publishing. pp. 440.
- [10] Enedah, I.C., Igbokwe, J.I., Ojiako, J.C., et al., 2015. Spatio-temporal analysis and mapping of urban development trends in the Federal Capital City (FCC) Abuja, Nigeria from 1990 to 2014. International Journal of Scientific Research and Engineering Studies. 2(9), 36-39.
- [11] Kessides, C., 2005. The Urban Transition in Sub-Saharan Africa: Implications for Economic Growth and Poverty Reduction. Africa Region Working Paper Series no. 97. New York: The World Bank.
- [12] Richardson, H.W., 2005. Polarization Reversal in Developing Countries. Papers in Regional Science. 45(1), 67-85.
- [13] Meshesha, D., Tsunekawa, A., Tsubo, M., 2012b. Dynamics and hotspots of soil erosion and management scenarios of the Central Rift Valley of Ethiopia. International Journal of Sediment Research. 27, 84-99
- [14] Mengistu, D.A., Waktola, D.K., Woldetsadik, M., 2012. Detection and analysis of land-use and land cover changes in the midwest escarpment of the Ethiopian Rift Valley. Journal of Landuse Land cover Science. 7(3), 239-260.
- [15] Ariti, A.T., van Vliet, J., Verburg, P.H., 2015. Land-use and land-cover changes in the Central Rift Valley

- of Ethiopia: Assessment of perception and adaptation of stakeholders. Applied Geography. 65, 28-37.
- [16] Molla, M., 2014. Land use/land cover dynamics in the CRV Region of Ethiopia: the case of Arsi Negele District. Academy Journal of Environment Science. 2(5), 74-88.
- [17] López-Carr, D., Ryan, S.J., Clark, M.L., 2022. Global Economic and Diet Transitions Drive Latin American and Caribbean Forest Change during the First Decade of the Century: A Multi-Scale Analysis of Socioeconomic, Demographic, and Environmental Drivers of Local Forest Cover Change. Land. 11(3), 326.
 - DOI: https://doi.org/10.3390/land11030326
- [18] Lambin, E.F., Turner, B.L., Geist, H., et al., 2001. The causes of land-use and land-cover change: moving beyond the myths. Global Environmental Change. 11(4), 261-269.
- [19] Geist, H.J., Lambin, E.F., 2002. Proximate causes and underlying driving forces of tropical deforestation. BioScience. 52(2), 143-150.
- [20] Contreras-Hermosilla, A., 2000. The underlying causes of forest decline. CIFOR Occasional Paper 30, Center for International Forestry Research, Bogor, Indonesia.
- [21] Fan, F., Weng, Q., Wang, Y., 2007. Landuse and Landcover Change in Guangzhou, China, from 1998-2003, Based on Landsat TM/ETM+ Imagery. Sensors. 7, 1323-1342.
- [22] Aroengbinanga, B.W., Kaswantoa, A., 2015. Driving force analysis of landuse and cover changes in Cimandiri and Cibuni Watersheds. Procedia Environmental Sciences. 24, 184-188.
- [23] Geist, H.J., Lambin, E.F., 2004. Dynamic causal patterns of desertification. BioScience. 54(9), 817-829.
- [24] Kaswanto, N.N., Arifin, H.S., 2010. Impact of Land Use Changes on Spatial pattern of landscape during two decades (1989-2009) in West Java region. HI-KOBIA. 15, 363-376.
- [25] Angelsen, A., Kaimowitz, D., 1999. Rethinking the causes of deforestation: lessons from economic modesls. World Bank Research Observer. 14(1), 73-98.
- [26] Crosthwaite, J.J., Callaghan, Q., Farmer-Bowers, C., et al., 2004. Land use changes, their drivers and impacts on native biodiversity. Department of sustainability and environment, Victoria, USA. Hillel D.



Journal of Geographical Research

https://ojs.bilpublishing.com/index.php/jgr

Retraction Notice

RETRACTED: Innovative Practices for the Promotion of Local/Indigenous Knowledge for Disaster Risk Reduction Management in Sudur Paschim Province, Nepal

Kabi Prasad Pokhrel^{1*} Shambhu Prasad Khatiwada¹ Narayan Prasad Paudyal¹ Keshav Raj Dhakal¹ Chhabi Lal Chidi² Narayan Prasad Timilsena³ Dhana Krishna Mahat⁴

- 1. Central Department of Geography Education, Tribhuvan University, Kathmandu, Nepal
- 2. Central Department of Geography, Tribhuvan University, Kathmandu, Nepal
- 3. Central Department of Science Education, Tribhuvan University, Kathmandu, Nepal
- 4. PhD Research Scholar of Geography Education, Tribhuvan University, Kathmandu, Nepal

This article has been retracted. The original article has previously been published elsewhere without disclosure to the editor, permission to republish, or justification (i.e., redundant publication). We apologise for any inconvenience this retraction may have caused readers.

Refers to:

RETRACTED: Innovative Practices for the Promotion of Local/Indigenous Knowledge for Disaster Risk Reduction Management in Sudur Paschim Province, Nepal

Kabi Prasad Pokhrel, Shambhu Prasad Khatiwada, Narayan Prasad Paudyal, Keshav Raj Dhakal, Chhabi Lal Chidi, Narayan Prasad Timilsena, Dhana Krishna Mahat

Journal of Geographical Research, Volume 4, Issue 3, July 2021

DOI of original article: https://doi.org/10.30564/jgr.v4i3.3223

*Corresponding Author:

Kabi Prasad Pokhrel,

Central Department of Geography Education, Tribhuvan University, Kathmandu, Nepal;



Journal of Geographical Research

https://ojs.bilpublishing.com/index.php/jgr

ARTICLE

A Hybrid Geostatistical Method for Estimating Citywide Traffic Volumes – A Case Study of Edmonton, Canada

Mingjian Wu* Tae J. Kwon Karim El-Basyouny

Department of Civil and Environmental Engineering, University of Alberta, Edmonton, AB, T6G2W2, Canada

ARTICLE INFO

Article history

Received: 10 March 2022 Revised: 30 March 2022 Accepted: 05 April 2022 Published Online: 16 April 2022

Keywords:
Traffic volume
Geographical information system
Spatial modelling
Hybrid geostatistics
Network regression kriging

1. Introduction

Traffic volume information has long played an important role in various transportation research areas, including but not limited to policy making, roadway design, safety analysis and air quality control ^[1-4]. However, collecting traffic count data over a large spatial area requires a significantly substantial, and potentially prohibitive, amount

ABSTRACT

Traffic volume information has long played an important role in many transportation related works, such as traffic operations, roadway design, air quality control, and policy making. However, monitoring traffic volumes over a large spatial area is not an easy task due to the significant amount of time and manpower required to collect such large-scale datasets. In this study, a hybrid geostatistical approach, named Network Regression Kriging, has been developed to estimate urban traffic volumes by incorporating auxiliary variables such as road type, speed limit, and network accessibility. Since standard kriging is based on Euclidean distances, this study implements road network distances to improve traffic volumes estimations. A case study using 10-year of traffic volume data collected within the city of Edmonton was conducted to demonstrate the robustness of the model developed herein. Results suggest that the proposed hybrid model significantly outperforms the standard kriging method in terms of accuracy by 4.0% overall, especially for a large-scale network. It was also found that the necessary stationarity assumption for kriging did not hold true for a large network whereby separate estimations for each road type performed significantly better than a general estimation for the overall network by 4.12%.

of manpower and financial costs ^[5]. For these reasons, local governments and transportation agencies are not able to place enough monitoring equipment for the whole road network, resulting in gaps and shortages of available data. Considering the irreplaceability of traffic volume data in transportation-related studies, the focus must advance from just 'measuring' 'well-estimating' ^[6]. Thus, over many years, transportation researchers and

Mingjian Wu,

Department of Civil and Environmental Engineering, University of Alberta, Edmonton, AB, T6G2W2, Canada;

Email: mingjian.wu@ualberta.ca

DOI: https://doi.org/10.30564/jgr.v5i2.4513

Copyright © 2022 by the author(s). Published by Bilingual Publishing Co. This is an open access article under the Creative Commons Attribution-NonCommercial 4.0 International (CC BY-NC 4.0) License. (https://creativecommons.org/licenses/by-nc/4.0/).

^{*}Corresponding Author:

practitioners have made considerable efforts to produce reliable estimations of traffic volumes by applying various methodologies and tools.

One of the most widely adopted methods to date is Ordinary Least Squares (OLS) regression while using as many explanatory variables as possible. For example, Xia et al. estimated traffic volumes for nonstate roads ^[7]. In their study, 450 count-monitoring stations were involved in the investigation with up to 12 initial variables (accessibility, socioeconomic, and road characteristics) included in the multiple regression model. Using a similar method, Zhao and Chung ^[8] predicted the annual average daily traffic (AADT) on multiple roadways in an urban area through a variety of land-use and accessibility measures. Mohamad et al. utilized a multiple regression model to incorporate relevant demographic variables such as population, state highway mileage, per capita income, and the presence of interstate highways ^[9].

Various methodologies other than regression models also have been employed. Tang et al. [10] compared time series, neural network, nonparametric regression, and Gaussian maximum likelihood (GML) techniques and found that GML methods were the most promising. Lam et al.'s [11] more recent study used nonparametric models and GML methods to forecast Hong Kong's traffic volumes. Davis and Yang proposed empirical Bayesian methods that were used to compute quantiles of the predictive probability distribution of the total traffic at a highway station, given a sample of daily traffic volumes from that station [12]. These activities were based on expressions for traffic data variability and the American Association of State Highway and Transportation Officials (AASHTO) reliability concept for pavement design. Goel et al. proposed a correlation-based approach to improve AADT estimation by exploiting the inherent underlying correlations between link flows [13]. These correlations arise partially because the inflows and outflows to a node are always constrained. In addition, when the network has many origin-destination (O-D) zones, and a relatively smaller number of links, the correlation between the link flows can be large.

With the growing availability of geographic information system (GIS) datasets and the evolution of spatial analysis techniques, researchers have started to explore geostatistical methods [14,15] that exploit the spatial context of traffic and other spatial data. Studies that are most closely related to this topic include Eom et al.'s [6] use of spatial regression methods to predict AADT for nonfreeway facilities in Wake County, North Carolina, and Selby B. and Kockelman, K.M. [16] compared the AADT estimation results between universal kriging and geographically

weighted regression for Texas. They conclude that the overall predictive capability of kriging methods eclipses traditional models as well as other spatial methods. Kriging presumes spatial dependence in error terms or unobserved factors, as a function of distance. Due to its capability of accounting for the variable's interaction over space and its ease of implementation for interpolating target variables at unmeasured locations, this method continues to gain popularity for application in many transportation fields in recent years [17-20]. Like all the other geostatistical methods, kriging uses Euclidean distance to quantify the spatial separation between variables during its interpolation procedures. However, when this approach is transferred to studies targeting traffic specific variables, logically the actual network distance should be a more reasonable metric. Some prior transportation-related research studies replaced Euclidean distance with network distance in their kriging models. For instance, Zhang and Wang [21] refined the standard kriging model by using subway system network to estimate the transit ridership in New York City. Although their findings indicate that kriging using subway routes outperforms the standard ones, they are based on two short subway lines whereby making their assessment less is conclusive. Likewise, a road network is much more complex than the subway network thus greater scrutiny is necessary in order to appreciate the true benefit of implementing road network distances for estimating traffic volumes. Selby B. and Kockelman, K.M. [16] evaluated universal kriging in estimating AADT using Euclidean distances and network distances for Texas but their dataset was limited to only one-year and may not be conclusive due to its limited temporal coverage. Datasets with a longer term of traffic volume observations need to be used to further validate its estimation performance.

Table 1 summarizes the reviewed literature including their corresponding study areas, road types, findings/ contributions, and limitations. In summary, a variety of models have been proposed and developed to estimate traffic volume information with kriging proving to be a promising method for generating reliable estimates. Nonetheless, there exist very few studies that incorporate local auxiliary information into the kriging method, and no studies that utilize city-scale and long-term traffic volume datasets. Likewise, due to the limited datasets and significantly higher computational costs, kriging with network distances has rarely been used in transportation studies involving a large urban network. Furthermore, the second-order stationarity assumption, which assumes the spatial pattern of a target variable is the same across the entire study area is the most fundamental assumption

behind kriging ^[15,22]. However, whether or not this holds true for traffic volumes across the urbanized network has not been investigated in past literature.

Therefore, the primary objective of this research is to develop a hybrid geostatistical interpolation framework, as well as validate its feasibility and robustness through a real-world case study. To summarize, the main novelty and contributions of this research work include the

following:

- Utilized local auxiliary variables to detrend the data within the interpolation framework, and to explain variations in traffic volumes with respect to different locations.
- Replaced Euclidean distance with road network distance to improve the estimation accuracy and model explanation power,

Table 1. Summary of the Selected Relevant Studies of Traffic Volumes Estimation

Author(s)	Study Area	Road Types	Method	Findings/Contributions	Limitations
Mohamad, et al., 1998	Indiana	County roads	Multiple regression	Data from multiple counties were used to validate the accuracy of the developed model	
Xia, et al., 1999	Broward County, Florida	Nonstate roads	Multiple regression	12 initial variables were involved in regression models	Regression models are not able to spatially map traffic volumes across the entire road network without adequate auxiliary variables as input.
Zhao & Chung, 2001	Broward County, Florida	Interstate highwaysExpress waysUrban roadsRural roads	Multiple regression	More explanatory variables with modified data and road classifications were used to extend the previous efforts	Adopted methods lacks the considerations of spatial characteristics of road networks.
Tang, et al., 2003	Hong Kong	Major road links	Time series model Neural network Nonparametric regression (NPR) Gaussian maximum likelihood (GML)	GML model appeared to generate the most accurate predictions among the four models.	Limited data input (road types, temporal coverage, etc.). Traffic volumes were assumed
Lam, et al., 2006	Hong Kong	Major road links	Time series model Neural network Nonparametric regression (NPR) Gaussian maximum likelihood (GML)	 Extended efforts using more observations to predict the hourly traffic flows. NPR and GML appeared to be more promising. 	to be normally distributed and time dependent. • Lack of spatial analysis of traffic volumes.
Davis & Yang, 2001	NA	• Highways	Empirical bayes method	Proposed method could estimate the probable ranges and associated probability distribution.	 Included road type is highway only. Adopted method is only able to provide point estimates.
Goel, et al., 2005	NA	Highways	Correlation-based method	Developed method exploit the correlation imposed by O-D path flow.	Adopted method is sensitive to the input data configuration.
Eom, et al., 2006	Wake County, North Carolina	Urban Suburban Rural	Spatial regression Universal kriging (UK)	Comparisons between spatial regression and ordinary regression method proved the former one could provide better predictions.	Euclidean distance was used in developing the models; however, it is not the true representation of the distance in road network. Lack of spatial interaction analysis of the traffic volumes.
Selby & Kockelman, 2013	Texas	From local roads to interstate freeways	Universal kriging (UK) Universal network kriging Geographically weighted regression (GWR)	UK provided better results than GWR in the study area. UK with network distance showed no enhanced performance.	Input data were lack of long-term observations. The network distance piece was only evaluated in a single network setting.
Zhang & Wang, 2014	New York City	Subway Line	Network universal kriging	With using network distance in kriging model, the standard kriging method using Euclidean distance was improved in terms of the spatial variability analysis.	A few subway lines were selected for the study, which was a relatively simple network. Lack of long-term observed data for model performance evaluation.

- Evaluated the applicability of the proposed method using a large-scale road network (i.e., city of Edmonton),
- Investigated the second-order stationarity assumption of kriging in relation to urban network traffic volume,
- Validated the consistency of the research findings using long term traffic volume data (i.e., 10 years)

In particular, this research also aims at answering the following questions which represent the main objectives of this study.

- What local factors would contribute to enhancing the traffic volume estimations?
- To what extent and in what situations would kriging with network distances outperform standard kriging with Euclidean distances?
- How to characterize the spatial dependence (spatial variation pattern) of traffic volumes and apply them to different network configurations?

The results of this study can be an important reference source for gaining knowledge on network regression kriging and network spatial variation pattern of traffic volumes. From a practical application perspective, since kriging is capable of spatially mapping traffic volume for all unmeasured locations across an urban area, our proposed framework provides a tool for transportation practitioners and engineers to estimate traffic volume at locations abstinent of any traffic information. With complete and accurate estimations of traffic volumes, city planners and transportation agencies will be able to benefit from this in various ways [23].

2. Methodology

2.1 Regression Kriging - The Idea

As described previously, a variety of techniques have been implemented to estimate traffic volumes. Each method takes known traffic counts and/or uses auxiliary information (e.g., land use, time-steps, road geometry attributes, etc.) to make an estimation. These estimates can be separated into future-year and present-year predictions. Future-year predictions use current and past traffic count data to estimate the traffic counts at a future date. On the other hand, current-year predictions use the available data to estimate traffic counts at unmeasured locations. Kriging is typically applied in the latter situation [24,25].

Kriging is one of the most commonly used geostatistical interpolation techniques that account for the uncertainty of the estimation. It relies on the second order stationarity assumption where the mean, variance and dependence structure of the target variable do not change over space [22]. Kriging predicts the values at unsampled locations from

the weighted average of nearby measured observations. The weights are determined based on their distance from the unsampled location and their closeness to each other. Commonly used variants of the kriging method include Ordinary Kriging (OK) and Regression Kriging (RK). The main difference between the two methods is that OK assumes the mean of the target variable to be unknown but constant locally, whereas RK assumes there to be a trend associated with the auxiliary variables (e.g., longitude, latitude) [26]. In this study, RK is adopted as it incorporates two conceptually different methods to model and map spatial variability to strengthen the explanation of the target variable. The estimations are made separately for the trend (OLS in this study) and residuals (via Kriging), and then added back together as shown in Equation (1).

$$\widehat{Z}(x) = \widehat{m}(x) + \widehat{e}(x) = \sum_{i=0}^{p} \widehat{\beta}_i \cdot q_i(x) + \sum_{k=1}^{m} \lambda_k \cdot e(x_k)$$
 (1)

where $\widehat{m}(x)$ is the fitted deterministic component (i.e., the trend), $\widehat{e}(x)$ is the interpolated residual, $\widehat{\beta}_i$ are coefficients of the estimated trend model, $\widehat{\beta}_0$ represents constant term, p is the number of auxiliary variables, λ_k are kriging weights and $e(x_k)$ is the regression residual. Kriging weights for each sampling location is estimated based on the parameters of the semivariogram model, introduced in the following paragraphs, and the relative distance of the specific point with other sampling points and the unknown point.

2.2 Semivariogram

As previously mentioned, the semivariogram model depicts the spatial dependence of the measured sample points [14,25,27], and is used for linear interpolation via RK, thus constructing a good quality semivariogram is critical as it determines the accuracy of estimation results. A semivariogram is the plot of the expected value of the semivariance of the variable of interest. It is a statistic that shows how the level of similarity between two known points decreases as their separation distance increases [27]. The semivariance value can be calculated by taking the average of the squared difference of two measurements in a study domain separated by a specific and defined lag distance. The equation generally used for semivariogram estimation is shown below:

$$\gamma(h) = \frac{1}{2n(h)} \sum_{i=1}^{n(h)} \left[z(x_i + h) - z(x_i) \right]^2$$
 (2)

Here, $\gamma(h)$ is the semivariance value. $z(x_i + h)$ and $z(x_i)$ are two measurements taken at the location x_i and $(x_i + h)$ which are separated by a lag distance, h. Figure 1 shows a typical semivariogram plot [18].

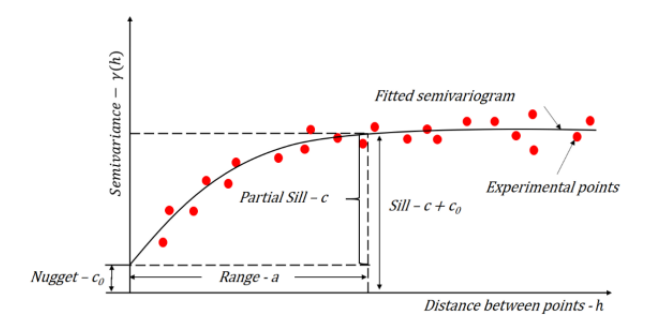


Figure 1. A Typical Semivariogram with Parameters

Three basic parameters associated with each semivariogram are the nugget, range and sill. According to theory, the semivariogram value at the origin should be zero, but due to stochastic errors such as measurement bias, the value of the semivariogram at the origin could differ significantly from zero and this is known as the nugget effect. The semivariance value at which the semivariogram levels off is known as the sill parameter. The lag distance at which the semivariogram reaches the sill value is known as the spatial range beyond which spatial dependence is considered non-existent. To assess the strength of the spatial dependence, the nugget-tosill ratio (NSR) is typically utilized as a dimensionless measure of the proportion of total observed variation that could not be explained by the observed spatial dependence of the target variable [28,29]. In other words, a small NSR represents a strong spatial dependence while a big NSR reflects a weak spatial dependence of the variable. To fit an experimental semivariogram based on observations made, there are several common theoretical forms $^{[30,27,31]}$ can be selected. The selection of fitted model types and adjustment of semivariogram parameters typically have effect on kriging estimation accuracy. However, these detailed selection/comparison processes are not the focus of this presented study, so to enforce a fair comparison between the different interpolation strategies, the spherical model (Equation (3)) was adopted for all.

Spherical model:

$$\gamma(h) = \begin{cases} 0 & ,h = 0\\ c_0 + (c - c_0) * \left(1.5\left(\frac{h}{a}\right) - 0.5\left(\frac{h}{a}\right)^3\right) & ,0 < h < a \\ c & ,h \ge a \end{cases}$$
 (3)

Here, h = lag distance, a = spatial range of continuity and c = sill.

2.3 Hybrid Geostatistical Interpolation Framework

The standard RK method, including the construction of the semivariogram model, is all based on the Euclidian distance metric; however, this might not be a reasonable way of interpolating traffic-related variables (i.e., traffic volumes in this study) which may strongly be correlated with the road network. Therefore, when constructing the semivariogram. Euclidean distances are replaced with road network distances thus providing a better representation of the spatial dependence between the measured traffic count points. This simple change makes the standard RK wholly based on the road network distance. Figure 2 illustrates the key steps of the hybrid geostatistical interpolation framework using network regression kriging. It is worth noting that the proposed framework as a whole is transferrable to other cities. Additionally, the target variable (traffic volume in this study) can be replaced with other traffic-related variables (e.g., traffic collisions, congestions, etc.); however, the detailed parameters (e.g., auxiliary variables for detrending data) involved in this framework needs to be recalibrated, which will depend on the type and availability of the input data.

The first step is to obtain the network distances between each point. This includes the distances between measured points and also the distances between measured points and unmeasured points of interest. This can be done by the Network Analyst extension in ArcGIS [32]. The second step is to remove the trend (i.e., the deterministic component) of the measured data points, to show only the true spatial variation of the traffic volumes. The detrended traffic volumes (i.e., the residuals) would be used as the input into the semivariogram modelling where python [33] and scikit-gstat package [34] are utilized. Kriging is then used to estimate the residuals for each point based on the semivariograms constructed in the previous step, and the final traffic volume estimates can be obtained by adding the estimated residuals and the deterministic components. Olea's study regarding the steps of constructing an appropriate semivariogram model is used as a guideline during the whole process [27].

To ensure that the semivariogram model is of good quality and to compare the estimation accuracy between different estimation strategies, cross-validation is utilized to check the estimation performance. In this study, the root-mean-square-error (RMSE) was calculated using the "leave one out" method that checks the prediction error of each point individually to ensure that the overall prediction accuracy is acceptable [35,27]. RMSE is an indicator of how closely the model estimates matches the measured values. For this reason, it is widely used in cross validation to evaluate the quality of the constructed semivariogram. The equation of RMSE can be found below.

$$RMSE = \sqrt{\frac{\sum_{i=1}^{i=n} (Z_i - \widehat{Z}_i)^2}{n}}$$
 (4)

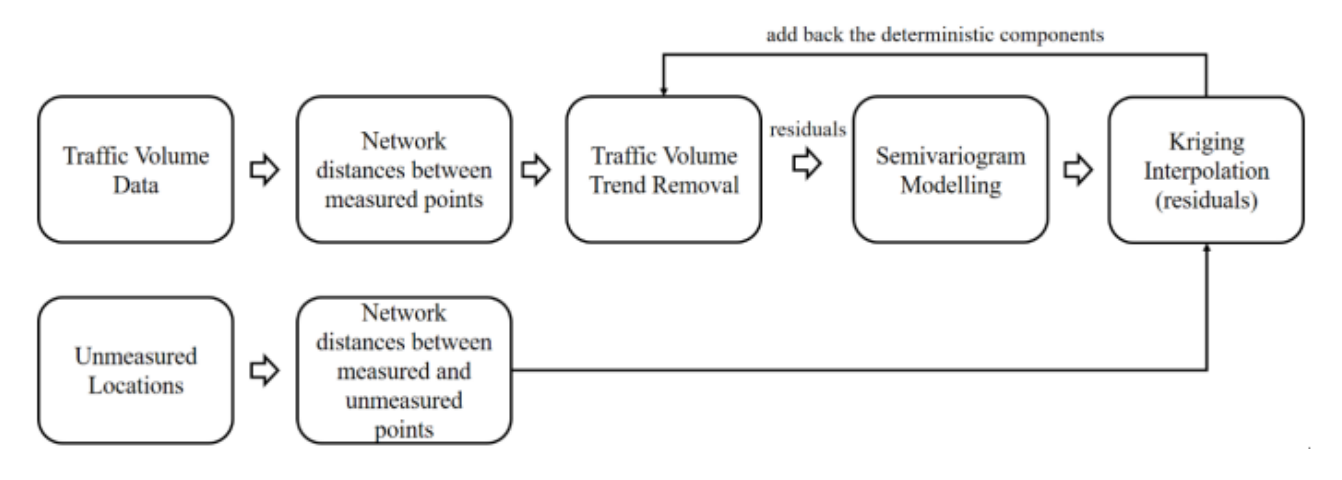


Figure 2. Proposed Hybrid Geostatistical Interpolation Framework

Here, n is the total number of measured points.

3. Case Study

3.1 Study Area: Edmonton, Alberta, Canada

As mentioned above, the road network for the city of Edmonton is used for the case study. To date, there are 233 arterials (1894 km), 699 collectors (886 km) and 2,394 local roads (2624 km) in total. Based on the function and traffic conditions of the city districts, the whole city is divided into two zones. The core zone is the dense areas in the centre of the city that have far more active transportation mode use like walking, cycling and public transportation. It mostly consists of local and collector roads and carries the main functions of residence and commerce. By contrast, the non-core zone is the rest of the city where social vehicles and trucks are the main modes of transportation. It is mainly used by commuters, intercity travelers, industrial, and agricultural industries.

3.2 Data Sources and Processing

Traffic volume data were obtained from the City of Edmonton Open Data Portal where the city road network shapefile and historical (2008-2018) traffic volume data were provided. The traffic volume data were collected by loop detectors or by manual counting on weekdays. Since not all the measurement locations had year-round monitoring, average-daily-traffic volume (ADT) for each detection site was calculated and used in this study. Table 2 summarizes the collected ADT data with descriptive statistics, while Figure 3 displays the study areas along with the different road types and the boundary

of the core zone. All detection sites are also shown in the same figure. The year 2017 was not included in the following analysis due to insufficient data. The road network distance between each pair of ADT points was obtained using the Network Analyst extension in ArcGIS [32], which lets us find the shortest route between locations along a network of transportation routes.

3.3 Trend Removal of Traffic Volumes

As previously described, the first step involved in the framework is to remove the trend of the target variable (i.e., the ADT) as much as possible so that the true spatial variation pattern of ADT can be observed. In this study, the linear regression with ordinary least squares (OLS) was adopted in removing the trend or the deterministic part of the kriging model. It is worth noting that linear regression is not the only method that can be employed here, however, the focus of this study is not on the detrending techniques while the linear regression model is one of the most widely used and effective methods that allows us to gain a deeper understanding of the influence that each covariate has in explaining the variations of ADT [6,20,16,21,8]. Available local auxiliary information in Edmonton for each detection site included the road type (eight types in total which were converted into numerical variables according to road class level), speed limit (30 km/h - 110 km/h) and local accessibility factors such as the distance to the nearest school and distance to the nearest senior residence, all of which were used in the stepwise multiple linear regression analysis by fitting a first-order polynomial model. The p-value was adopted to confirm the statistical significance between ADT and the auxiliary variables in a 5% significance level. Table

Table 2. Descriptive Statistics of the Collected Average Daily Traffic (ADT) Volume Data

Year	# measured ADT points	Maximum ADT	Minimum ADT	Average ADT	Standard Deviation	Proportions in Arterial/Collector/Other roads
2008	415	26196.0	17.5	7478.8	6034.6	84.3%/ 15.0%/ 0.7%
2009	425	33989.0	28.5	5742.3	5961.9	68.7%/ 30.8%/ 0.5%
2010	494	39520.0	38.0	5796.0	5956.6	68.2%/ 31.1%/ 0.6%
2011	581	45142.0	59.0	6070.8	7337.3	62.5%/ 37.1%/ 0.4%
2012	521	52727.0	49.5	8269.6	8965.1	75.0%/ 24.8%/ 0.2%
2013	700	50818.0	16.5	9546.7	9189.5	82.8%/ 15.8%/ 1.3%
2014	905	53171.5	56.5	10016.5	9141.8	84.7%/ 14.5%/ 0.8%
2015	1174	60066.0	78.5	10646.2	9209.0	81.6%/ 17.7%/ 0.6%
2016	1035	47176.0	43.5	9961.5	7896.4	85.3%/ 13.8%/ 0.9%
2017	8	7129.0	561.5	3018.0	2406.9	62.5%/ 37.5%/ 0.0%
2018	238	49487.0	130.5	9105.0	7646.4	89.9%/ 8.0%/ 2.1%

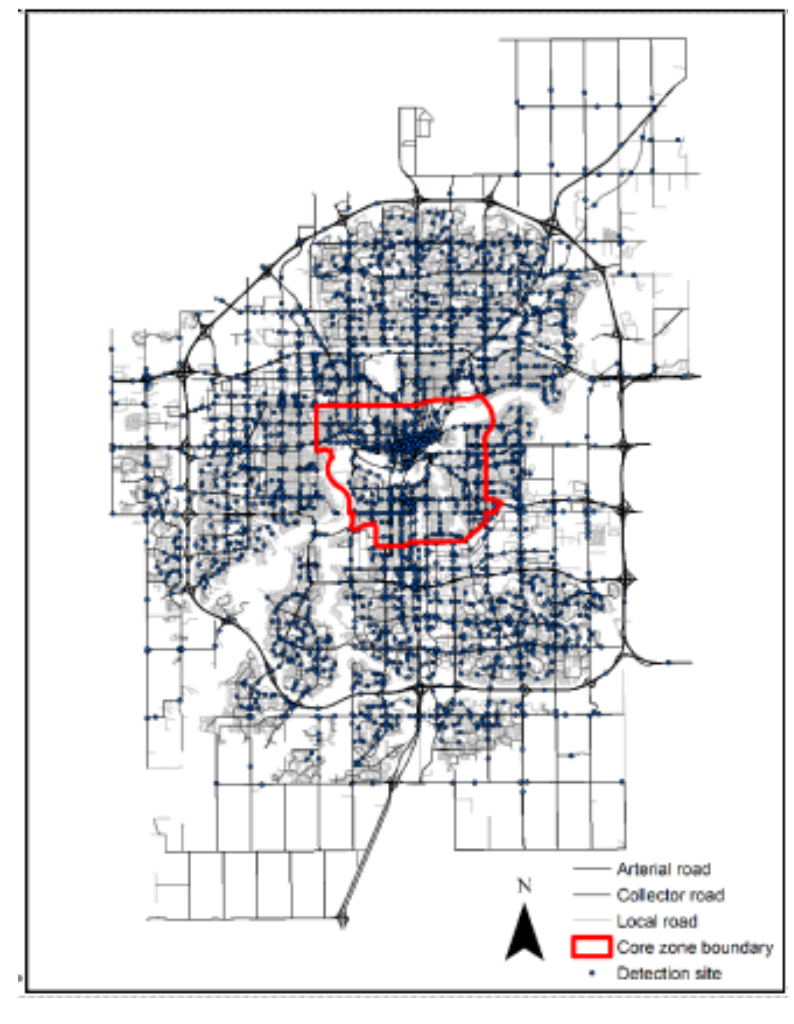


Figure 3. The Study Area – Edmonton, Alberta

Table 3. Linear Regression Results for Traffic Volume Trend Remov
--

Year	Road Type	Speed Limit	Distance to Nearest Senior Residence Distance to Nearest School		R2
2008	-5185.387	1687.224	99.019	_	30.6%
2009	-10800.105	1330.000	223.670	-	36.4%
2010	-12610.012	1270.851	256.203	-	39.6%
2011	-17979.301	1308.853	375.761	-1.234	48.0%
2012	-21996.595	1369.502	447.581	-1.278	59.2%
2013	-22324.391	2185.237	389.300	-	51.2%
2014	-22547.419	1991.376	414.489	-	48.3%
2015	-24068.033	2045.341	461.151	-1.224	53.1%
2016	-17932.787	2082.277	327.148	-	42.0%
2018	-30951.479	899.345	647.308	-	52.0%

Note: eight road types are converted into numerical variables.

- Arterial-Class A (Primary Highway Truck Route) = 8;
- Arterial-Class B (Non-Primary Highway Truck Route) = 7;
- Arterial-Class C (Truck Route Low speeds) = 6;
- Arterial-Class D (Non-Truck Route Low speeds) = 5;
- Collector-Commercial (Adjoining lots zoned > 50% Commercial) = 4;
- Collector-Industrial (Adjoining lots zoned > 50% Industrial) = 3;
- Collector-Residential = 2;
- Other (e.g., local roads) = 1.

3 summarizes the calibrated parameters, and only those variables with *p*-values less than $\alpha = 0.05$ are included.

As can be seen from the linear regression results, road type, speed limit, and distance to the nearest senior residence are all consistently significant variables that can explain the variation of ADTs in each year. In 2011, 2012 and 2015, the distance to the nearest school is also a significant variable in this step. Signs of the calibrated coefficients all make sense, as higher classes of roads (e.g., primary highway truck route) hold more traffic volumes compared with lower classes (e.g., local roads); roads with higher speed limits also tend to hold more traffic volumes as they are either interstate highways or arterials that serve the most commuters. In terms of the local accessibility factors that may only be applicable to Edmonton, the shorter the distance to a senior residence is, the larger the traffic volume tends to be, as most of the senior residences in Edmonton are located near major arterial roads. This also partially applies to the schools, but it depends on the locations of detection sites in specific years, implying that changing sampling locations may have an impact on the estimation performance of the regression.

Although the regression models were able to moderately remove underlying spatial trend, the low R² values indicate the need for performing spatial interpolation via kriging using residual values to further improve the estimation accuracy. The next is to construct semivariogram models based on the residuals of the regression models and implement regression kriging under different scenarios

and road network configurations.

3.4 Semivariogram and Regression Kriging

In this section, the comparison results including the spatial dependence and estimation accuracy between standard kriging and network kriging are presented. As shown in Table 2, ADT values can vary a lot between each year, and to understand the network model performance in different network settings, as well as assess the stationarity assumption of ADT, the study repeated the same analysis procedures for three different network configuration groupings. The first grouping (Case I) considers the whole city-wide network, the second grouping (Case III) is the district functions of core and non-core zones, and the final grouping (Case III) is a separation between arterial and collector road types. As mentioned previously, all semivariograms were fitted using the spherical model in order to enforce a consistent and fair comparison.

3.4.1 Case I: Whole Network

Following the steps of the standard kriging and network kriging (Figure 2), the semivariogram models of two distance metrics for each year were first constructed based on the same data points. Figure 4 includes all the semivariogram models that were developed by carefully following the procedures and guidelines from Olea's publication [27].

As can be seen from Figure 4, the general shapes

and sill values remain similar in each pairing while the nugget values of network models are consistently smaller compared with the standard ones. This also leads to different spatial dependence patterns between the two models. Figure 5 vividly shows the comparisons between the four parameters of the two types of semivariogram models, *t*-tests were also employed to examine the significance of the differences (Note: * represents the *p*-value is significant at 5% significance level).

From the t-test values, it can be concluded that the nugget and the nugget-to-sill ratio (NSR) values of network-distance semivariogram models are significantly smaller as compared to their Euclidean distance counterpart. This means the stochastic effect or the variance of ADT within a very short lag distance are reduced dramatically and thus the stronger spatial dependence of ADT can be observed. The reason can be the use of network distance takes the actual road network into account which avoids the situation where one low traffic volume road segment is considered adjacent to a highway segment even if there is no direct connection between them. In addition, the nugget and NSR values change dramatically over the 10-year period, which implies that the spatial configuration of the ADT detection sites has an impact on the representativeness of the ADT spatial variation pattern. The travel behavior changes over time (i.e., temporal pattern) in the city of Edmonton is also one of the possible reasons. This will need further investigation in the future, but unfortunately, it will be out of scope for this study. Figure 5 suggests that there is no significant difference present in the sill values, and this is because sill values represent the maximum variance between ADT values within the sampling scale, points that are far away from each other in Euclidean distances are likely to be far away from each other in network distance as well, thus the use of network distance does not affect sill value much. For the range values of semivariograms, it is a parameter that is highly correlated with the ADT sampling distribution and thus makes estimating the true range complicated hampering its use in comparisons [36]. Thus, for the other two groups, only the nugget and NSR values calibrated from their corresponding semivariograms were used for comparisons.

After the semivariogram models were constructed, the cross-validation was implemented to compare the estimation accuracy between the two-distance metrics. RMSE values suggest that using network distance led to an average improvement of 4.0% for all of the years. The *t*-statistic between them is 5.473 with the *p*-value being equal to 0.000, which means network kriging is able to consistently provide significantly more accurate estimates

compared to the standard one for the whole city road network.

It is worth noting that the percentages of the improvement vary for each year (i.e., 1% to 9%). The reason for the variation can be attributed to the sampling distribution of the measured ADT points, as the city keeps expanding its scale during these 10 years thus changing most of the locations of the ADT detection sites every year.

Since the computational costs of the network model are exponentially higher than the standard one, it is important to distinguish the situations under which applying network kriging is worth the increased effort. In other words, there is a need to identify the situations where the network semivariogram model and RK method can significantly outperform the standard ones.

3.4.2 Case II: Core Zone and Non-core Zone

The same comparison procedures are repeated between core zone (downtown) and non-core (suburb) zone of the city to see if the model would perform differently under varying network configurations. Calibrated nugget and NSR values are compared in Table 4. Years with insufficient data for both zones are excluded from this analysis.

Although results show that the network kriging model is able to reduce the nugget effect, better represent spatially dependence, and generate more accurate results in both core and non-core zones, the t-test values indicate that the differences were seen in the RMSE values between standard and network models are not statistically significant in the core zone (t-statistic: 0.919; p-value: 0.194) while they do differ significantly in the non-core zone (t-statistic: 2.057; p-value: 0.039). The reason for this can be attributed to the density and scale of the networks. For example, the core zone has a smaller spatial scale than that of the non-core zone and that varying distance metrics do not play a significant role due to having higher network density. Additionally, the shape of the road segments within the core-zone is mostly straight thus making the differences between Euclidean and network distance kriging less dramatic.

Therefore, it can be concluded that the marginal benefits gained by using network kriging on a small and dense network with straight road segments is not worth the extra effort. By contrast, a widely spread-out network, or a network with a considerable number of curvy roads, can benefit significantly more from the network model. Additionally, calibrated nugget and NSR values in Table 4 also imply the same conclusion as discussed in Case I, regardless of the zone area, ADT detections sites' configuration affects the semivariogram model. The

temporal pattern of travel behavior also needs future investigation. Another point worth mentioning here is that the semivariogram models for each year were very different between the core and non-core zones, which infers that the stationarity assumption (i.e., translation invariance) of ADT may not hold true across large urban

area. In other words, one single semivariogram model may not be able to represent the spatial pattern of all ADTs in the network as a whole thereby warranting a need to develop separate semivariogram models by taking into account the underlying characteristics of road networks under investigation.

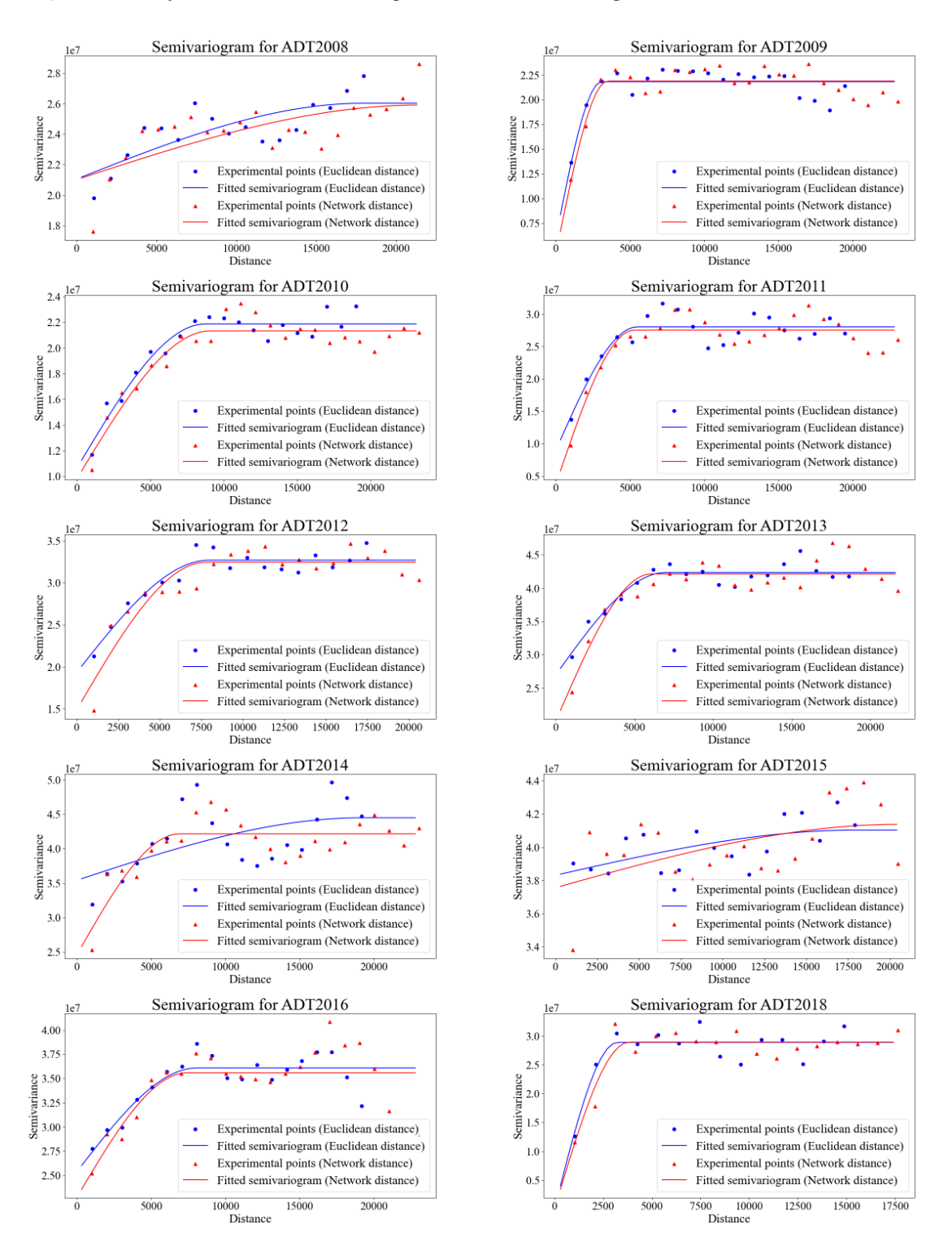


Figure 4. Constructed Semivariogram Models

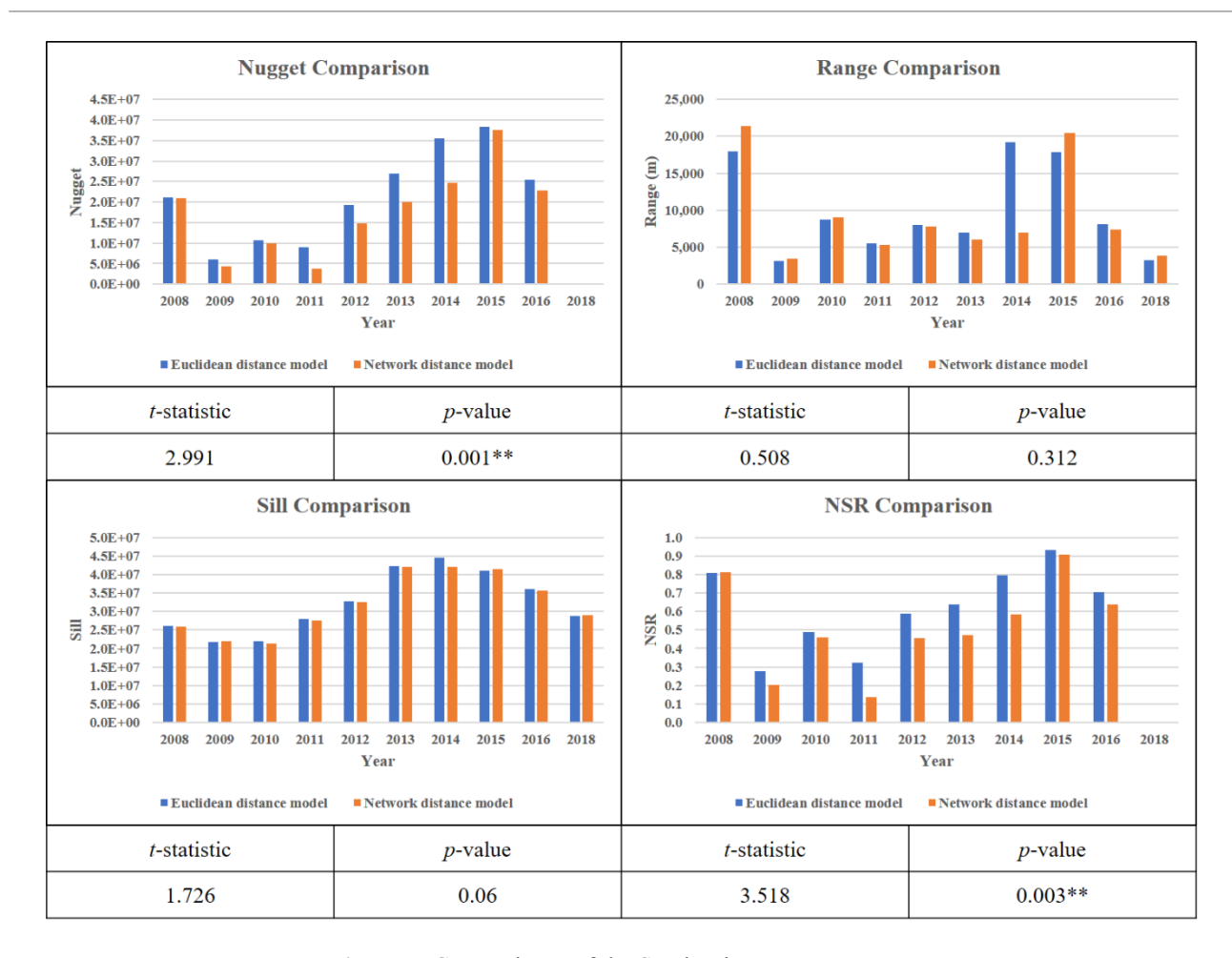


Figure 5. Comparisons of the Semivariogram Parameters

Table 4. Calibrated Semivariogram Parameters for Core vs Non-core Zones

Year	Core Zone (Euclidean)		Core Zone (Network)		Non-core Zone (Euclidean)		Non-core Zone (Network)	
	Nugget	NSR	Nugget	NSR	Nugget	NSR	Nugget	NSR
2008	6.3E+06	3.4E-01	7.3E+06	4.0E-01	3.1E+07	7.6E-01	2.2E+07	5.7E-01
2009	-	-	-	-	1.3E+07	3.7E-01	1.1E+07	2.9E-01
2010	1.2E+07	6.0E-01	1.1E+07	5.5E-01	1.6E+07	4.1E-01	1.6E+07	3.9E-01
2011	2.3E-06	9.1E-14	5.2E+05	2.0E-02	2.5E+07	4.2E-01	1.7E+07	2.8E-01
2012	2.2E+07	9.9E-01	1.9E+07	8.4E-01	6.0E+07	6.5E-01	3.0E-10	3.3E-18
2013	2.1E+07	7.6E-01	1.7E+07	6.2E-01	2.9E+06	2.9E-02	7.9E+06	7.9E-02
2014	2.1E+07	6.1E-01	5.3E+06	1.7E-01	7.4E-09	7.6E-17	1.1E-06	1.1E-14
2015	3.8E+07	9.9E-01	3.0E+07	1.0E+00	8.1E+07	8.0E-01	7.4E+07	7.2E-01
2016	2.2E+07	6.6E-01	2.2E+07	6.6E-01	3.6E+07	5.2E-01	3.5E+07	5.1E-01
2018	-	-	-	-	1.0E+07	1.4E-01	6.0E+06	8.3E-02

3.4.3 Case III: Arterial and Collector

To further examine whether the stationarity assumption is true or not for the study area, this section investigates the differences between semivariogram models tailored for different road types, namely, arterial and collector roads. The model development procedures remain the same as described in the previous sections, and the years with insufficient data for both road types are again excluded from this analysis. All models were fitted using the same spherical form. Their calibrated semivariogram parameters are shown in Table 5.

It is implied that the spatial dependence pattern can be very different between the two road types, as the calibrated parameters differ from each other significantly. For example, the nugget values in arterials are dramatically bigger than those in collectors, this is because arterial roads tend to carry most of the traffic flows of the city especially for intercity trips, and industrial and agricultural travels, thus the magnitude of the variances can be also higher for this road type. In addition, the calibrated semivariogram parameters vary over time regardless of the road type. This implies that the impact of ADT detection sites' configuration and the temporal pattern of travel behavior in the city of Edmonton will require further investigation in future work.

The ultimate goal of this research is to provide more

2016

2018

2.8E+07

8.7E-08

6.8E-01

2.8E-15

2.5E+07

6.7E-07

accurate estimates of traffic volumes, cross-validation was conducted to assess the estimation accuracy for the separate estimations for arterial and collector roads. RMSE values were used to compare and contrast the ADT estimates from the various semivariogram models developed using separate road types, keeping all roads together, and network distances. Results show that compared to using Euclidean distance in kriging without separating the road types, network distance kriging while considering semivariograms separately can, once again, improve the ADT estimation accuracy by 4.12% on average for the entire urban network while the *t*-test also validates that it is a statistically significant improvement (*t*-statistic: 5.828; *p*-value: 0.000).

3.5 Spatial Mapping of Traffic Volumes

With the semivariogram models calibrated and validated for each year, the proposed hybrid geostatistical approach was used to interpolate the missing ADTs for the entire city network. This method utilized the midpoints of each road segment that are split by intersections as shown in Figure 6.

As described previously, the major difference in implementing network kriging compared with the standard one is to replace the Euclidean distance with the network distance. Therefore, the network distance matrix based on the shortest path for all measured and unmeasured

Year _	Arterial (Euclidean)		Arterial (Network)		Collector (Euclidean)		Collector (Network)	
	Nugget	NSR	Nugget	NSR	Nugget	NSR	Nugget	NSR
2008	2.4E+07	8.1E-01	1.9E+07	6.7E-01	2.6E+06	6.8E-01	2.3E+06	5.7E-01
2009	3.8E+05	1.3E-02	9.7E-10	3.2E-17	1.8E-13	5.0E-20	6.5E-09	1.9E-15
2010	1.7E+07	5.4E-01	1.4E+07	4.8E-01	1.7E+06	4.3E-01	1.6E+06	4.0E-01
2011	2.6E-02	6.3E-10	6.4E-11	1.6E-18	4.1E+05	6.8E-02	2.8E-09	4.7E-16
2012	2.9E+07	6.6E-01	2.3E+07	5.6E-01	3.0E-07	5.0E-14	4.3E-10	7.1E-17
2013	3.0E+07	6.1E-01	2.4E+07	4.8E-01	-	-	-	-
2014	3.5E+07	6.8E-01	2.6E+07	5.4E-01	1.6E-11	1.0E-18	1.3E+07	1.0E+00
2015	4.3E+07	9.3E-01	4.2E+07	9.0E-01	4.3E-05	2.1E-12	6.8E-13	3.4E-20

6.2E-01

2.2E-14

1.1E-09

1.5E-16

3.4E+05

 Table 5. Calibrated Semivariogram Parameters for Arterial vs Collector

4.6E-02

locations were generated firstly via ArcGIS [32] and then input into kriging along with the corresponding best-fitted spherical semivariogram models. As a result, 2008, 2009, 2010, 2011, 2012, 2013, 2014, 2015, 2016 utilized the separated-road type network semivariograms while 2013, 2018 utilized their citywide network semivariograms. These interpolated ADT values reflect the true spatial distribution pattern as the ring road and the areas within it is shown to have higher traffic volumes as compared to the areas outside the ring road (i.e., the far northern and far southern parts of the city where people rarely go). Furthermore, years with interpolation using separated semivariogram models (with * marked in title) tend to distinguish the traffic volume differences more prominently between road types.

Although more case studies using different network sizes and traffic related variables (e.g., collision frequency) are required to further attest to the conclusiveness of the results generated herein, the findings of this study provide significant contributions to areas in need of utilizing

accurate traffic volume information with limited traffic detectors.

3.6 Summary of Research Findings

With the adoption of the proposed hybrid interpolation framework to estimate and spatially map ADT across the city of Edmonton, several findings were made from the three case studies (i.e., Case I, II, III). These findings are summarized below:

- Network semivariogram was able to better represent the spatial variation pattern of ADT within the road network. When compared with semivariogram models using Euclidean distance (Case I, II, III), network semivariogram has lower nugget and NSR values [37].
- Estimating ADT using network kriging was consistently more accurate than standard kriging with Euclidean distance ^[21]. This finding was supported by cross-validation results using the 10 years of data (Case I).
- Small and dense networks where roads are fairly straight were not worth performing network kriging due

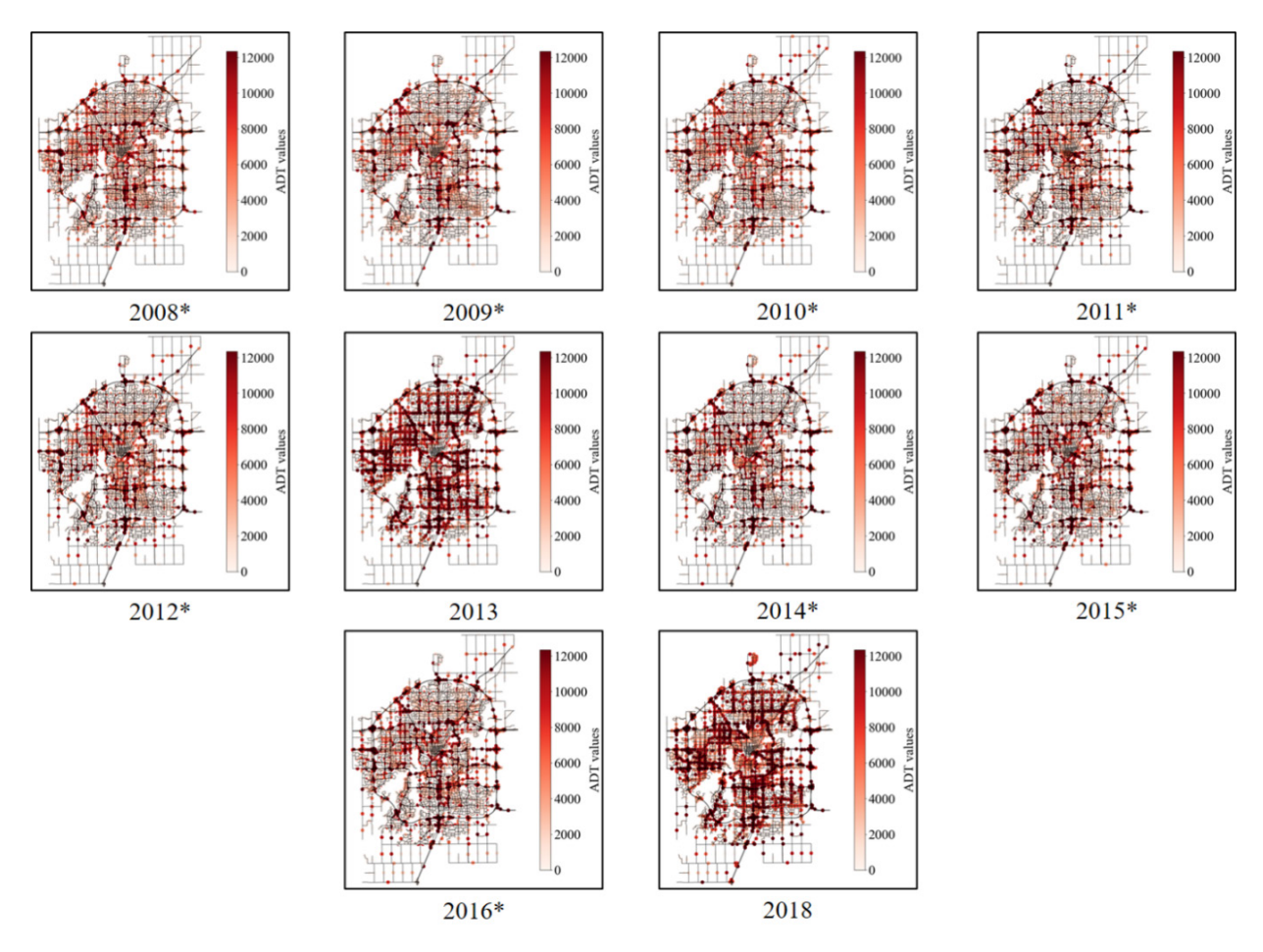


Figure 6. Interpolated ADT maps via Network Regression Kriging

to its low return and substantial computational cost. In Case II, estimated ADT values using two distance metrics have no significant difference in the non-core zone, which supports this finding.

- The imposed stationarity assumption of ADT did not hold true for the entire study area. This was evident from the different semivariogram parameters calibrated with respect to different city zones and road types (Case II, III).
- Estimating ADT using network kriging with multiple road types and semivariograms (Case III) was significantly more accurate than estimating using Euclidean distance with a single semivariogram.
- Semivariogram parameters (e.g., nugget, range, NSR) changed dramatically over time regardless of zone and road types, which implies that the configuration of ADT detection sites has an impact on the spatial variation pattern representativeness, and thus will potentially affect the overall estimation accuracy. The temporal pattern of travel behavior in the city of Edmonton also needs further investigation.
- Interpolated ADT (Figure 6) using our proposed method was able to successfully reflect the true spatial distributions of the traffic volumes in the city.

Since the data employed in this case study covers 10 years of ADT observations, and our findings regarding the network regression kriging performance are consistent with previous relevant studies [11,38,16,7,21], it can be said that our proposed hybrid geostatistical interpolation framework and research findings are transferrable and applicable to other cities as well as other traffic related variables. One thing to note is, some of the detailed parameters or settings (e.g., variables in detrending step, semivariogram type, etc.) may differ depending on the data of interest and availability.

4. Conclusions and Future Research

In this research, a hybrid geostatistical interpolation framework for estimating city-wide traffic volumes was developed by applying linear regression models to remove trends within ADT and performed kriging with network distances using semivariogram models constructed for each estimation year. A case study in Edmonton was conducted to compare the estimation accuracy between the standard and network models. Linear regression models consistently show that road types, speed limits and accessibility to senior residences are significant explanatory variables over the 10 years, and accessibility to schools may also be a significant variable depending on the distribution of sample sites. Overall, the network semivariogram model better represents the spatial interaction pattern of the traffic volumes. It significantly

reduces the nugget effect while also forming a stronger spatial dependence by generating a lower NSR. For a large road network (e.g., the whole city network, noncore zone), network kriging consistently and significantly outperforms standard kriging by providing more accurate traffic volume estimates. By contrast, on a small scale and dense road network with road segments that are not very curvy (e.g., core-zone), the standard kriging method based on Euclidean distance is still able to provide reliable estimates, and the semivariogram model is also able to adequately represent the spatial interaction of traffic volumes. Furthermore, it is also found that the stationarity assumption for traffic volumes does not hold true thereby indicating that the semivariogram model constructed over a particular zone/network configuration may not be representative of the actual spatial interaction for all zones or different road types in the city. This also suggests that separate estimates for different road types using their corresponding semivariogram models can produce more accurate estimates overall.

In conclusion, within the area of traffic estimation, our research provides several contributions. First, a hybrid geostatistical interpolation framework was developed, which involves the use of local auxiliary variables and road network metrics. This interpolation framework is a powerful tool that transportation agencies can employ when their traffic information is limited. In addition, this is also the first time that long-term and large urban datasets are used to prove the feasibility and robustness of our proposed framework. And lastly, it was demonstrated that with semivariogram models, using network distances can allow us to better understand the spatial variation patterns of traffic volume. Furthermore, this research also contributes to identifying situations where the application of network kriging is not necessary considering the substantially high computational costs required of it. Furthermore, the imposed stationarity assumption placed on the whole network did not hold true since semivariogram models developed for different zones and road types led to improved estimation performance. It is expected that with more accurate ADT estimation/ mapping results (as shown in Figure 6) and a better understanding of the ADT spatial pattern, transportation authorities can make more robust and accurate decisions on transportation-related activities.

This research can be extended in several directions. First, the same approach proposed in this study can be directly implemented in any other traffic-related cases where the use of network distance is more reasonable. Given the studies done in the past using Euclidean distances, there are lots of studies that can be re-done

using network distances such as traffic congestion, collisions, emissions and so on [38-40]. Secondly, the distribution of the sampling sites is suspected to affect the modeling and estimation performance as can be seen from the 10-year RMSE values and calibrated nugget values. Therefore, additional efforts into developing optimal traffic-count sampling strategies will be required to optimize the traffic monitoring capabilities and to further improve estimation performance. It would be also beneficial to use the data collected over same geographic locations but over different years in an attempt to further validate the conclusiveness and transferability of our findings. Thirdly, instead of converting road types into numerical values, they can also be hot-coded or binarycoded (e.g., major roads vs other roads) to quantify the effect of different road types have on ADT and their contributions to improving the accuracy of interpolating citywide traffic volumes. Lastly, the calibrated parameters of our linear regression models (i.e., coefficients of the auxiliary variables) and semivariograms (e.g., range) tend to vary drastically, which implies that people's travel behavior within the city of Edmonton is changing over time. Further investigation of this temporal pattern can be a potential future research topic.

Acknowledgement

The authors would like to thank the City of Edmonton for providing financial support and the data used in this study. The authors would also like to acknowledge the anonymous reviewers for their suggestions that have contributed to improving the quality and the readability of the manuscript.

Conflict of Interest

All authors declare that they have no conflicts of interest.

References

- [1] Elvik, R., Høye, A., Vaa, T., et al., 2009. The Contribution of Research to Road Safety Policy-Making. The Handbook of Road Safety Measures, Emerald Group Publishing Limited. pp. 117-141.
 DOI: https://doi.org/10.1108/9781848552517-006.
- [2] Minderhoud, M.M., Botma, H., Bovy, P.H.L., 1997. Assessment of Roadway Capacity Estimation Methods. Transportation Research Record. 1572(1), 59-67.
 - DOI: https://doi.org/10.3141/1572-08
- [3] Rakowska, A., Wong, K.C., Townsend, T., et al., 2014. Impact of traffic volume and composition on

- the air quality and pedestrian exposure in urban street canyon. Atmospheric Environment. 98, 260-270.
- DOI: https://doi.org/10.1016/j.atmosenv.2014.08.073
- [4] Wu, M., Kwon, T.J., El-Basyouny, K., 2020. A Citywide Location-Allocation Framework for Driver Feedback Signs: Optimizing Safety and Coverage of Vulnerable Road Users. Sustainability. 12(24), 10415.
 - DOI: https://doi.org/10.3390/su122410415
- [5] Skszek, S.L., 2001. State-of-the-art report on non-traditional traffic counting methods. Arizona.
- [6] Eom, J.K., Park, M.S., Heo, T.Y., et al., 2006. Improving the Prediction of Annual Average Daily Traffic for Nonfreeway Facilities by Applying a Spatial Statistical Method. Transportation Research Record. 1968(1), 20-29.
 - DOI: https://doi.org/10.1177/0361198106196800103
- [7] Xia, Q., Zhao, F., Chen, Z., et al., 1999. Estimation of Annual Average Daily Traffic for Nonstate Roads in a Florida County. Transportation Research Record. 1660(1), 32-40.
 - DOI: https://doi.org/10.3141/1660-05
- [8] Zhao, F., Chung, S., 2001. Contributing factors of annual average daily traffic in a Florida county: exploration with geographic information system and regression models. Transportation Research Record. 1769(1), 113-122.
 - DOI: https://doi.org/10.3141/1769-14
- [9] Mohamad, D., Sinha, K.C., Kuczek, T., et al., 1998. Annual Average Daily Traffic Prediction Model for County Roads. Transportation Research Record. 1617(1), 69-77.
 - DOI: https://doi.org/10.3141/1617-10
- [10] Tang, Y.F., Lam, W.H.K., Ng, P.L.P., et al., 2003. Comparison of four modeling techniques for short-term AADT forecasting in Hong Kong. Journal of Transportation Engineering. 129(3), 271-277. DOI: https://doi.org/10.1061/(ASCE)0733-947X (2003)129:3(271)
- [11] Lam, W.H.K., Tang, Y.F., Chan, K.S., et al., 2006. Short-term Hourly Traffic Forecasts using Hong Kong Annual Traffic Census. Transportation. 33(3), 291-310.
 - DOI: https://doi.org/10.1007/s11116-005-0327-8
- [12] Davis, G., Yang, S., 2001. Accounting for uncertainty in estimates of total traffic volume: an empirical Bayes approach. Journal of Transportation and Statistics. 4(1), 27-38.
- [13] Goel, P.K., McCord, M.R., Park, C., 2005. Exploiting Correlations between Link Flows to Improve Estimation of Average Annual Daily Traffic on Coverage Count Segments: Methodology and Numerical Study.

- Transportation Research Record. 1917(1), 100-107. DOI: https://doi.org/10.1177/0361198105191700112
- [14] Matheron, G., December 1963. Principles of geostatistics. Economic geology. 58(8), 1246-1266.DOI: https://doi.org/10.2113/gsecongeo.58.8.1246
- [15] Chiles, J., Delfiner, P., 2009. Geostatistics: modeling spatial uncertainty, John Wiley & Sons.
- [16] Selby, B., Kockelman, K.M., 2013. Spatial prediction of traffic levels in unmeasured locations: applications of universal kriging and geographically weighted regression. Journal of Transport Geography. 29, 24-32. DOI: https://doi.org/10.1016/j.jtrangeo.2012.12.009
- [17] Kwon, T.J., Fu, L., 2017. Spatiotemporal variability of road weather conditions and optimal RWIS density—an empirical investigation. Canadian Journal of Civil Engineering. 44(9), 691-699. DOI: https://doi.org/10.1139/cjce-2017-0052
- [18] Wu, M., 2020. Evaluating the Safety Effects of Driver Feedback Signs and Citywide Implementation Strategies.
 - DOI: https://doi.org/10.7939/r3-xwkc-1112
- [19] Biswas, S., Wu, M., Melles, S.J., et al., 2019. Use of Topography, Weather Zones, and Semivariogram Parameters to Optimize RoadWeather Information System Station Density across Large Spatial Scales. Transportation Research Record. 2673(12), 301-311. DOI: https://doi.org/10.1177/0361198119846467
- [20] Gu, L., Wu, M., Kwon, T.J., November 2019. An Enhanced Spatial Statistical Method for Continuous Monitoring of Winter Road Surface Conditions. Canadian Journal of Civil Engineering. 47(10), 1154-1165.
 - DOI: https://doi.org/10.1139/cjce-2019-0296
- [21] Zhang, D., Wang, X.C., 2014. Transit ridership estimation with network Kriging: a case study of Second Avenue Subway, NYC. Journal of Transport Geography. 41, 107-115.
 - DOI: https://doi.org/10.1016/j.jtrangeo.2014.08.021
- [22] Gneiting, T., Genton, M.G., Guttorp, P., 2006. Geostatistical space-time models, stationarity, separability, and full symmetry. Monographs On Statistics and Applied Probability. 107, 151.
- [23] Roll, J., 2019. Evaluating Streetlight Estimates of Annual Average Daily Traffic in Oregon.
- [24] Cressie, N., 1990. The origins of kriging. Mathematical Geology. 22(3), 239-252.
 DOI: https://doi.org/10.1007/BF00889887
- [25] Lichtenstern, A., 2013. Kriging methods in spatial statistics.
- [26] Hengl, T., Heuvelink, G., Stein, A., 2003. Comparison of kriging with external drift and regression krig-

- ing. ITC Enschede, Netherlands.
- [27] Olea, R.A., 2006. A six-step practical approach to semivariogram modelling. Stochastoc Envrionment Research and Risk Assessment. 20(5), 307-318. DOI: https://doi.org/10.1007/s00477-005-0026-1
- [28] Cambardella, C.A., Moorman, T.B., Novak, J.M., et al., 1994. Field-scale variability of soil properties in central Iowa soils. Soil Science Society of America Journal. 58(5), 1501-1511.
 DOI: https://doi.org/10.2136/sssaj1994.03615995 005800050033x
- [29] Sun, X.L., Yang, Q., Wang, H.L., et al., 2019. Can regression determination, nugget-to-sill ratio and sampling spacing? Catena. 181, 104092. DOI: https://doi.org/10.1016/j.catena.2019.104092
- [30] Bohling, G., 2005. Introduction to geostatistics and variogram analysis. Kansas Geological Survey. pp. 1-20
- [31] Solana-Gutiérrez, J., Merino-de-Miguel, S., 2011. A Variogram Model Comparison for Predicting Forest Changes. Procedia Environmental Sciences. 7, 383-388.
 - DOI: https://doi.org/10.1016/j.proenv.2011.07.066
- [32] Desktop, ESRI ArcGIS, 2011. Release 10. Redlands, CA: Environmental Systems Research Institute. 437, 438
- [33] Van Rossum, G., Drake, F.L., 2009. Python 3 Reference Manual, Scotts Valley, CA: CreateSpace.
- [34] Mälicke, M., Schneider, H.D., 2019. Scikit-GStat 0.2.6: A scipy flavoured geostatistical analysis toolbox written in Python. (Version v0.2.6). Zenodo.
- [35] Oz, B., Deutsch, C.V., 2000. Cross Validation for Selection of Variogram Model and Kriging Type: Application to IP Data from West Virginia. Center for Computational Geostatistics Annual Report Papers. pp. 1-13.
- [36] Brooker, P.I., 1986. A parametric study of robustness of kriging variance as a function of range and relative nugget effect for a spherical semivariogram. Mathematical Geology. 18(5), 477-488.

 DOI: https://doi.org/10.1007/BF00897500
- [37] Skøien, J.O., Merz, R., Blöschl, G., 2006. Top-kriging geostatistics on stream networks. Hydrology and Earth System Sciences. 10(2), 277-287.
 DOI: https://doi.org/10.5194/hess-10-277-2006
- [38] Miura, H., 2010. A study of travel time prediction using universal kriging. 18(1), 257-270. DOI: https://doi.org/10.1007/s11750-009-0103-6
- [39] Thakali, L., Kwon, T.J., Fu, L., 2015. Identification of crash hotspots using kernel density estimation and kriging methods: a comparison. Journal of Modern

Transportation. 23(2), 93-106.

DOI: https://doi.org/10.1007/s40534-015-0068-0

[40] Bayraktar, H., Turalioglu, F.S., 2005. A Kriging-based approach for locating a sampling site-

in the assessment of air quality. Stochastic Environmental Research and Risk Assessment. 19(4), 301-305.

DOI: https://doi.org/10.1007/s00477-005-0234-8



Journal of Geographical Research

https://ojs.bilpublishing.com/index.php/jgr

ARTICLE

Open Space Implications in Urban Development: Reflections in Recent Urban Planning Practices in Nepal

Krishna Prasad Timalsina^{1*} Bhim Prasad Subedi²

- 1. Central Department of Geography, Tribhuvan University, Kathmandu, Nepal
- 2. University Grants Commission, Tribhuvan University, Nepal

ARTICLE INFO

Article history

Received: 20 March 2022 Revised: 12 April 2022 Accepted: 20 April 2022 Published Online: 29 April 2022

Keywords:

Open space

Urban development Planning practices Land development

1. Background

Open space planning for cities has been a growing concern among planners, development activists, and academicians worldwide. The open space is considered as the lungs of city life by which people discover the

ABSTRACT

Open space has various implications in urban development planning and has been integrated into recent urban planning approaches and practices in Nepal. The open spaces are not only important for (re)shaping the urban form but are also important for enhancing urban social life and disaster risk management, particularly for dense cities. As most of the cities in Nepal have been growing haphazardly, the cities lack sufficient open space. However, the value of open space in dense cities like Kathmandu has been recognized more after the Gorkha Earthquake in 2015 as the open space were extensively used for risk relief, treatment, recovery, and rehabilitation during and after the earthquake. With this background, this paper presents the major planning initiatives in Nepal and discusses how recent urban plans have provisioned and initiated open spaces development by reviewing concurrent urban planning practices, particularly reviewing Periodic Plans, Integrated Urban Development Plans, Smart City Plans, and Land Development Plan. The development of open areas has not been given much attention in the earlier urban planning practice but recent urban development planning has emphasized with a special focus which is very important for sustainable and safer city development and is expected to address the current bulging urban issues of spatiality and sociability. Therefore, it is very important for integrating open space implications in city planning and such open space should be conceptualized according to the city's geography, landscape as well as socio-cultural contexts.

value and benefits of public life activities [1-3]. The term "open space" in this article denotes those spaces that are available to urban residents without any restrictions for social, economic, cultural, environmental, and political uses, and these are contributing environmental benefits and shaping the urban physical form [4]. These spaces

Krishna Prasad Timalsina,

Central Department of Geography, Tribhuvan University, Kathmandu, Nepal;

Email: krishnadhading@gmail.com

DOI: https://doi.org/10.30564/jgr.v5i2.4544

Copyright © 2022 by the author(s). Published by Bilingual Publishing Co. This is an open access article under the Creative Commons Attribution-NonCommercial 4.0 International (CC BY-NC 4.0) License. (https://creativecommons.org/licenses/by-nc/4.0/).

^{*}Corresponding Author:

are shared resources, which are not closed or blocked up and provide access for people and express conditions of public life, civic culture, and everyday activities [5]. Therefore, open space for the cities underpins many social, ecological, environmental, political, and economic activities that are essential to the healthy functioning of urban life and the city environment. Thus, urban open spaces are the agent of shaping urban morphology and are contributing to the social, economic, environmental life of urban people. Different urban planning practices address open spaces to make the city livable, live, and functional even though the details and depth intensity of open spaces implications may be contextual and varies according to physiography, landscape, social and cultural settings, etc. Planners, urban authorities, and development activists working in urbanism, therefore, have been giving attention to integrating open space provisions in city planning practices.

Cities, countries, and organizations in the world have different criteria and practices for provisioning open spaces in city planning. Cities such as New York, Hongkong, Johannesburg, etc. use per capita; cities like London, Singapore, Sidney, Vancouver, and Stockholm use distance from the household residence to open space. Similarly, organizations like WHO use per capita whereas ECI (European Common Indicators), US EPA (US Environment Protection Agency) use distance to open spaces and Un-Habitat uses both per capita and distance to open spaces [4]. Table 1 reveals the major provisions and practices by world cities/towns and agencies to make open space functional and efficient.

Table 1. Open Space Provisions in the Major Cities

Cities/ Agencies	% of Open Space	Open Space Per Capita	Distance to Open Space
Bogota		10 m^2	
Hongkong		2 m ²	
Johannesburg		24 m ²	
London			400 m
New York		10 m ²	
Singapore			400 m
Sidney			400 m
Stockholm			200 m
Vancouver			5 min walk
Mumbai		2 m ²	
Kathmandu	5% of the metro city area	2.05 m^2	
UN-Habitat	15% of the city area		400 m
WHO		9 m ²	300 m
ECI			300 m
US EPA			500 m

Source: UN-Habitat, 2018; MoUD, 2015

The data reveal that Johannesburg seems the highest per capita open space then followed by New York. However, cities in developing countries like Mumbai and Kathmandu have the least open space available for public use. Mumbai has below 2 m² per capita open spaces whereas KMC (Kathmandu Metropolitan City) has 2.05 m² per capita [6,4,20]. It implies that open spaces are important for urban life as many developed countries are giving high attention to making the cities efficient, life, and functional with spacious open space provisions. However, our position is very poor in terms of open space availability and access of it to the urban people. So, we are in danger of running out of open space in the cities [7]. Sufficient green space, recreational spaces, public plazas, squares, rest places, etc. are the heart of such cities which would provide a good place for public life activities. Open space contributes to societal well-being and provides a safe place for disaster risk management. Evidence shows that there were thousands of people on the street and open spaces in Kathmandu during the earthquake in 2015 living outside their "home" [8]. Although the open space in city planning needs to be a central focus, there is less discussion on how urban planning practices have embedded open space planning in practice. In light of this background, this paper will explore how recent urban planning practices have conceptualized open space planning for city planning and development in Nepal.

2. Chronological Planning Practices in Nepal

It is pertinent to discuss here briefly the histography of the urban planning initiatives in Nepal. The first urban planning was started in Nepal in 1944 as the "Rajbiraj Plan" which was initiated to develop a grid road plan with the skeleton physical urban forms of the administrative town of Rajbiraj. Similarly, the first physical development planning was started as "The Physical Development Plan for the Kathmandu valley" in 1969 [9]. Thereafter, several planning practices have been executed for town/municipal development in Nepal. Master Planning, Structure Planning, Physical Development Planning, Integrated Action Planning, and Periodic Planning were the major planning practices that were used in town/municipal planning. Recently, the government has introduced Integrated Urban Development Planning (IUDP) and Smart City Planning for the sectoral integration of urban development efforts which is yet to be implemented [10]. The historiographic development planning initiatives in Nepal have been presented in chronological order as follows (Table 2).

Table 2. Chronological Planning Practice in Nepal

Timeline	Major Urban Planning Initiatives in Nepal		
1944	Rajbiraj Plan (the first planned administrative town plan)		
1956	National level periodic planning started		
1962	Kathmandu Beautification Program: Visual Beautification of Kathmandu Valley (Occasion of Royal visit of Elizabeth under UN Technical Assistance)		
1963	Town Development Committee Act, 1963		
1965	Third National Plan (1965-1970) (Divided the country into 3 watersheds namely Koshi, Gandaki, and Karnali River)		
1969	Physical Development Plan of Kathmandu Valley prepared under technical assistance from UNDP, led by Karl Pusha		
1973	Revised PDP of Kathmandu Valley 1969 (Revised by national professionals and land use plan of Kathmandu Valley)		
1975	Construction of Ring Road in Kathmandu Valley		
1974-1984	Bhaktapur Development Project (successfully implemented) with German assistance		
1976	The Revised Comprehensive General Plan for Kathmandu 1969/1973		
1987-1988	Structural plan for major urban centers including greater Kathmandu (20 years plan) in support of GTZ/MSUD		
1990	Integrated Action Plan (IAP)		
1991	Kathmandu Valley Urban Development Plans and Programs – Hal Crow Fox/ DHUD/ ADB		
1993	Study of Kathmandu Valley Urban Road Development – JICA		
1999	Kathmandu Valley Mapping Program (KVMP)		
2002	Long Term Vision for Kathmandu Valley Development (Vision 2020)		
2005-2015	Periodic Planning (Various municipalities)		
2015	Vision 2035 and Beyond: 20 years Strategic Development Plan (2015-2035)		
2016 onwards	Integrated Urban Development Planning (IUDP)		
2018 onwards	Smart City Planning (three piloting municipalities in the first phase and 10 other municipalities in the second phase)		

Source: NTPCO, 2019a, 2019b and DUDBC, 2020a and 2020b

The periodic planning approach was largely adopted for town/municipal planning in Nepal for a long-time before the IUDP and is still in practice in municipal planning. However, most municipalities now prefer integrated planning to integrate different sectors in the urban development which is supposed to integrate various development sectors identifying the leading development sector(s) for the municipality.

The implications of open space in urban planning are diverse. Open space contributes not only to enhancing the urban forms of the town but also helps to enable social and physical well-being [7] of urban communities. Moreover, open spaces will contribute as a place for disaster risk management in dense cities like KMC as most open spaces were extensively used in disaster risk relief, treatment, recovery, and rehabilitation [8,11] during the 2015 earthquake. Planning practices such as Physical Development Planning, Periodic Planning, Integrated Urban Development Planning, and Smart City Planning have embedded some slots of open space development in city planning. Although it was not highlighted much about open space development in periodic planning except for identifying the potential sites for land development projects and open space allocations in the plan which is a good initiation for open space development for the towns.

3. Methods and Materials

The methodology of this paper is based on constructive criticism of various urban plans prepared by the Department of Urban Development and Building Construction (DUDBC), New Town Project Coordination Office (NTPCO), and Municipalities. The propositions of open space development within the plans were reviewed and discussed how these plans have focused to contain open space in the city planning and practices. Depth review of Periodic Plans, Integrated Urban Development Plans, Smart City Plans, and Land Development projects/Plans was the basis for identifying open space implications in the planning practices. Maps have been prepared by using the data acquired from DUDBC, NTPCO, and the Municipalities and further overlay in google earth images. The overall methodology of preparing this paper has been presented below (Figure 1).

As far as data is available, DUDBC has prepared 58 municipalities' periodic plans, 186 municipalities' IUDPs, 13 municipalities' smart city plans, and about 27 block land development plans [15-17,20-23]. To make representatives for reviewing the different planning practices, 11 municipalities for periodic planning, 34 municipalities for integrated urban development planning, 4 smart city planning, 4 land development plans were selected randomly by listing out all the municipalities in different thematic columns e.g., periodic planning, integrated urban development planning, smart city planning, and land development planning. The reviewed plans are; 11 municipalities' periodic plans namely Bidur, Dhangadhi, Ghorahi, Birjung, Rajbiraj, Siraha, Baglung, Kathmandu, Attariya (renamed now as Godabari), Jharipipaladi (renamed now as Shuklaphanta), Ilam; 34 municipalities

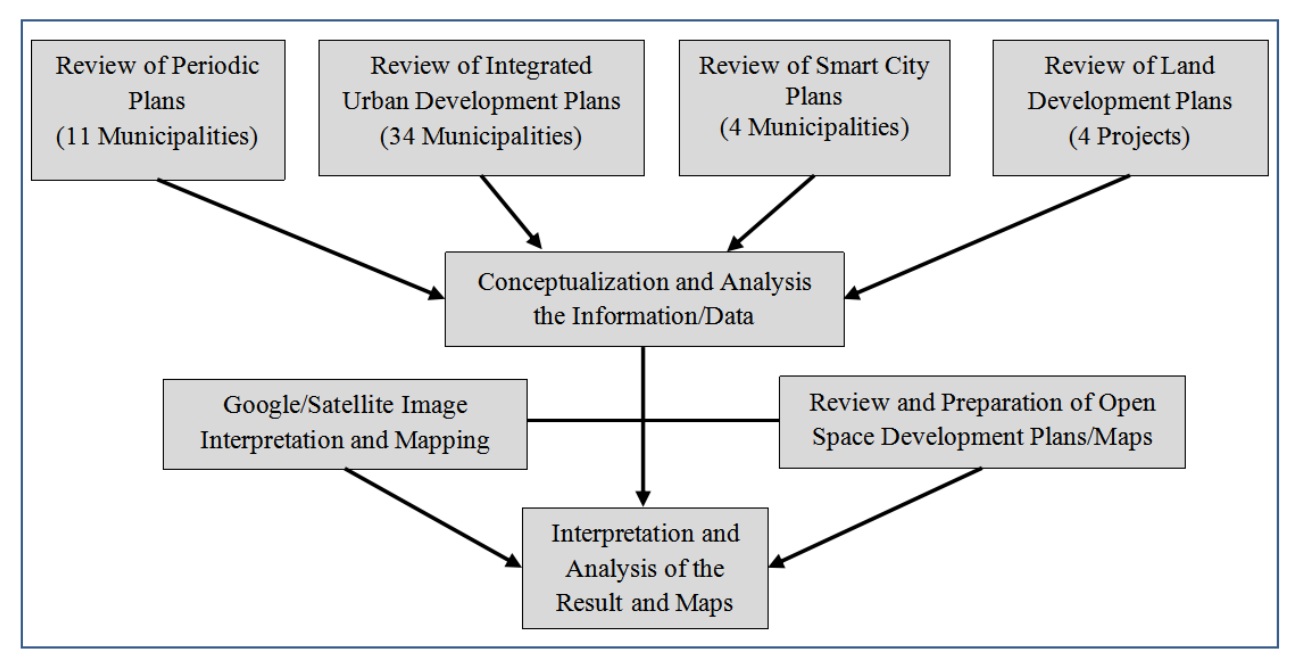
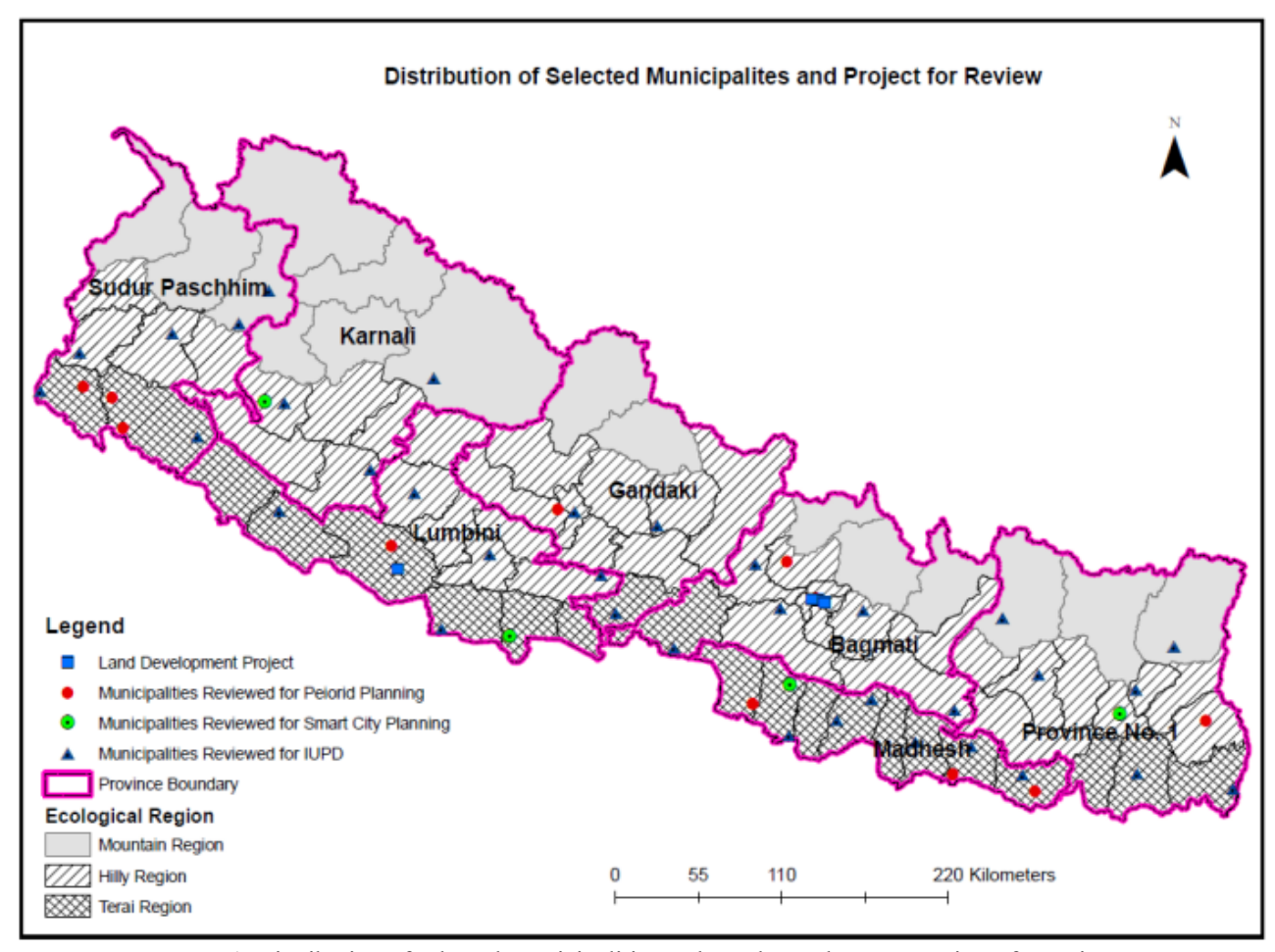


Figure 1. Process and Methods



Map 1. Distribution of selected Municipalities and Land Development Projects for review

integrated urban development plans namely *Phungling*, Bhadrapur, Belbari, Laligurans, Solududkunda, Rupakot Majuwagadhi, Shambhunath, Golbazar, Chhireshwornath, Barahathawa, Lalbandi, Dudhauli, Panchkhal, Neelakantha, Thaha, Simraungadh, Madi, Myadhyanepal, Kushma, Rampur, Krishnanagar, Sandhikharka, Bagchaur, Kohalpur, Narayan, Tripurasundari, Budhinanda, Tribeni, Dipavalsilgadhi, Punarbas, Mahakali, Parashuram, Madhyabindu, Rolpa; 4 municipalities' smart city plans namely Nijgadh, Lumbini, Dullu, and Chandrapur and 4 Land Development Plans namely Pepsicola Town Planning, Nayabazar Khusibu Town Planning of Kathmandu District, Divyaswari Planning of Bhaktapur District and Lamahi Town Planning, Dang District. Details of plans prepared by DUDBC and No. of reviewed are presented in Table 3. The selected municipalities for review are from different provinces, and ecological zones as presented in the map below (Map 1).

Table 3. No of Plans (municipalities) Selected for Review

S. No	Plans	Plans Prepared by DUDBC	Selected Municipalites for review
1	Periodic Plans	58	11
2	Integrated Urban Development Plans (IUDP)	186	34
3	Smart City Plans	13	4
4	Land Development Projects/Plans	27	4

4. Results and Discussions

Open Spaces in the Municipal Periodic Planning

In 1999 the Local Self Governance Act (LSGA) was enacted with subsequent LSG (Local Self Governance) regulations in 2000 which empowered periodic planning for urban development to the municipalities [12]. The Tenth Plan 2002-2007 also prioritized the preparation of periodic plans of the municipalities and in 2002 the Guideline was prepared by the Ministry of Local Development [13]. The periodic plan was expected to be efficient to integrate different sectors to achieve short-term, mid-term, and long-term planning goals and avoid duplication of sectoral plans and programmes by the government line agencies and others that serve as planning, implementing, and project executions in the municipalities. The plan would require a municipal profile, sectoral integration plan with Logical Framework Analysis (LFA)-based participatory planning for municipalities.

The periodic plan is a long-term, comprehensive parti-

cipatory, and inclusive plan prepared for 5 years action plan with a long-term vision, goal, and objectives for municipal development. A rational and participatory planning method would be applied as bottom-up planning methods. Ward-level projects and municipal-level projects would be prepared with the integration of different thematic plans such as social, economic, environmental, physical, financial, and institutional plans. This plan would ensure that the concerned stakeholders in the respective district authorities get due support in the overall periodic planning process to translate the legal provision into action [12]. Sectoral integration would be based on the nature of the program, resource availability, and the performance indicators as a tool for monitoring the plan implementation. Although the integration of sectoral plans, the physical development plan was the main goal of regulating spatial city forms and development for the municipality. This plan would foster municipalities to initiate and direct future city expansion, development, and regulation for urban development where the potential expansion is inevitable.

The method includes profile-based planning based on the primary and secondary data, physical investigations, a participatory approach for a long-term development vision, developing the sectoral goals, identification of lead development sectors, output indicators using Logical Framework Approach (LFA), program identification at municipal and ward levels and preparation of implementation plan with the role and responsibilities of possible line agencies. Although the plan would be beneficial in many aspects of municipal development because of its integrated nature of physical, social, and institutional planning, it has some limitations. The lengthy planning process, absence of municipal data, elites' participation and free riding their voices, collection of a list of scanty projects, insufficient budget for implementations, less effort on depth fieldwork and analysis may mislead to drive the municipality to the targeted direction and, of course, lack of proper implementation mechanisms in the municipality are some of the major limitations. Hence, municipal authorities started to see the periodic plan as just to fulfill their Minimum Criteria Performance Measure (MCPM) requirement for the government's evaluation process to receive a regular grant. So, the municipal periodic plan was not successfully implemented on the ground.

Although the periodic plans were to contribute to spatial development planning having a focus on a physical development plan, they could not address and regulate the physical forms of the town/city effectively. Allocation of open spaces within the physical plan could be one of

the guiding principles for spatial planning that was not well initiated in this plan. Planning and building by-laws and their effective implementation would be the best tool for the implementation of spatial regulation which was not embedded in the plan. Therefore, the periodic plan could not effectively guide spatial development directions to the municipalities as it had poorly embedded planning and construction by-laws in the plans. The open spaces provisions were just spoken in the plan as Right of Way (RoW), which was not proposed strongly in most of the periodic planning. It means periodic plans do not adequately address open space planning for the municipalities but address the local and municipal level needs assessment and direct municipalities to integrate the different sectors as a whole to meet the intended longterm vision of the city/town.

Open Spaces in the Integrated Urban Development Planning (IUDP)

Integrated Urban Development Planning (IUDP) is the integration of all development sectors involved in urban/ city development. IUDP was started in 2017 by DUDBC initiating for preparation of 185 municipalities' plans. It was one of the remarkable planning activities initiated by DUDBC. IUDP comprises a system of interlinked actions, which seeks to bring about a lasting improvement in the economic, physical, social, and environmental conditions of a city or an area within the city [14]. The integration process involves sectoral integrations in the plan and process integration from the bottom-up to topdown strategic planning. The main scopes of IUDP are i) to coordinate the work of local and other spheres of government in a coherent plan to improve the quality of life for all the people living in an area considering the existing conditions and problems and balance allocation of resources available for development, and ii) to ensure equal opportunity for different sub-areas and different social and age groups in urban society which includes gender-mainstreaming planning, ensure balanced development planning with growing social and spatial inequalities, and it aims to help preserve social harmony with equity and equality [15].

The procedural steps of IUPD would start with reviewing the existing plan documents and conceptualizing the sectoral integration for municipal/town development. Induction workshops that are supposed to disseminate the planning process and outcomes at the municipality would be conducted at the municipality to start the IUDP. It is then followed by tole/community level problems and issues identification to which ward/cluster of wards level workshops and discussions would be conducted. Such community-level issues would guide the planning team

to prepare sectoral strategic plans and project formulation at the municipal level. In the second stage, municipal level workshops for vision setting, participatory SWOT (Strength, Weakness, Opportunities, and Threats) analysis, and municipal sectoral planning issues identification would be conducted to establish municipal sectoral goals and objectives. The municipal scenario would be presented among the broad stakeholders' participants and feedback would be collected through brainstorming among the stakeholders. The participatory process of vision setting, development of sectoral goals, and strategies would foster rationality of planning and lead municipal development in which leading sector(s) and the projects that the IUDP should intervene for the municipality would be identified and proposed in the plans.

Besides the sectoral integrations, the strengths of IUDP are base maps and planning and building bye-laws for the municipality. Previous plans were less focused on base maps although some thematic maps were prepared in periodic and physical development plans. The IUDP has mainly focused on preparing base maps with 1:2500 and 1:5000 scales for core and other urban areas of the entire municipal area respectively. On the one hand, planning and building by-laws would be a guiding tool for regulating spatial development directions. On the other hand, the base map would be prepared by using the latest archive satellite imagery. All the sectoral analysis would perform on the base map rationally. Right of Way (RoW), Floor Area Ratio (FAR), land use zones, development controls regulation would be prepared and proposed by the planning by-laws to regulate growth control. The bylaws would control and regulate urban growth as spacious urban development regulating ground coverage, building heights, RoW (right of way), and provisions of open spaces in the city development. The by-laws thus would be an effective tool for guiding spatial planning especially for enforcing to regulation of city morphology and open space provisioning for the city. For the first time, with a separate planning and building by-laws volume for the municipality development regulation, the IUDP has addressed open space planning for shaping the city in the

Similarly, the strategic plans in the form of proposed development plans would be prepared on the base map that would guide rationally for municipal development in many respects. Existing physical, social, and environmental conditions would be assessed through the maps and potential development could be monitored on the maps as the base maps would guide where the suitable area is located for what purposes through suitability analysis. Thus, one of the greatest achievements of IUDP is that

it integrates sectoral development and is backed up by a rational planning process with reference to updated base maps. Planning of recreational space, green spaces, land use zoning with delineation of risk-sensitive areas where development growth needs to be restricted were identified and proposed in the maps. Such sectoral analysis would provide the basis for the municipality for spacious planning to preserve sufficient open spaces, green space, and prohibit settlement development in risk-sensitive areas.

Planning of open space in the IUDP has been proposed within broad land use zones and sub-zones (e.g., green area, open space, cultivation, residential, commercial, industrial, institutional, water body, etc.). Based on the suitability analysis, the development zones as residential, mixed-use, commercial, forest, waterbody, conservation, and green area development zones were proposed for the municipality (Figures 2 and 3). Conservation and green area development zone including open space development zones would enhance the city's form and spatiality. The zones and open spaces development in the municipalities

have been proposed considering the potential urban development areas and future growth trend prospects. The proposed open space development plans would be proposed considering settlement growth trends, settlement hierarchy, connectivity, and regional positioning and networks of the towns. However, the scale and size of open space in the plans vary according to their growth potentiality, existing physiography, landscape, settlement forms and patterns, and socio-cultural contexts. It means open space planning for the Terai municipalities may differ from the hilly municipalities as these municipalities pose different physiographic characteristics and different social-cultural settings. Similarly, open space within a city may vary as open space in the core area of KMC is found more culturally driven and bounded [2] whereas open space in the outer areas is community-driven [7]. But all the open spaces whether they are cultural, religious, institutional or public; all of these are valued in terms of the city's landscaping, enhancing the environment, and contributing

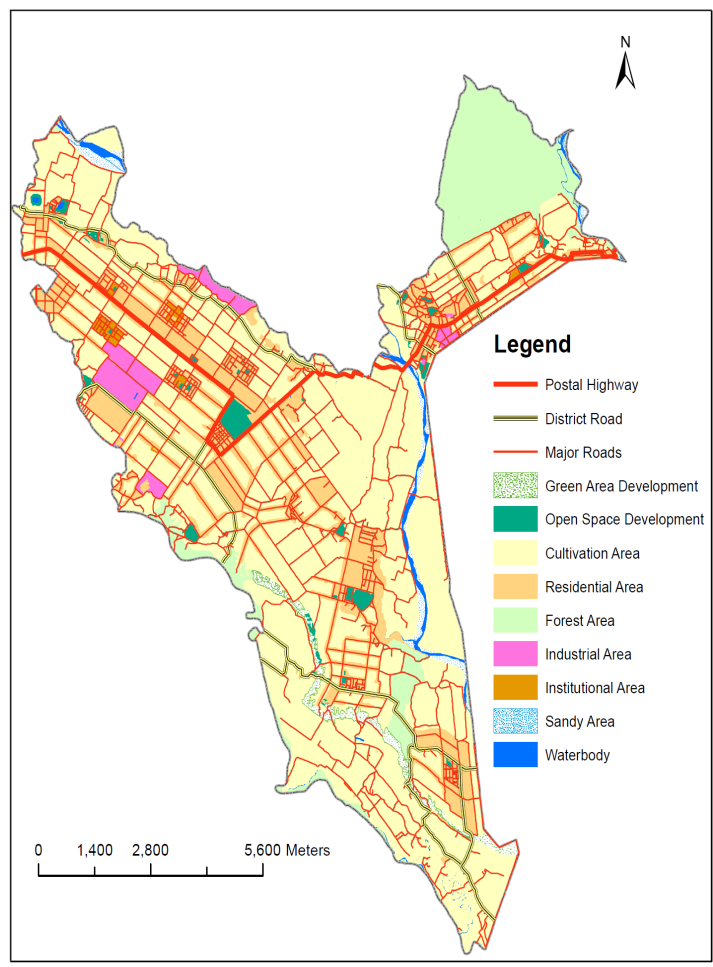


Figure 2. IUDP Land Use Zoning with Open Space Development Plan, Punarbas Municipality, Kanchanpur District

Source: DUDBC, 2020

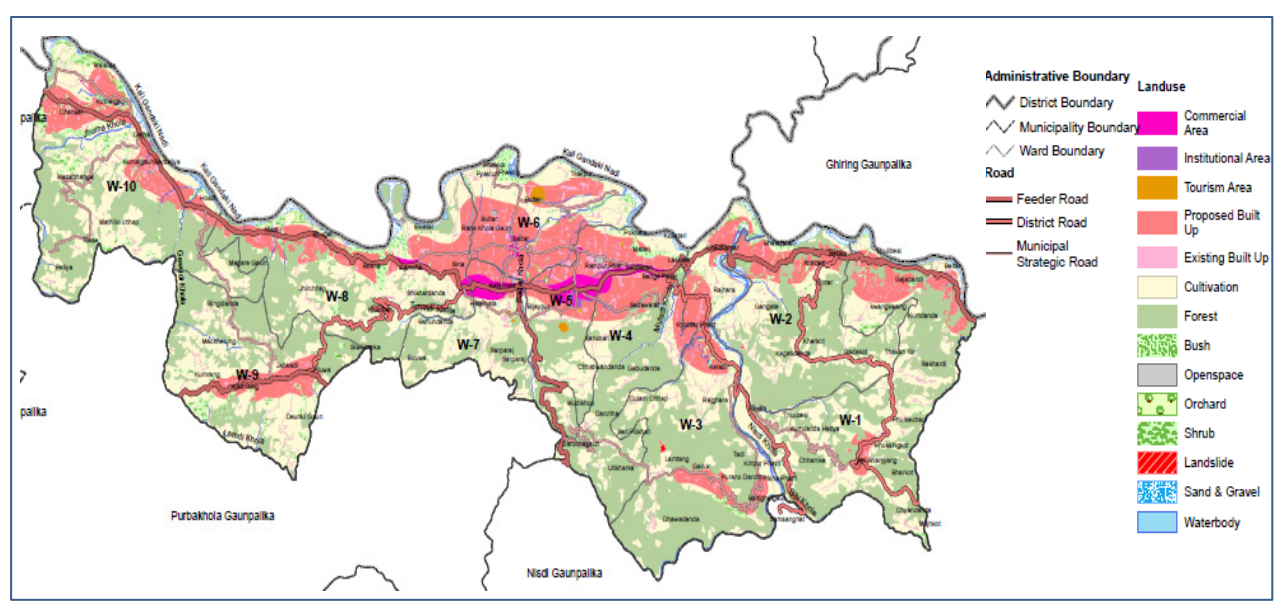


Figure 3. IUDP Land Use Zoning with Open Space Development Plan, Rampur Municipality, Palpa District

Source: DUDBC, 2020

to social well-being. Figures 2 and 3 are presented from some of the municipal IUDP to show how the open has been envisioned in the IUDP taking cases of *Punarbas Municipality* located in the Terai Region of Kanchanpur District and *Rampur Municipality*, located in Hilly Region of Palpa District [15].

Open Spaces in the Smart City Planning

Smart city development is a recent urban development planning practice across the world. Nepal government has also initiated Smart City Planning intending to integrate the benefits of Information Communication Technology (ICT) in urban development and growth management. The smart city concept especially focuses on the increasing efficiency of land use, infrastructure, and urban service delivery through the use of ICT. A smart city is defined as a city that is sustainable and innovative, where high-quality urban services are provided to all citizens effectively and efficiently through the optimum use of technologies including ICT as a tool to improve the quality of urban life, the efficiency of urban services, and competitiveness [9,10]. Thus, smart city planning is a combination of sectoral development and ICT integrations envisioning the future urban development strategy to plan smartly.

The government of Nepal has prepared 13 municipal smart city plans for implementing ICT embedded plans for municipal development. Three municipalities namely *Nijgadh* (Bara District), *Lumbini* (Rupandehi District), and *Palungar* (Gorkha-Tanahu Districts) were planned as piloting for smart city development, then followed by other 10 municipalities in different provinces of Nepal. The main objective of preparing smart city plans

are: a) contained population growth management and regulate urban development through the uses of ICT in the municipality, b) promote green, spacious, and sustainable city development through land-use zoning and regulation and environment-friendly development initiatives, c) integrate the application and benefit of ICT in the functionality of the city, especially for mobility, community development, service delivery, governance and infrastructure development in the city [9,10,16,17]. It indicates that ICT development is essential for smart city planning integrating it with other physical infrastructure and sectoral development for the city.

The crux of smart city planning is indicator-based strategic planning by which targeted outcomes would be achieved through the intended action plans. Therefore, the fundamental basis of smart city planning is to target some level of achievement set out in the indicators. The indicators include four broad pillars a) Smart People, b) Smart Governance, c) Smart Infrastructures, and d) Smart Economy. Within the four broad smart city indicators, 31 components and 117 indicators were defined [9,10]. The smartness of a city would be measured based on the targeted level of achievement on the defined indicators.

The process of formulating a smart city plan is also the participatory method by which the local needs would be addressed in the plan. Induction workshops, local/community level consultations/workshops for need/gap identifications, vision setting, lead sector identification, participatory SWOT analysis, strategic sectoral planning through municipal level workshops are the process of plan formulation. Besides, indicator-based analysis and planning have been proposed for the

development of different sectors such as the physical, social, environmental aspects of the city. But one of the innovative ideas of smart city planning is the integration of ICT components which is not addressed in any other planning approach of Nepal. So, sectoral plans would be strongly tied up with ICT-based planning in smart city planning. Thus, smart city planning also advocates for participatory planning that would address the local needs effectively.

Open space planning has been highlighted more in the smart city plans targeting 40% of municipal ground coverages by an open/green space (Smart City Indicators-C.3.1) as supporting indicators for urban planning and land use components under the smart environmental infrastructure of Smart City Indicators. The proposed ground coverage includes green development areas, open spaces, ecological conservation areas, etc. which could be available for the use of municipal residents as open areas in terms of recreational space, public space, or green space. Including the planning and building by-laws, this plan has strongly proposed the allocation of sufficient open spaces in the city. Land-use zoning and regulation, RoW, FAR, building heights and services spaces, setback, density control, road access, etc. have been proposed to regulate urban development with spacious spatial planning. This has opened an opportunity to preserve green areas and open spaces for the city which could initiate to development of sufficient open spaces/ areas in the city for the future. Delineation of conservation areas with keeping intact forest coverage and agricultural zones for the city would guide growth control for the city.

In Smart City Planning, open space has been proposed as an ecological corridor, greenfield development, and pond site green development zone in the case of Lumbini Sanskritik municipality whereas a population densitybased plan would control urban growth and regulate open area for the city in case of Nijgadh municipality. The proposed areas have supposed to be preserved for open space/green area development for the municipality which could serve as sufficient open space in the future. Various zones have been proposed to regulate land use for future development control (Figures 4 and 5). ICT development at community and city levels is intended to ease urban life so as to smooth service delivery and governance. Proposed infrastructure development would always be developed in favor of spacious planning based on the proposed by-laws. Board land-use zoning and allocation of potential sites for settlement development, green area/ open area development, and other potential zones were proposed for spacious urban development in the smart city.

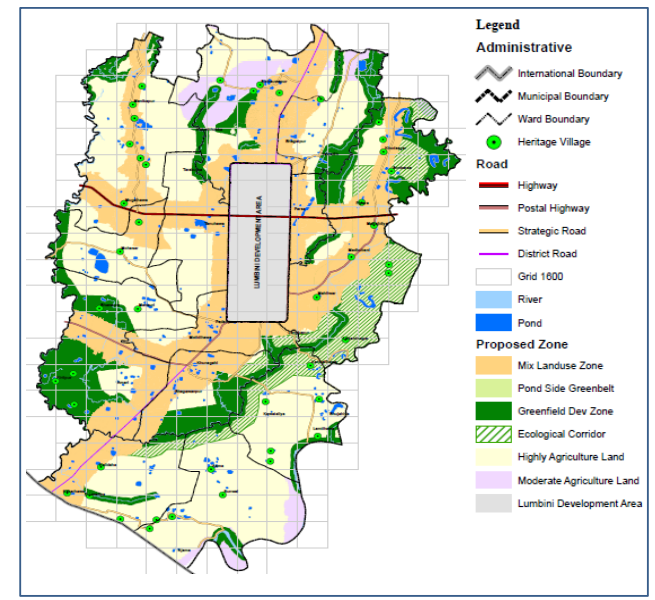


Figure 4. Land Use Zone with Open Space Development in Lumbini Sanskritik Municipality, Rupandehi District

Source: NTPCO, 2019b

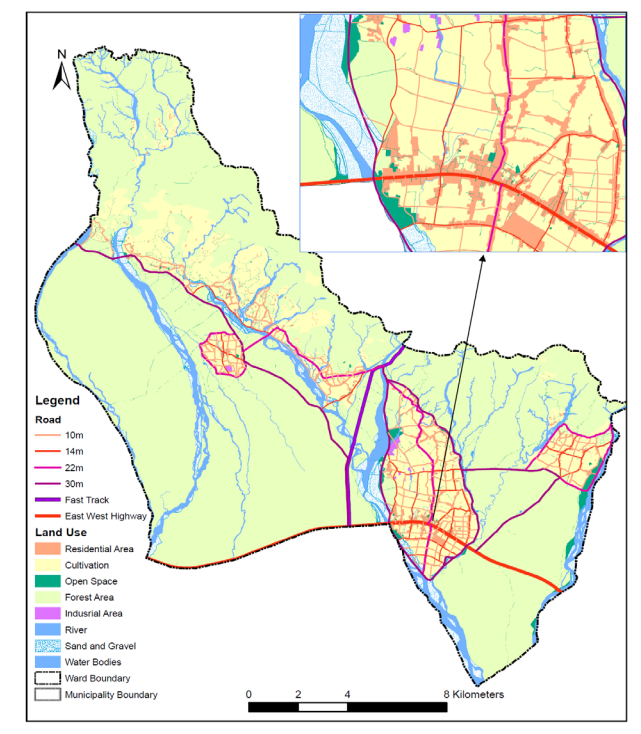


Figure 5. Land Use Zone with Open Space Development in Nijgadh Municipality, Bara District

Source: NTPCO, 2019a

Plans in Action: Open Space in Land Development Plan

Land development plans are action plans with small area development as a part/component of the city. It is an implementation of the physical plan of the city/town. While

planning small area development, land development (also called land pooling) is a popular method of implementing the plans. Land pooling could be a process of planned urban islands to city transformation [18]. Globally it shows that land pooling can transform entire cities in a planned form which means land pooling can transform a city into a planned development area. The concept of land pooling is that a portion of the urban area is pooled for residential development with provisions of urban infrastructures, open spaces, and other basic services and distributed proportionately among the landowners. The landowners contribute the land proportionately for site and services development within the area. The landowners agree to contribute land for infrastructure development by which their land value would be increased to compensate for their contributed land. Some examples of land development areas are presented below (Figures 6 and 7). The main strength of such land development is that it allocates open spaces with adequate road networks and connectedness between settlements/households. In a properly planned land development area, road connectivity, basic urban infrastructure, sufficient open space and even building structures will be regulated so that the chaotic development of a city could be discouraged. Since the land pooling could be possible in a small site, whole city development takes time but expansions of such a developed island could transform the city into a planned city form [18,24,25,27]. Such plans are also important to develop sustainable cities and spacious urban development that could foster spatiality and sociability [7,26-29].

The action plans in the form of a land development plan reflect a spacious development plan that addresses planned settlement development in an area or a city. There are many land development projects completed in Nepal which have a good provision of open space. 25 land pooling projects in Kathmandu Valley and 17 projects outside Kathmandu Valley have been developed as land development/land pooling projects by different government institutions of Nepal and the Kathmandu Valley alone holds 6,684 Ropani of land with 15,160 developed plots [19]. Among these, 27 projects were designed by DUDBC which is successfully implemented with good provision of open spaces.

Provisions of open space in land development project sites regulate urban development patterns, provide spacious urban landscapes, and preserve open space for the city. Land development sites of some projects in different parts of Nepal are presented in Figures 6 and 7 above in which Pepsicola town planning-Kathmandu (A), Khusibu town planning-Kathmandu (B), Divyaswari town planning-Bhaktapur (C), and Lamahi town planning-Dang (D) reveal that open space development in the planned area is well developed with good road networks. Therefore, such land development with a good provision of open space could be a successful strategy of open space planning for a town/city. Such plans will integrate good road connectivity, preserve urban form, regulate urban growth, and provide urban people with spacious space for residential development. Examples of some land development plans are presented in Figures 6 and 7.

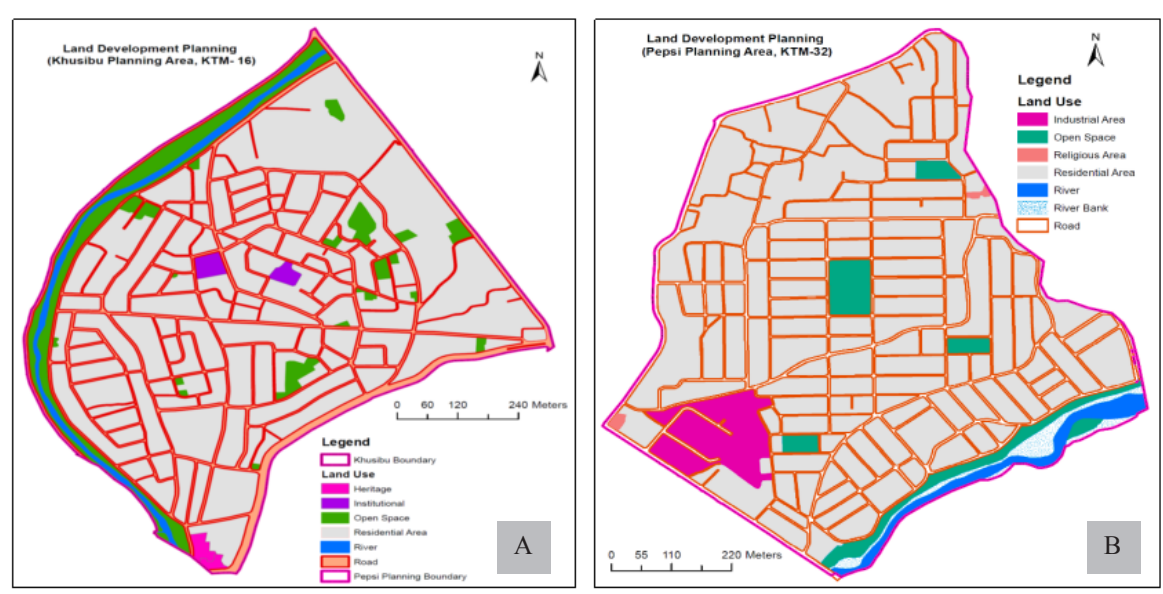
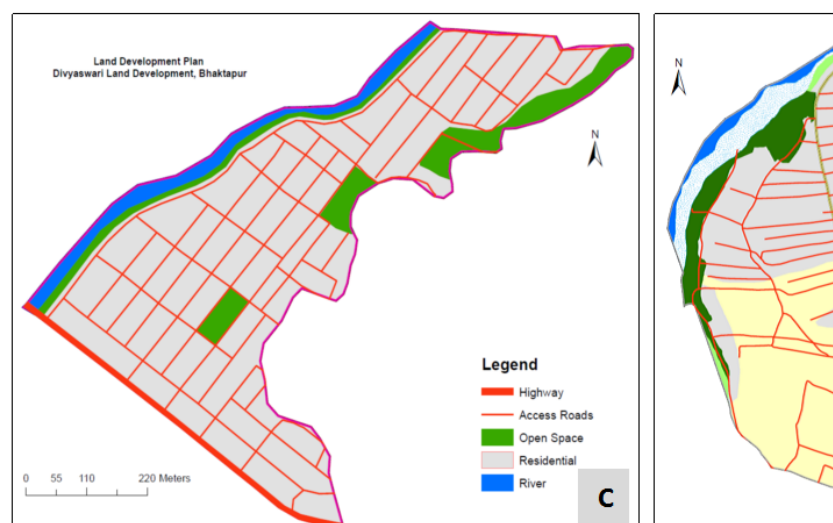


Figure 6. Land Development with Provisions of Open Space (A-Khusibu and B-Pepsicola land development area, Kathmandu Metropolitan City)

Source: Periodic Plan of KMC, 2011, and Google Map, 2021.



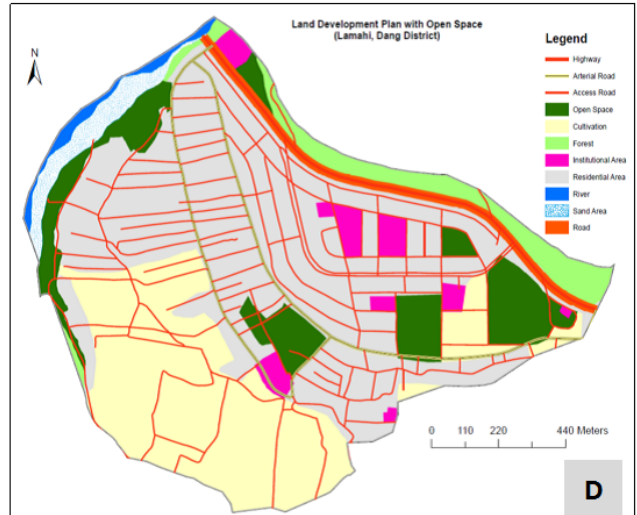


Figure 7. Land Development with Provisions of Open Space (C-Divyashwori, Bhaktapur District and D-Lamhi Dang District)

Source: Google Image-Based Data, 2020 and DUDBC, 2015

However, there are many land development sites flourishing in the major cities by the private sectors in Nepal which have been planned without proper provisioning of basic services and facilities (e.g. lack of public open space, improper infrastructures and facilities, unsuitable locations, and poor physical conditions, etc.). The sites are developed by the private sector with their own interests and the government institutions have not been able to scrutinize/monitor them effectively. Hence, government institutions should govern and regulate such private sectors for adequate and proper physical infrastructures and services while developing private housing/land pooling projects.

5. Conclusions

This paper aimed to look at the implications of open space in urban planning with reference to recent planning practices such as Periodic Planning, IUDP, Smart City Planning, and Land Development Planning of Nepal. This paper is prepared by reviewing 11 periodic plans, 34 IUDPs, 4 smart city plans, and 4 land development plans which were selected randomly among the list of prepared plans/projects. The concept of open space development in the plans before periodic planning was very limited. Recent planning practices have been giving attention to sectoral integration with open space development for spacious planning. Periodic planning, IUDP, and smart city planning are the concurrent practices that have addressed open space for resilient cities. The periodic plan integration of sectoral plans focuses on physical development plans in which open space development was initiated within the physical development plan. IUDP has highlighted the open space development for the city specifying it in the planning and building by-laws as a tool to regulate sufficient open space and proposing broad zoning of land use plan. Such a land-use plan addresses open space development within the networks and different hierarchies of settlements of a town. Similarly, the smart city plan has more focused on open space development in the city with indicators-based planning. For the first time, it has established 40% open/green space coverage as an indicator for a smart city. Therefore, the latest planning practices are more rational in open space provisions in city planning in Nepal. However, the scale of an open space development proposal in the plans varies according to the geographic as well as socio-economic characteristics of the municipalities as the municipalities of the Terai and the Hilly region pose different natures of physiography and social, cultural settings and have different propositions of open space development in the plans.

A land development plan as an action plan presents how a land pooling project is designed for spacious planning preserving open space within a small area of a city/town. Land pooling projects are successful land planning in various towns and cities in Nepal. Such plans could be a tool for implementing Periodic Plans, IUDP, and Smart City Plans to provide accessible and sufficient open space to the residents. Such plans will regulate urban development with a proper provision of open space including basic urban services. However, the witness of a growing private sector's land development planning in major cities of Nepal which needs effective regulation and monitoring by the government institutions. The importance of open space provisions in urban planning

has now been well acknowledged by the urban authorities for disaster risk management as urban people extensively used open spaces during the Gorkha Earthquake in 2015. It has been well conceptualized that the recent planning practices including land development planning are well recognized by city designers, residents, and authorities for spacious open space provisions to make a resilient and sustainable city.

Acknowledgment

The authors would like to acknowledge the Department of Urban Development and Building Construction (DUDBC) and New Town Project Coordination Office (NTPCO) for providing data, base maps, and reports for reviewing the plans. We would also like to acknowledge PhD Cosupervisor, Dr. Kanhaiya Sapkota. Acknowledgment also extends to Dr. Sanjaya Uprety, Dr. Kedar Dahal, Mr. Kishore Kr. Jha, Mr. Narayan Prasad Khanal for their support in different stages of preparing plans during the project period in preparing the plans.

Conflict of Interest

There is no conflict of interest.

References

- [1] Tiwari, S.R., 1989. Tiered temples of Nepal. Sunita Tiwari Publication: Kathmandu.
- [2] Chitrakar, R.M., 2015. Transformation of public space in contemporary urban neighbourhoods of Kathmandu valley, Nepal: an investigation of changing provision, use and meaning. (Ph.D. Thesis), School of Civil Engineering and Built Environment Faculty of Science and Engineering Queensland University of Technology.
- [3] KVDA, 2015. Atlas of open space. KVDA, Kathmandu
- [4] UN-Habitat, 2018. Developing public space and land values in cities and Neighborhoods (discussion paper). Kathmandu: UN-Habitat.
- [5] Wooley, H., 2003. Urban open space. London and New York: Tailor and Francis.
- [6] KMC, 2011. Periodic plan of Kathmandu Metropolitan City. Department of Urban Development and Building Construction, Kathmandu.
- [7] Timalsina, K.P., 2020. Public open space in crises: Appraisal and observation from metropolitan Kathmandu. Journal of Geography and Regional Planning. 13(4), 77-90. DOI: https://doi.org/10.5897/JGRP2020.0797
- [8] Shrestha, S.R., Sliuzas, R., Kuffer, M., 2018. Open

- spaces and risk perception in post-earthquake Kathmandu city. Applied Geography. ELSEVEIR: Amsterdam. 93, 81-91.
- [9] NTPCO, 2019a. Preparation of Smart City for Developing Nijgadh as a Smart City. NTPCO (DUDBC), Babarmahal, Kathmandu.
- [10] NTPCO, 2019b. Preparation of Smart City for Developing Lumbini as a Smart City. NTPCO (DUDBC), Babarmahal, Kathmandu.
- [11] Poudel, K., 2017. Open space vanishing fast. New spotlight magazine. 11, 08.
- [12] MoFAGA, 1999. Local Self Governance Act, Kathmandu: MoFAGA.
- [13] MoFAGA, 2000. Local Self Governance Regulation, Kathmandu: MoFAGA.
- [14] ADB, 2020b. Guidelines for preparation of Integrated Urban Development Plan (Draft). ADB, A-9384 NEP: Regional Urban Development Project. Kathmandu: DUDBC.
- [15] DUDBC, 2020. Preparation of Integrated Urban Development Plan of Various Municipalities. DUDBC: Kathmandu.
- [16] NTPCO, 2020a. Preparation of Smart City for Developing Chandrapur as a Smart City. NTPCO (DUD-BC), Babarmahal, Kathmandu.
- [17] NTPCO, 2020b. Preparation of Smart City for Developing Dullu as a Smart City. NTPCO (DUDBC), Babarmahal, Kathmandu.
- [18] ADB, 2020a. Land pooling in Nepal from planned urban "islands" to city transformation. ADB South Asia Working Paper Series, ADB: Manila, Philippines.
- [19] ADB, 2017. Land pooling projects in Nepal: A consolidated document. Regional - Capacity Development Technical Assistance (R-CDTA), ADB/OIE, Kathmandu.
- [20] MoUD, 2015. Planning Norms and Standards. DUD-BC, MoUD: Kathmandu.
- [21] Bhadrapur Municipality, 2017. Integrated Urban Development Plan of Bhadrapur Municipality. Bhadrapur, Jhapa.
- [22] DUDBC, 2015. Physical development plan and GIS based base map of Lamahi TDC area, Dang. DUDBC: Kathmandu.
- [23] DUDBC, 2018. Preparation of Integrated Urban Development Plan of Dudhauli Municipality, Sindhuli District, DUDBC: Kathmandu.
- [24] French, E.M., 2017. Designing public open space to support seismic resilience: A systematic review. Master's Thesis (unpublished), The University of Guelph, Ontario, Canada.
- [25] Koren, D., Rus, K., 2019. The potential of open space

- for enhancing urban seismic Resilience: A literature review. Sustainability, MDPI. 11.
- DOI: https://doi.org/10.3390/su11215942
- [26] NRA, 2016. Nepal earthquake 2015: Post-disaster recovery framework, 2016-2020. Kathmandu: National Reconstruction Authority, Government of Nepal.
- [27] Pelling, M., 2003. The vulnerability of cities: Natural
- disasters and social resilience. London: Earthscan.
- [28] USAID, 2010. Planning for disaster risk reduction, urban governance and community resilience guidelines. USAID, Asian Disaster Preparedness Center (ADPC).
- [29] www.newsghana.com. and www.theatlantic.com (Accessed on 22 May 2020)

